ISSN 1307-8798

Official Publication of the Turkish Society of Anatomy and Clinical Anatomy

www.anatomy.org.tr

anatomy

An International Journal of Experimental and Clinical Anatomy

Volume 12 / Issue 3 / December 2018

Published three times a year

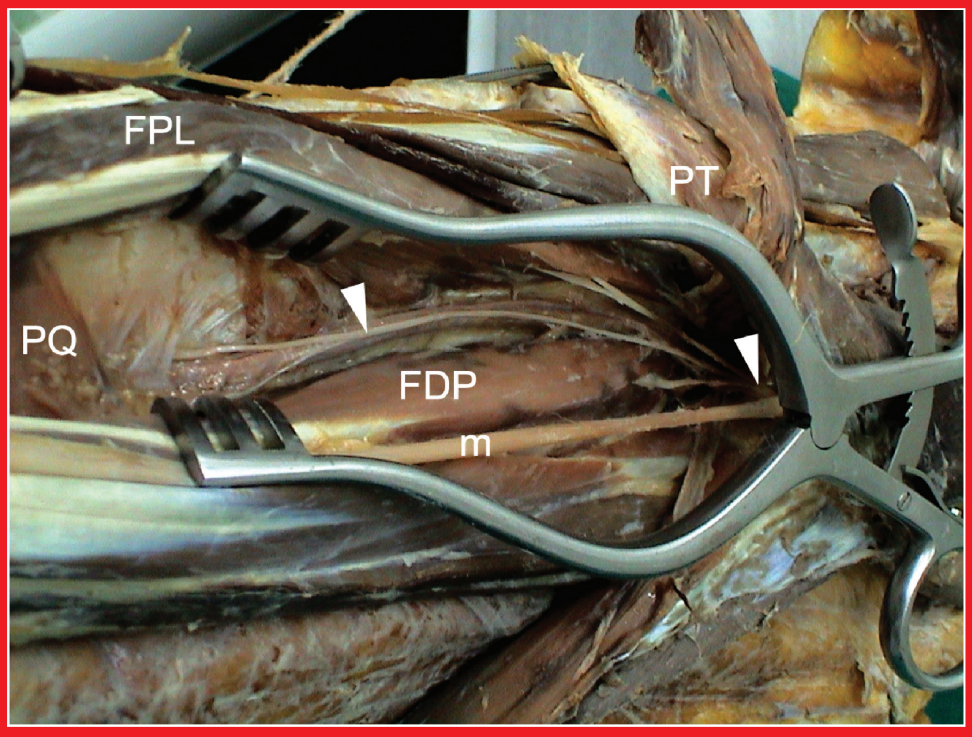

deomed®

www.anatomy.org.tr

anatomy

An International Journal of Experimental and Clinical Anatomy

Official Publication of the Turkish Society of Anatomy and Clinical Anatomy

Aim and Scope

Anatomy, an international journal of experimental and clinical anatomy, is a peer-reviewed journal published three times a year with an objective to publish manuscripts with high scientific quality from all areas of anatomy. The journal offers a forum for anatomical investigations involving gross, histologic, developmental, neurological, radiological and clinical anatomy, and anatomy teaching methods and techniques. The journal is open to original papers covering a link between gross anatomy and areas related with clinical anatomy such as experimental and functional anatomy, neuroanatomy, comparative anatomy, modern imaging techniques, molecular biology, cell biology, embryology, morphological studies of veterinary discipline, and teaching anatomy. The journal is currently indexing and abstracting in TUBITAK ULAKBIM Turkish Medical Index, Proquest, EBSCO Host, Index Copernicus and Google Scholar.

Publication Ethics

Anatomy is committed to upholding the highest standards of publication ethics and observes the principles of Journal's Publication Ethics and Malpractice Statement which is based on the recommendations and guidelines for journal editors developed by the Committee on Publication Ethics (COPE), Council of Science Editors (CSE), World Association of Medical Editors (WAME) and International Committee of Medical Journal Editors (ICMJE). Fore detailed information please visit the online version of the journal which is available at www.anatomy.org.tr

Authorship

All persons designated as authors should have participated sufficiently in the work to take public responsibility for the content of the manuscript. Authorship credit should be based on substantial contributions to (1) conception and design or analysis and interpretation of data, (2) drafting of the manuscript or revising it for important intellectual content and, (3) final approval of the version to be published. The Editor may require the authors to justify assignment of authorship. In the case of collective authorship, the key persons responsible for the article should be identified and others contributing to the work should be recognized with proper acknowledgment.

Copyright

Publication Information

Anatomy (p-ISSN 1307-8798; e-ISSN 1308-8459) is published by Deomed Publishing, Istanbul, for the Turkish Society of Anatomy and Clinical Anatomy, TSACA. Due the Press Law of Turkish Republic dated as June 26, 2004 and numbered as 5187, this publication is classified as a periodical in English language.

Ownership
On behalf of the Turkish Society of Anatomy and Clinical Anatomy,
Ahmet Kağan Karabulut, MD, PhD; Konya

Responsible Managing Editor
Nihal Apaydın, MD, PhD; Ankara

Administrative Office
Güven Mah. Güvenlik Cad. Onlar Ap. 129/2 Aşağı Ayrancı, Ankara
Phone: +90 312 447 55 52-53

Publisher
Deomed Publishing
Gür Sok. No:7/B Kadıköy, İstanbul, Turkey
Phone: +90 216 414 83 43 (Pbx) / Fax: +90 216 414 83 42
www.deomed.com / e-mail: medya@deomed.com

deomed®

Submission of Manuscripts

Contributions should be submitted for publication under the following categories to:

Gülgün Şengül, MD
Editor-in-Chief, *Anatomy*

Department of Anatomy,
Faculty of Medicine, Ege University,
35100, Bornova, Izmir, Turkey
Phone: 0090 232 390 39 84
Fax: 0090 232 342 21 42
e-mail: gulgun.sengul@gmail.com; gulgun.sengul@ege.edu.tr

Categories of Articles

- ***Original Articles*** describe substantial original research that falls within the scope of the Journal.
- ***Teaching Anatomy*** section contains regular or all formats of papers which are relevant to comparing teaching models or to introducing novel techniques, including especially the own experiences of the authors.
- ***Reviews*** section highlights current development in relevant areas of anatomy. The reviews are generally invited; other prospective authors should consult with the Editor-in-Chief.
- ***Case Reports*** include new, noteworthy or unusual cases which could be of help for basic notions and clinical practice.
- ***Technical Note*** articles cover technical innovations and developments with a specific technique or procedure or a modification of an existing technique. They should be sectioned like an original research article but not exceed 2000 words.
- ***Viewpoint*** articles give opinions on controversial topics or future projections, some of these are invited.
- ***Historical View*** category presents overview articles about historical sections from all areas of anatomy.
- ***Terminology Zone*** category is a platform for the articles which discuss some terminological controversies or opinions.

The categories above are peer-reviewed. They should include abstract and keywords. There are also categories including Letters to the Editor, Book Reviews, Abstracts, Obituary, News and Announcements which do not require a peer review process.

For detailed instructions concerning the submission of manuscripts, please refer to the Instructions to Authors.

Subscription

Please send your order to Deomed Publishing, Gür Sok. No: 7/B Kadıköy, Istanbul, Turkey. e-mail: alikoz@deomed.com

- ***Annual rates:*** Institutional 100 EUR, Individual 50 EUR (include postage and local VAT). Supplements are not included in the subscription rates.

Membership of the Turkish Society of Anatomy and Clinical Anatomy, TSACA includes a reduced subscription rate to this journal.

- ***Change of address:*** Please send to the publisher at least six weeks in advance, including both old and new addresses.
- ***Cancellations:*** Subscription cancellations will not be accepted after the first issue has been mailed.

The online version of this journal is available at www.anatomy.org.tr

Advertising and Reprint Requests

Please direct to publisher. e-mail: medya@deomed.com

Printing and Binding

Yek Press, İstanbul, Turkey, Phone: +90 212 430 50 00
Printed in Turkey on acid-free paper (February 2019).

Editorial Board

www.anatomy.org.tr

anatomy
An International Journal of Experimental and Clinical Anatomy

anatomy
www.anatomy.org.tr
An International Journal of Experimental and Clinical Anatomy

Instructions to Authors

Anatomy, an international journal of experimental and clinical anatomy, is the official publication of the Turkish Society of Anatomy and Clinical Anatomy, TSACA. It is a peer-reviewed journal that publishes scientific articles in English. For a manuscript to be published in the journal, it should not be published previously in another journal or as full text in congress books and should be found relevant by the editorial board. Also, manuscripts submitted to Anatomy must not be under consideration by any other journal. Relevant manuscripts undergo conventional peer review procedure (at least three reviewers). For the publication of accepted manuscripts, author(s) should reveal to the Editor-in-Chief any conflict of interest and transfer the copyright to the Turkish Society of Anatomy and Clinical Anatomy, TSACA.

In the Materials and Methods section of the manuscripts where experimental studies on humans are presented, a statement that informed consent was obtained from each volunteer or patient after explanation of the procedures should be included. This section also should contain a statement that the investigation conforms with the principles outlined in the appropriate version of 1964 Declaration of Helsinki. For studies involving animals, all work must have been conducted according to applicable national and international guidelines. Prior approval must have been obtained for all protocols from the relevant author's institutional or other appropriate ethics committee, and the institution name and permit numbers must be provided at submission.

Anatomical terms used should comply with Terminologia Anatomica by FCAT (1998).

No publication cost is charged for the manuscripts but reprints and color printings are at authors' cost.

Preparation of manuscripts

During the preparation of the manuscripts, uniform requirements of the International Committee of Medical Journal Editors, a part of which is stated below, are valid (*see* ICMJE. Uniform requirements for manuscripts submitted to biomedical journals. Updated content is available at www.icmje.org). The manuscript should be typed double-spaced on one side of a 21x 29.7 cm (A4) blank sheet of paper. At the top, bottom and right and left sides of the pages a space of 2.5 cm should be left and all the pages should be numbered except for the title page.

Manuscripts should not exceed 15 pages (except for the title page). They must be accompanied by a cover letter signed by corresponding author and the Conflicts of Interest Disclosure Statement and Copyright Transfer Form signed by all authors. The contents of the manuscript (original articles and articles for Teaching Anatomy category) should include: 1- Title Page, 2- Abstract and Keywords, 3- Introduction, 4- Materials and Methods, 5- Results, 6- Discussion (Conclusion and/or Acknowledgement if necessary), 7- References

Title page

In all manuscripts the title of the manuscript should be written at the top and the full names and surnames and titles of the authors beneath. These should be followed with the affiliation of the author. Manuscripts with long titles are better accompanied underneath by a short version (maximum 80 characters) to be published as running head. In the title page the correspondence address and telephone, fax and e-mail should be written. At the bottom of this page, if present, funding sources supporting the work should be written with full names of all funding organizations and grant numbers. It should also be indicated in a separate line if the study has already been presented in a congress or likewise scientific meeting. Other information such as name and affiliation are not to be indicated in pages other than the title page.

Abstract

Abstract should be written after the title in 100–250 words. In original articles and articles prepared in IMRAD format for Teaching Anatomy category the abstract should be structured under sections Objectives, Methods, Results and Conclusion. Following the abstract at least 3 keywords should be added in alphabetical order separated by semicolumns.

References

Authors should provide direct references to original research sources. References should be numbered consecutively in square brackets, according to the order in which they are first mentioned in the manuscript. They should follow the standards detailed in the NLM's Citing Medicine, 2nd edition (Citing medicine: the NLM style guide for authors, editors, and publishers [Internet]. 2nd edition. Updated content is available at www.ncbi.nlm .nih.gov/books/NBK7256). The names of all contributing authors should be listed, and should be in the order they appear in the original reference. The author is responsible for the accuracy and completeness of references. When necessary, a copy of a referred article can be requested from the author. Journal names should be abbreviated as in *Index Medicus*. Examples of main reference types are shown below:

• **Journal articles:** Author's name(s), article title, journal title (abbreviated), year of publication, volume number, inclusive pages

– *Standard journal article:* Sargon MF, Celik HH, Aksit MD, Karaagaoglu E. Quantitative analysis of myelinated axons of corpus callosum in the human brain. Int J Neurosci 2007;117:749–55.

– *Journal article with indication article published electronically before print:* Sengul G, Fu Y, Yu Y, Paxinos G. Spinal cord projections to the cerebellum in the mouse. Brain Struct Funct Epub 2014 Jul 10. DOI 10.1007/s00429-014-0840-7.

• **Books:** Author's name(s), book title, place of publication, publisher, year of publication, total pages (entire book) or inclusive pages (contribution to a book or chapter in a book)

– *Entire book:*

- *Standard entire book:* Sengul G, Watson C, Tanaka I, Paxinos G. Atlas of the spinal cord of the rat, mouse, marmoset, rhesus and human. San Diego (CA): Academic Press Elsevier; 2013. 360 p.

- *Book with organization as author:* Federative Committee of Anatomical Terminology (FCAT). Terminologia anatomica. Stuttgart: Thieme; 1998. 292 p.

- *Citation to a book on the Internet:* Bergman RA, Afifi AK, Miyauchi R. Illustrated encyclopedia of human anatomic variation. Opus I: muscular system [Internet]. [Revised on March 24, 2015] Available from: http://www.anatomyatlases.org/AnatomicVariants/AnatomyHP.shtml

– *Contribution to a book:*

- *Standard reference to a contributed chapter:* Potten CS, Wilson JW. Development of epithelial stem cell concepts. In: Lanza R, Gearhart J, Blau H, Melton D, Moore M, Pedersen R, Thomson J, West M, editors. Handbook of stem cell. Vol. 2, Adult and fetal. Amsterdam: Elsevier; 2004. p. 1–11.

- *Contributed section with editors:* Johnson D, Ellis H, Collins P, editors. Pectoral girdle and upper limb. In: Standring S, editor. Gray's anatomy: the anatomical basis of clinical practice. 29th ed. Edinburgh (Scotland): Elsevier Churchill Livingstone; 2005. p. 799–942.

– *Chapter in a book:*

- *Standard chapter in a book:* Doyle JR, Botte MJ. Surgical anatomy of the hand and upper extremity. Philadelphia (PA): Lippincott Williams and Wilkins; 2003. Chapter 10, Hand, Part 1, Palmar hand; p. 532–641.

Illustrations and tables

Illustrations and tables should be numbered in different categories in the manuscript and Roman numbers should not to be used in numbering. Legends of the illustrations and tables should be added to the end of the manuscript as a separate page. Attention should be paid to the dimensions of the photographs to be proportional with 10x15 cm. Some abbreviations out of standards can be used in related illustrations and tables. In this case, abbreviation used should be explained in the legend. Figures and tables published previously can only be used when necessary for a comparison and only by giving reference after obtaining permission from the author(s) or the publisher (copyright holder).

Control list

- Length of the manuscript (max. 15 pages)
- Manuscript format (double space; one space before punctuation marks except for apostrophes)
- Title page (author names and affiliations; running head; correspondence)
- Abstract (100–250 words)
- Keywords (at least three)
- References (relevant to *Index Medicus)*
- Illustrations and tables (numbering; legends)
- Conflicts of Interest Disclosure Statement and Copyright Transfer Form
- Cover letter

Original Article

www.anatomy.org.tr
Received: November 12, 2018; Accepted: November 28, 2018
doi:10.2399/ana.18.026

anatomy
An International Journal of Experimental and Clinical Anatomy

Morphometry of the anterior interosseous nerve: a cadaveric study

Sibel Kibar[1,2], Burak Bilecenoğlu[1,3], Luis Filgueira[4], Aysun Uz[1,4,5]

[1]*Department of Anatomy School of Medicine, Ankara University, Ankara, Turkey*
[2]*Department of Physical Medicine and Rehabilitation, FizyoCare Medical Center, Ankara, Turkey*
[3]*Department of Anatomy, School of Dentistry, Ankara University, Ankara, Turkey*
[4]*Department of Medicine Anatomy, Faculty of Sciences, University of Fribourg, Fribourg, Switzerland*
[5]*Department of Neuroscience, Graduate School of Health Sciences, Ankara University, Ankara, Turkey*

Abstract

Objectives: Pathophysiology and etiology of anterior interosseous nerve (AIN) syndrome are still controversial. This anatomical dissection study aimed to understand the anatomy of AIN.

Methods: From a random sample of upper extremities of whole-body human cadavers (n=10), 20 upper extremities were included in the study. Two of the cadavers were females and 8 were males (age range 34–62 years). Specimens were dissected with the elbow in extension, wrist in neutral position and forearm in pronation. After superficial dissection, the pronator teres muscle was released, and the branching pattern of the AIN and the separation of the nerve from the interepicondylar line were recorded. The branches to the pronator teres, flexor pollicis longus, flexor digitorum profundus and flexor digitorum superficialis were recorded according to their distance from the interepicondylar line.

Results: The AIN branched from the main trunk 5.1 to 47.89 mm (mean 37.58±11.25 mm) distal to the interepicondylar line. AIN gave off 1–4 branches to the pronator teres. The first branch left the AIN 10.05–83.84 mm proximal and entered the muscle 23.49–43.72 mm distal to the interepicondylar line. AIN gave 1–4 branches to the flexor pollicis longus, flexor digitorum profundus and flexor digitorum superficialis at varying distances. The origin of the branches of AIN, as well as the innervation by one or multiple branches for a muscle, was variable.

Conclusion: This study provides a detailed map of the anterior interosseous nerve innervating flexor pollicis longus, flexor digitorum profundus and flexor digitorum superficialis muscles, to serve as a guide for location of AIN block in patients with upper extremity spasticity and AIN syndrome.

Keywords: anterior interosseous nerve; cadaver; morphometry

Anatomy 2018;12(3):111–114

Introduction

The anterior interosseous nerve syndrome (AINS) is a rare forearm nerve neuropathy. Compression of the nerve due to different anatomical variations such as Gantzer's muscle[1,2] and inflammation of the anterior interosseous nerve (AIN) are the prominent considerations for the etiology of AINS.[3,4] Previously, AINS has also been described as a clinical manifestation of neuralgic amyotrophy (Personage-Turner syndrome).)[5,6] Thickening of AIN and widespread muscle oedema at the distal third of the forearm, demonstrated by magnetic resonance imaging, also support the inflammatory pathophysiology.[3,4]

The patients can usually reach spontaneous recovery by conservative treatment methods in one year.[7] Before surgical treatment, they can be followed with conservative treatments such as injections, electrical stimulation and strengthening of the remaining muscles from 3 months to 1 year.[7–9] While a compressive lesion or a precise compression level are found by magnetic resonance imaging and electroneuromyography, corticosteroid or anesthetic injections can be applied to the injury level on the purpose of treatment or to diagnose the accurate surgery level. The corticosteroid and local anesthetic injections to the proximal side of the injury level of the nerve are effective treat-

ment options to relieve peripheral nerve neuropathy.[10] Infiltration of the pronator teres muscle with corticosteroids has been reported as an effective treatment method in patients with pronator teres syndrome.[11]

Ideal timing of surgery for AINS is controversial. Proper treatment depends on precise and accurate diagnosis.[9] Injection techniques to the AIN have been studied previously.[12,13] Diagnostic lidocaine AIN block can help to specify the spastic muscles for botulinum toxin injection to improve the contractures of interphalangal joints.[13] Most of the studies focused on the motor entry points of the median nerve branches to find the accurate localization of forearm botulinum toxin injections.[14,15] However, there are a few studies on the detailed morphology of the AIN.[16,17] The AIN arises from the posterior part of the median nerve in various forms.[17,18] Canova et al.[18] reported that the AIN of the forearm and its branches showed the least variability. Studies on the distribution of the AIN on the pronator teres muscle are controversial. Some reported the AIN arising between the ulnar and humeral heads of the pronator teres, and some more distally from the heads of the pronator teres. AIN has a branch to the flexor indicis profundus and innervates the flexor digitorum profundus of the middle finger and distally supplies the pronator quadratus muscle.[17]

Investigation of the morphological distribution of the AIN within the pronator teres muscle is important for the development of the proper injection techniques. AIN transfer has also become popular in recent years. Especially in proximal ulnar nerve injuries, reconstruction is usually performed transferring the distal branch of the AIN to the distal motor branch of the ulnar nerve.[8,19,20] Therefore, anatomical variations of the distal branches of the AIN are significant. The purpose of this cadaver study was to identify the trajectory and morphology of the AIN for augmenting its clinical applications.

Materials and Methods

Twenty upper extremities of 10 formalin fixed cadavers were dissected with Zeiss OPMI 9-FC surgical microscope (Carl Zeiss, Goettingen, Germany) starting from the middle third of the forearm to the wrist. Two of the cadavers were females and 8 were males (age: 34–62 years). All specimens were preserved by intra-arterial injection of 10% formalin solution, and dissected while the elbow was in extension, the wrist in neutral position and forearm in pronation. After dissection of the skin and the superficial fasciae of the flexor compartment, the pronator teres muscle was exposed and the location of the AIN was recorded with respect to this muscle. Thereafter, the pronator teres was released from its origin at the medial epicondyle (humeral portion) and the separation of the AIN was recorded as laterally, medially or posteriorly (towards the deep compartment). The distance of the nerve from the interepicondylar line was recorded in millimeters. Later, AIN branches to the flexor pollicis longus and the flexor digitorum superficialis muscles were recorded in relation to their distance from the interepicondylar line.

The cadavers used in our institution were unclaimed bodies which were delivered from Forensic Medicine according to the rules of Turkish legislation, studied according to the Helsinki protocol.

Results

The AIN separated from the main trunk posteriorly in 14 upper extremities, laterally in 5 upper extremities and medially in only 1 upper extremity (**Figures 1** and **2**). The AIN branched from the main trunk 5.1 to 47.89 mm (mean 37.58±11.25 mm) distal to the interepicondylar line.

The AIN separated from the main trunk of the median nerve before the level of the pronator teres (in the proximal 1/3 of the forearm) in 7 upper extremities and at the level of the pronator teres (in the middle 1/3 of the forearm) in 13 upper extremities (**Figures 1** and **2**), in accordance with the textbooks stating that the AIN separates usually within the pronator teres.

The AIN gave off 1–4 branches to the pronator teres. In 15 extremities, the AIN was giving a single branch to pronator teres. In 3 upper extremities, there were 2 branches, while there were 4 branches in two extremities. All the branches to the pronator teres branched from the AIN proximal to the interepicondylar line and entered the muscle distal to the interepicondylar line. In the extremities which the pronator teres had more than one branch, additional branches were highly variable, while we measured more consistent values for 15 extremities, including only 1 branch to the pronator teres (**Figure 2**). The first branch to the pronator teres parted from the AIN 10.05–83.84 proximal to interepicondylar line and entered the muscle 23.49–43.72 mm distal to the interepicondylar line. The AIN gave off 2–3 branches to the flexor pollicis longus and 1–3 branches to the radial part of the flexor digitorum profundus (**Figure 2**).

There were two branches from the AIN to the flexor pollicis longus in 14 extremities and three branches in 6 upper extremities. The first nerve to the flexor pollicis longus originated between 22.82–69.32 mm (mean 49.69± 18.52 mm) and terminated between 97.94–109.41 mm (mean 102.06±3.68 mm) from the interepicondylar line (**Figure 2**). The second nerve to the flexor pollicis longus originated 35.79 to 80.9 mm (mean 59.37±16.77 mm) and terminated between 89.26 to 121.04 mm (mean 109.6±

11.43 mm) from the interepicondylar line. Furthermore, if a third nerve to the flexor pollicis longus was present, it originated between 63.87 to 110.42 mm (mean 87.15± 32.92 mm) and terminated between 128.65 to 163.77 mm (mean 146.21±24.83 mm) from the interepicondylar line.

The branches to the flexor digitorum profundus muscle were similarly variable. The AIN gave 1 branch to the flexor digitorum profundus in four extremities, 2 branches in 10 upper extremities and 3 branches in six upper extremities. The first branch to the flexor digitorum profundus separated from the AIN between 53.15–69.79 mm (61.59± 7.11 mm) and terminated between 61.20–90.61 mm (78.79±10.61 mm) from the interepicondylar line. The second nerve to the flexor digitorum profundus originated between 69.32–114.05 mm (81.59±18.87 mm) and terminated between 87.72–161.94 mm (114.30±30.73 mm) from the interepicondylar line. If present, the third nerve to the flexor digitorum profundus originated between 111.62–116.57 mm (114.1±3.5 mm) and terminated between 134.8–139.12 mm (136.96±3.05 mm) from the interepicondylar line.

The AIN gave a single branch to the flexor digitorum superficialis in 14, and 2 branches in 6 upper extremities. The first branch to the flexor digitorum superficialis showed high variability, being separated from the AIN between 55.2 mm proximal to 35.16 mm distal to the interepicondylar line. The first branch to the flexor digitorum superficialis entered the muscle 47.54–78.65 mm, and the second branch 64.85–130.21 mm (85.96±23.05 mm) distal to the interepicondylar line, and terminated 159.86–161.05 mm (160.16±0.26 mm) distal to the epicondylar line (**Figure 2**).

After giving off these branches, the AIN reached the pronator quadratus muscle and terminated at the deep surface of this muscle, 174–187.69 mm and 178.6±2.65 mm distal to the interepicondylar line, respectively (**Figure 1**).

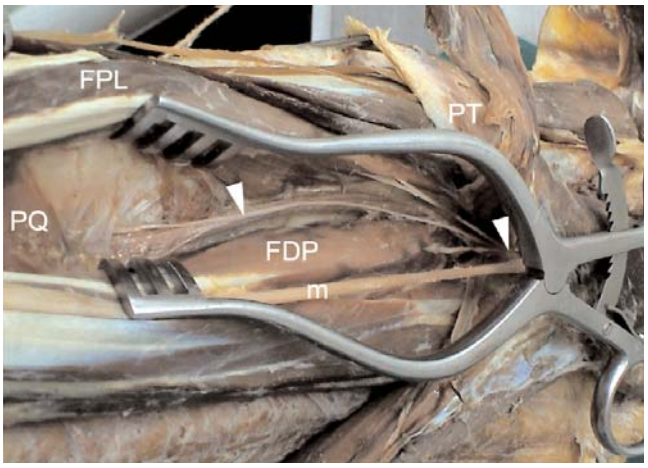

Figure 1. Course of the anterior interosseous nerve (AIN). **Arrowheads:** AIN; **FDP:** flexor digitorum profundus; **FPL:** flexor pollicis longus; **m:** median nerve; **PQ:** pronator quadratus; **PT:** pronator teres. [Color figure can be viewed in the online issue, which is available at www.anatomy.org.tr]

Discussion

This study aimed to reveal the anatomical location and branching of the AIN innervating the flexor digitorum profundus, flexor pollicis longus and pronator quadratus muscles. Additionally, we tried to expose other branches of the AIN to understand the precise distribution of the nerve on the forearm.

In contrast to previous published studies demonstrating that the AIN separates from the main trunk posteriorly, we found that it separated not only posteriorly, but also laterally from the main trunk in 5 (25%) upper extremities and medially in one upper extremity (5%).[16,21,22] The AIN separated from the main trunk 37.58 mm from the interepicondylar line. This measurement is close to the measurements of previous studies as 45 mm and 43 mm from the interepicondylar line.[16,21] The small standard deviation of our measurement (11.25 mm) signified a little variability in this location.

Vincelet et al.[16] reported that the AIN gave two branches to flexor pollicis longus and 72±15 mm distance to the interepicondylar level. However, Lepage et al.[15] demonstrated a single branch to the flexor pollicis longus. We observed that the AIN usually gave off 2 branches to the flexor pollicis longus, and the number of the branches was 2 or 3. The level of the separation of the nerves and the level of the entry to the muscle were different from

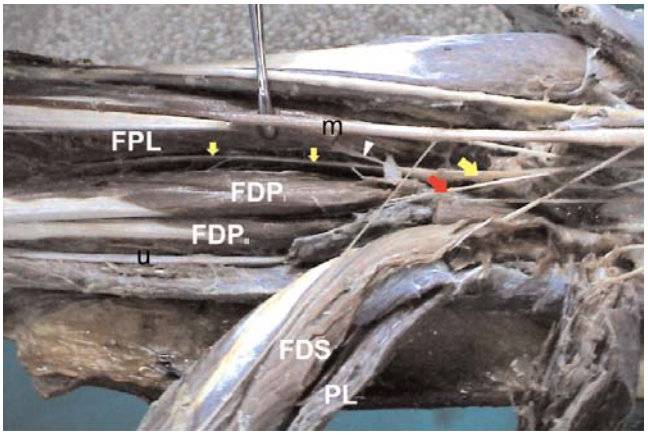

Figure 2. Branches of the anterior interosseous nerve (AIN). **FDP:** flexor digitorum profundus; **FDS:** flexor digitorum superficialis; **FPL:** flexor pollicis longus; **m:** median nerve; **PL:** palmaris longus; **u:** ulnar nerve; **yellow arrows:** AIN; **red arrow:** nerve to FDP; **arrowhead:** nerve to FPL. [Color figure can be viewed in the online issue, which is available at www.anatomy.org.tr]

each other. Nevertheless, a significant relationship was not found between these values. In this study, the flexor pollicis longus branches separated from the main trunk 22.82–110.42 mm distal to the interepicondylar line. We demonstrated more variability for the flexor pollicis longus branches compared to other studies.[16,21] The AIN gave off 1–3 branches to the flexor digitorum profundus, similar with the previous studies.[16,21]

Conclusion

In this study, we showed that the origin of the branches of the AIN, as well as the innervation by one or multiple branches for a muscle, was highly variable. However, the level of the origin of the AIN was less variable compared to other branches of the median nerve. Therefore, we conclude that the anterior interosseal nerve is probably the best option for free muscle transfer to restore flexion of fingers. By knowing the exact location of the AIN, the surgical operations in this area will be safer, particularly for nerve transfer. This study also provided a detailed map of the AIN innervating the flexor pollicis longus, the flexor digitorum profundus and the pronator quadratus, to serve as a guide for the location of the proper nerve block in patients with upper extremity spasticity and AINS.

References

1. Bilecenoğlu B, Uz A, Karalezli N. Possible anatomic structures causing entrapment neuropathies of the median nerve: an anatomic study. Acta Orthop Belg 2005;71:169–76.
2. Roy J, Henry BM, Pekala PA, Vikse J, Ramakrishnan PK, Walocha JA, Tomaszewski KA. The prevalence and anatomical characteristics of the accessory head of the flexor pollicis longus muscle: a meta-analysis. Peer J 2015;3:e1255.
3. Maldonado AA, Amrami KK, Mauermann ML, Spinner RJ. Reinterpretation of electrodiagnostic studies and magnetic resonance imaging scans in patients with nontraumatic "isolated" anterior interosseous nerve palsy. Plast Reconstr Surg 2016;138:1033–9.
4. Dunn AJ, Salonen DC, Anastakis DJ. MR imaging findings of anterior interosseous nerve lesions. Skeletal Radiol 2007;36:1155–62.
5. Gaitzsch G, Chamay A. Paralytic brachial neuritis or Parsonage-Turner syndrome anterior interosseous nerve involvement. Report of three cases. Ann Chir Main 1986;5:288–94.
6. Rennels GD, Ochoa J. Neuralgic amyotrophy manifesting as anterior interosseous nerve palsy. Muscle Nerve 1980;3:160–4.
7. Rodner CM, Tinsley BA, O'Malley MP. Pronator syndrome and anterior interosseous nerve syndrome. J Am Acad Orthop Surg 2013;21:268–75.
8. Lubahn JD, Cermak MB. Uncommon nerve compression syndromes of the upper extremity. J Am Acad Orthop Surg 1998;6:378–86.
9. Alexandre A, Alexandre AM, Zalaffi A. Considerations on the treatment of anterior interosseous nerve syndrome. Acta Neurochir Suppl 2011;108:247–50.
10. Eker HE, Cok OY, Aribogan A, Arslan G. Management of neuropathic pain with methylprednisolone at the site of nerve injury. Pain Med 2012;13:443–51.
11. Morris HH, Peters BH. Pronator syndrome: clinical and electrophysiological features in seven cases. J Neurol Neurosurg Psychiatry 1976;39:461–4.
12. Grutter PW, Desilva GL, Meehan RE, Desilva SP. The accuracy of distal posterior interosseous and anterior interosseous nerve injection. J Hand Surg Am 2004;29:865–70.
13. Alfaro A. Anterior interosseous nerve blocks to treat finger flexor muscle spasticity. Muscle Nerve 2012;46:645.
14. Yang F, Zhang X, Xie X, Yang S, Xu Y, Xie P. Intramuscular nerve distribution patterns of anterior forearm muscles in children: a guide for botulinum toxin injection. Am J Transl Res 2016;8:5485–93.
15. Lepage D, Parratte B, Tatu L, Vuiller F, Monnier G. Extra- and intramuscular nerve supply of the muscles of the anterior antebrachial compartment: applications for selective neurotomy and for botulinum toxin injection. Surg Radiol Anat 2005;27:420–30.
16. Vincelet Y, Journeau P, Popkov D, Haumont T, Lascombes P. The anatomical basis for anterior interosseous nerve palsy secondary to supracondylar humerus fractures in children. Orthop Traumatol Surg Res 2013;99:543–7.
17. Caetano EB, Vieira LA, Sabongi Neto JJ, Caetano MBF, Sabongi RG. Anterior interosseous nerve: anatomical study and clinical implications. Rev Bras Ortop 2018;53:575–81.
18. Canovas F, Mouilleron P, Bonnel F. Biometry of the muscular branches of the median nerve to the forearm. Clin Anat 1998;11:239–45.
19. Bilecenoglu B, Uz A, Karalezli N, Issi S. Two anatomic variations in the arm related to the median nerve. Saudi Med J 2005;26:1827–8.
20. McNamara B. Clinical anatomy of median nerve. Advances in Clinical Neuroscience and Rehabilitation 2003;2:19-20.
21. Canovas F, Mouilleron P, Bonnel F. Biometry of the muscular branches of the median nerve to the forearm. Clin Anat 1998;11:239–45.
22. Sunderland S. The intraneural topography of the radial, median and ulnar nerves. Brain 1945;68:243–99.

Online available at:
www.anatomy.org.tr
doi:10.2399/ana.18.026
QR code:

Correspondence to: Sibel Kibar, MD, PhD
Alacaatlı Cad., 2587 Sok., No: 7, Çayyolu,
Çankaya 06580 Ankara, Turkey
Phone: +90 505 688 87 24
e-mail: sibelkbr@gmail.com

Conflict of interest statement: No conflicts declared.

Original Article

www.anatomy.org.tr
Received: May 10, 2018; Accepted: September 14, 2018
doi:10.2399/ana.18.034

anatomy
An International Journal of Experimental and Clinical Anatomy

Gross anatomical investigation of the posterolateral aspect of the forearm for ulnar nerve block in Black Bengal goat *(Capra hircus)*

Tuli Dey[1], Sonnet Poddar[2], Abdullah Al Faruq[2], Jabin Sultana[3], Salma Akter[4]

[1]*Department of Medicine and Surgery, Chittagong Veterinary and Animal Sciences University, Khulshi, Chittagong, Bangladesh*
[2]*Department of Anatomy and Histology, Chittagong Veterinary and Animal Sciences University, Khulshi, Chittagong, Bangladesh*
[3]*Department of Physiology, Biochemistry and Pharmacology, Chittagong Veterinary and Animal Sciences University, Khulshi, Chittagong, Bangladesh*
[4]*Department of Medicine, Surgery and Obstetrics, Hajee Mohammad Danesh Science and Technology University, Dinajpur, Bangladesh*

Abstract

Objectives: The aim of this study was to investigate the gross anatomical features of the ulna and radius bones on the posterolateral aspect of the forearm in Black Bengal goat *(Capra hircus)* to determine the site for ulnar nerve block.

Methods: 15 radius and ulna bones of Black Bengal goats from three different age groups (Group A: 1–2 years; Group B: 2–3 years; Group C: >3 years) were studied. Measurements of the length between the olecranon tuberosity and styloid process on the posterolateral aspect of radius and ulna bones were made, and the mean midpoints on this line were determined.

Results: Ulna was always fused with the radius except on the posterolateral interosseous spaces at the proximal and distal ends. The ulnar nerve coursed posterior to the ulna, between the flexor carpi ulnaris and ulnaris lateralis muscles, and remained superficial at the midpoint of ulna. Mean lengths of the midpoint on the posterolateral aspect of the ulna (on the line between the olecranon tuberosity to the styloid process) were 7.27±0.16, 7.67±0.34 and 8.29±0.73 cm in Groups A, B and C, respectively.

Conclusion: These anatomical findings indicate that these mean midpoints are the most convenient sites for ulnar nerve block in these three age groups of Black Bengal goats.

Keywords: blocking site; forearm; gross anatomy; ulnar nerve; Black Bengal goat

Anatomy 2018;12(3):115–117

Introduction

The forearm of Black Bengal goat *(Capra hircus)* consists of two large bones named radius and ulna. It extends in a vertical direction from elbow joint.[1,2] Radius is much larger, but not longer than the ulna bone. The posterior surface of the radius bone is concave and fused with the cranial surface of the shaft of ulna bone except for the two interosseous spaces situated at the proximal and distal ends of the bone.[1,3] Proximal part of the ulna bears the olecranon tuberosity and the trochlear notch. The caudal border of the ulna is straight, thick and rounded. Styloid process is a pointed projection of the distal end of ulna which faces the posterolateral aspect of the radius. The ulnar nerve courses along the posterior border of the ulna.[1,4] Block of the ulnar nerve for surgical purposes can be performed at various levels along its course in the forearm region. There are very few studies performed for determination of the site of ulnar nerve block.[4,5] Therefore, this study was planned to to determine the site for ulnar nerve block in Black Bengal goats with gross anatomical investigation of the posterolateral aspect of the forearm.

Materials and Methods

The study was conducted on the forearm of Black Bengal goats between March 2 and May 10, 2016. Fifteen forearms from different aged groups of Black Bengal goats were collected from the local market, Khulshi, Chittagong, Bangladesh. The bones were graved for 2 months, excavated out and processed as described by

Gofur and Khan (2010).[6] The radius and ulna bones of Black Bengal goats were divided into three groups according to their age. Group A: between 1–2 years Group B: between 2–3 years, and Group C: older than 3 years. Gross anatomical investigation of the posterolateral aspect of the forearm was performed at the Department of Anatomy and Histology, Chittagong Veterinary and Animal Sciences University (CVASU), Khulshi, Chittagong, Bangladesh.

Gross anatomical investigation of the radius and ulna bones from Groups A, B and C were made at their posterolateral aspects. Measurements of the length between the olecranon tuberosity and styloid process on the posterolateral aspect of radius and ulna bones were made, and the mean midpoints on this line were determined. After this, the most suitable site for ulnar nerve block was determined.

Results

The body of thw radius bone was flattened craniocaudally. The ulna was longer and fused with radius along its posterolateral aspect, except at the proximal and distal interosseous spaces (**Figure 1**). Proximal end of the ulna was expanded with a rough prominence called the olecranon tuberosity. On the distal end, there was a pointed projection named the styloid process of the ulna. The mean midpoint on the line between the olecranon tuberosity and the styloid process were 7.27±0.16, 7.67±0.34 and 8.29±0.73 cm in Groups A, B and C, respectively (**Table 1**). At the forearm region, the ulnar nerve coursed poste-

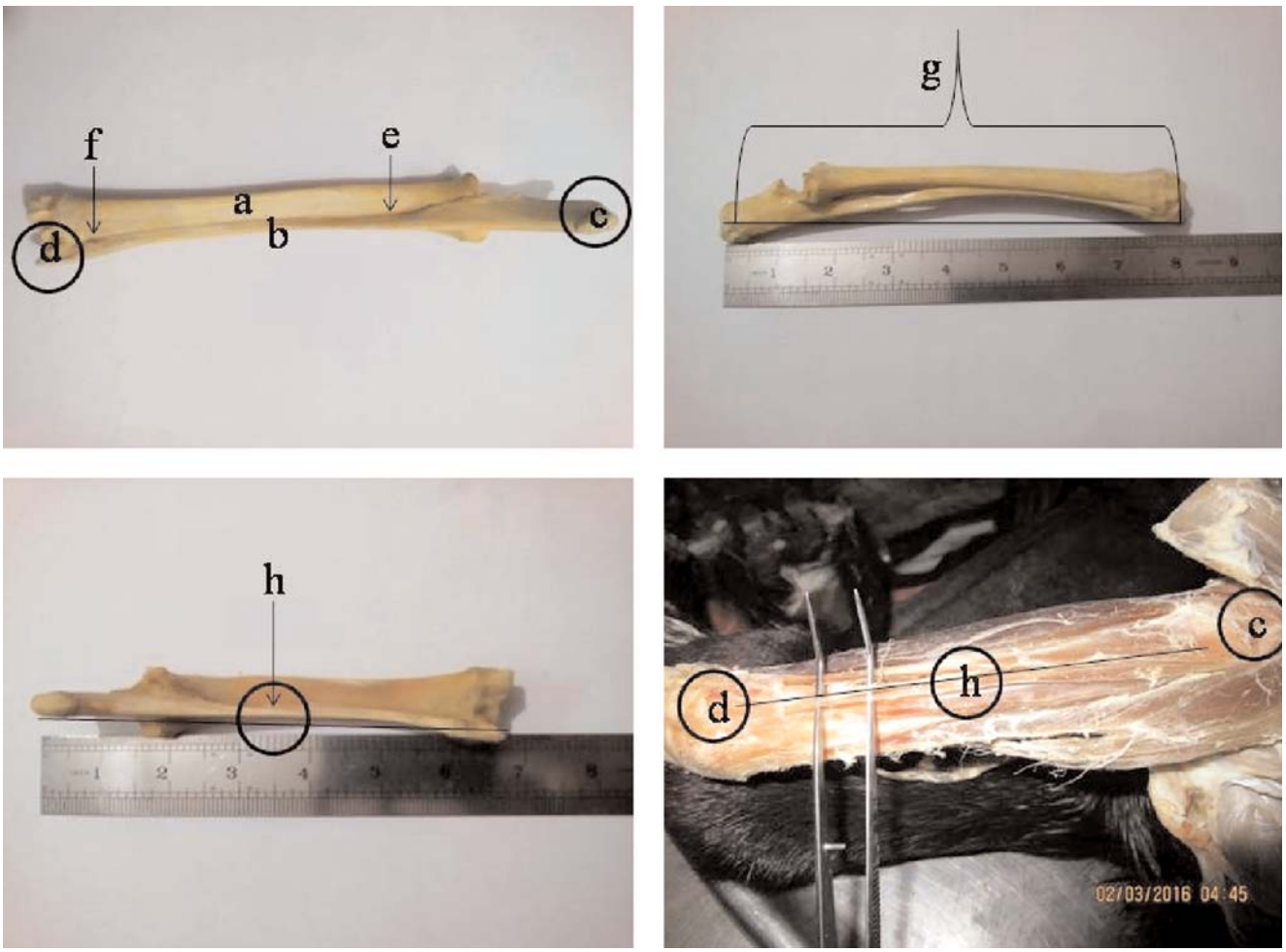

Figure 1. Radius and ulna bones, and the midpoint on the line between the olecranon tuberosity and the styloid process for ulnar nerve block. **a**: radius; **b**: ulna; **c**: olecranon tuberosity; **d**: styloid process; **e**: proximal interosseous space; **f**: distal interosseous space; **g**: total length along olecranon tuberosity to styloid process; **h**: midpoint on the line between the olecranon tuberosity and the styloid process. [Color figure can be viewed in the online issue, which is available at www.anatomy.org.tr]

Table 1
Length between the olecranon tuberosity to styloid process of ulna (posterolateral aspect) in different aged groups of Black Bengal goats (Mean±SD).

Age groups	Number of bones	Mean length between OT and SP	Mean midpoint distance (cm)
Group A: 1–2 years	5	14.53±0.16	7.27±0.16
Group B: 2–3 years	6	15.33±0.34	7.67±0.34
Group C: >3 years	4	16.58±0.73	8.29±0.73

rior to the ulna and passed between the flexor carpi ulnaris and ulnaris lateralis muscles.

Discussion

In this study, we found that the ulna bone was fused with the radius along its posterolateral aspect except for the proximal and distal interosseous spaces, similar with the findings of Getty,[1] Mahmud and Mussa,[7] and Siddiqui et al.[8] The olecranon tuberosity and styloid process of the ulna was observed in every bone, similar with the findings of Ghosh,[2] Neil and May,[3] and Siddiqui et al.[8] The mean midpoint length along the olecranon tuberosity and styloid process were 7.27±0.16, 7.67±0.34 and 8.29±0.73 cm in Groups A, B and C age group Black Bengal goats, respectively. At the midpoint of the forearm, the ulnar nerve courses more superficially to pass between the flexor carpi ulnaris and ulnaris lateralis muscles.[1,4] So, the midpoint of the the distance between the olecranon tuberosity and the styloid process of ulna on the posterolateral aspect was the most convenient site for ulnar nerve block Black Bengal goats (**Figure 1**).

Conclusion

Gross anatomical investigation of the radius and ulna revealed that the ulna is fused with radius on its posterolateral aspect. For surgical purposes, ulnar nerve block can be performed at various levels along its the course in the forearm region, but is more convent at the midpoint of the line between the olecranon tuberosity and the styloid process of the ulna on its posterolateral aspect.

References

1. Getty R. Session and Grossman's the anatomy of the domestic animals. 2nd ed. Vol. 1. Philadelphia (PA): W.B. Saunders; 1975.
2. Ghosh RK. Primary veterinary anatomy. 5th ed. Kolkata: Current Books International; 2012.
3. May NDS. Anatomy of the sheep. 2nd ed. Brisbane: University of Queenesland Press; 1964.
4. Skarda RT, Tranquilli WJ. Local anesthetics. In: Tranquilli WJ, Thurmon JC, Grimm KA, editors. Lumb and Jone' veterinary anesthesia and analgesia. 4th ed. Ames (IA): Blackwell Publishing; 2007. p. 395–418.
5. Ghadirian S, Vesal N. Brachial plexus block using lidocaine/epinephrine or lidocaine/xylazine in fat-tailed sheep. Vet Res Forum 2013;4:161–7.
6. Gofur MR, Khan MSI. Development of a quick, economic and efficient method for preparation of skeleton of small animals and birds. International Journal of BioResearch 2010;2:13–7.
7. Mahmud AA, Mussa, T. Comparative macro anatomy of forelimb bones of Black Bengal Goat and indigenous dog: an overview. American Journal of Agricultural Science Engineering and Technology 2016;3:1–10.
8. Siddiqui MSI, Khan MZI, Sarma M, Moonmoon S, Islam MN, Jahan MR. Macro-anatomy of the bones of the limb of Black Bengal goat *(Capra hircus)*. Bangladesh Journal of Veterinary Medicine 2008;6: 59–66.

Online available at:
www.anatomy.org.tr
doi:10.2399/ana.18.034
QR code:

Correspondence to: Sonnet Poddar, DVM, MS
Department of Anatomy and Histology, Chittagong Veterinary and Animal Sciences University, Khulshi, Chittagong, Bangladesh
Phone: +8801721429218
e-mail: sonnetcvasu@gmail.com

Conflict of interest statement: No conflicts declared.

anatomy
www.anatomy.org.tr
An International Journal of Experimental and Clinical Anatomy

Original Article

www.anatomy.org.tr
Received: October 20, 2018; Accepted: November 24, 2018
doi:10.2399/ana.18.074

Alpha-lipoic acid attenuates iron overload-induced structural changes in the liver of the laboratory mouse *(Mus musculus)*

William O. Sibuor, Fidel O. Gwala, Jeremiah K. Munguti, Moses M. Obimbo

Department of Human Anatomy, School of Medicine, University of Nairobi, Nairobi, Kenya

Abstract

Objectives: The role of alpha-lipoic acid in the amelioration of iron overload-induced hepatic damage remains largely under-explored. Therefore, this paper aimed at describing the structural effects of alpha-lipoic acid on the liver following iron overload in mice.

Methods: After ethical approval, a total of 24 male mice were used. Twenty mice were randomly divided into two groups: A and B. Group A rats received 50 mg/kg of iron dextran intraperitoneally daily for 49 days, while those in Group B received a daily oral dose of 100 mg/kg alpha-lipoic acid by gavage in addition to the treatment in Group A. Four mice were used as normal controls. At the endpoint of the experiment, the livers were harvested and studied for iron deposition, parenchymal histoarchitecture and hepatocyte densities. Photomicrographs were taken using a digital photomicroscope for morphometric analysis.

Results: Treatment of mice with iron led to a distortion of the histoarchitecture of the liver which was attenuated with co-administration of alpha-lipoic acid. Additionally, co-treatment of iron with alpha-lipoic acid resulted in significant lowering of hepatic iron deposition ($p<0.001$), reduction in leukocyte infiltration and significantly greater hepatocyte densities ($p<0.001$).

Conclusion: Alpha-lipoic acid considerably attenuates the structural damage in the liver induced by iron overload.

Keywords: alpha-lipoic acid; iron; liver

Anatomy 2018;12(3):118–123

Introduction

Iron overload is a common clinical problem that occurs in conditions such as hereditary hemochromatosis and transfusion dependent anaemia including sickle cell disease and beta thalassemia.[1,2] Since the liver is the main storage site for iron, it is among the key organs to be adversely affected by iron overload toxicity resulting in hepatic fibrosis and hepatocellular necrosis.[3,4]

Currently, management of iron overload involves iron chelation therapy and phlebotomy. These modalities however, have several limitations including high cost, patient incompliance and numerous associated side effects.[5–7] Furthermore, phlebotomy is contraindicated in anaemic patients.[8] Thus, there is need for better avenues to augment the management of iron overload.

Alpha-lipoic acid (ALA) is a widely available cheap but potent antioxidant. It has lately been in use in the management of diabetic polyneuropathies where it scavenges reactive oxygen species (ROS) produced as a result of glucose auto-oxidation induced by hyperglycemia.[9] A few studies have documented the possible iron chelating properties of ALA. For instance, Goralska et al.[10] showed that treating isolated cultured lens epithelial cells with ALA significantly lowered the size of the free intracellular iron. In another study by Suh et al.,[11] feeding ALA to aged rats for 2 weeks showed a reversal of the age-related accumulation of iron in the cerebral cortex. However, these studies were conducted under conditions of normal body iron levels. Hitherto, there are hardly any studies that have investigated the effects of ALA on the liver following iron overload. This study therefore

aimed to describe the structural effects of ALA on the liver of the mouse following iron overload.

Materials and Methods

ALA was supplied by Nature's Bounty, Inc. (Bohemia, NY, USA) while iron dextran (Dawafer) was supplied by Chongqing Fangtong for Dawa Limited (Kenya). The injections were administered using 30 gauge (BD Micro-Fine™ Plus; Becton Dickinson and Co., Franklin Lakes, NJ, USA) insulin syringes and a gavage tube for mice was used for oral drug administration.

A total of 24 male 8 week old mice *(Mus musculus)* were purchased from The Department of Zoology, University of Nairobi, Kenya. Ethical approval to conduct the study was obtained from the Animal Use and Ethics Committee, Faculty of Veterinary Medicine, University of Nairobi, Kenya. The handling and care of the animals were in accordance with the guidelines provided by the same committee.

Four mice were randomly selected for use as normal controls. One of the 4 mice selected as controls was used to show the baseline histomorphology of the liver. The remaining 20 mice were then randomly divided into two equal groups: A and B. Group A received a daily intraperitoneal (i.p.) injection of 50 mg/kg/day of iron dextran followed by daily oral gavage of 0.3 ml of normal saline, while Group B received a daily i.p. injection of 50 mg/kg/day iron dextran followed by daily oral gavage of 100 mg/kg/day of ALA. The normal control mice were given a daily i.p. normal saline (30 µl) followed by daily oral gavage of 0.3 ml normal saline. The dose of iron dextran used was based on the study by Zhang et al.,[12] while that of ALA was based on the studies by Budin et al.[13] and Ahmadvand and Jamor.[14] Three mice from each group were sacrificed at day 16 and 32 of the experiment while the remaining 4 in each group were sacrificed at day 49.

The livers were harvested *en masse* and stored in 10% formalin. Independent uniform random sampling, as described by Marcos et al.,[15] was used to select 5 random fragments from each liver for histological processing and staining with haematoxylin and eosin.

Photomicrographs of the stained sections were taken using a 12 mega pixel Canon camera mounted on a photomicroscope.

Estimation of iron deposition was done using the Cavalieri principle of point counting[16] and data expressed as volumetric densities (%). Following the technique described by Gundersen et al.[17] and Bancroft and Cook,[18] the selected histological areas were analysed using a superimposed 80-point grid on the digital images on a monitor screen using ImageJ software (National Institutes of Health, Bethesda, MD, USA) (**Figure 1**).

Hepatocyte density estimation was done using the Cavalieri's principle of point counting.[16] Using the Image J software, grid squares were superimposed on the images then the cells within a square and those crossed by the inclusion line were counted (**Figure 2**).

Quantitative data on volumetric densities of iron deposits and hepatocyte densities was entered into the Statistical Package for Social Sciences (SPSS for Windows, version 21.0; SPSS Inc., Chicago, IL, USA) for analysis. Cell densities were expressed in mm2 while iron deposition was expressed as a percentage. Kruskal-Wallis H test was used to compare medians of the quantitative data across the various harvesting periods within each group while Mann-Whitney U test was used to compare the medians between Group A and B. A p value ≤0.05 was considered significant at 95% confidence interval. Data are presented in photomicrographs and graphs.

Results

Iron treatment resulted in a progressive increase in the volumetric densities of the iron deposits from 6.4% at day 16 to 12.03% and 27.26% at days 32 and 49, respectively ($p<0.001$). Co-administration of iron with ALA resulted in

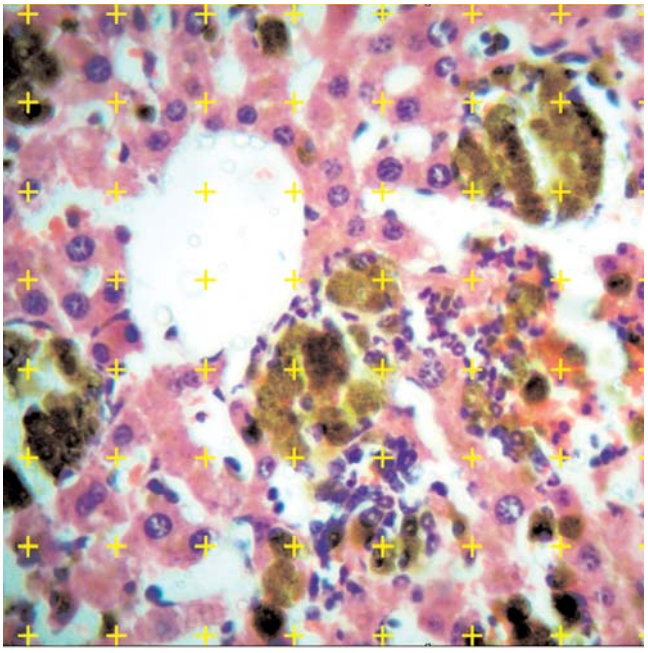

Figure 1. The point counting method to estimate the volumetric density of the iron deposits. The volume densities of the iron deposits were calculated by the formula Vv = Pp/Pt, where Vv is the volume density, p is the component under consideration (iron deposits), Pp is the number of test points associated with p, and Pt is the total number of points of the test system. [Color figure can be viewed in the online issue, which is available at www.anatomy.org.tr]

significantly lower volumetric densities across all the harvesting periods ($p<0.001$). The percentages in the ALA group were 3.76%, 7.52% and 15.79% at day 16, 32 and 49, respectively (**Figure 3**).

Iron treatment resulted in distortion of the normal hepatic histoarchitecture proportional to the duration of treatment. There was marked degeneration of hepatocytes with distortion of the hepatocyte cords. The nuclei of hepatocytes were enlarged and showed fragmented nucleoli. There was also infiltration of deeply basophilic leukocytes around several clusters of large iron deposits.

ALA co-administration resulted in a reduction of the magnitude of the iron overload induced histoarchitectural changes as evidenced by the reduction in the sizes and area of the iron deposits. The cord like arrangement of the hepatocytes was also preserved with discernible boundaries between cells in adjacent cords. The nuclei of hepatocytes showed less enlargement and fragmentation. The leukocyte infiltrates were also reduced (**Figure 4 a–f**).

Iron treatment resulted in a progressive decline in the hepatocyte densities from 1433.33/mm^2 at day 16 to 1383.33 and 689.89/mm^2 at day 32 and 49 respectively ($p<0.001$). Time matched mice treated with iron and ALA showed higher hepatocyte densities compared with the mice treated with iron alone ($p<0.001$). The densities for the mice treated with iron and ALA were 1572.22, 1583.33 and 1055.56/mm^2 at day 16, 32 and 49 respectively (**Figure 5**).

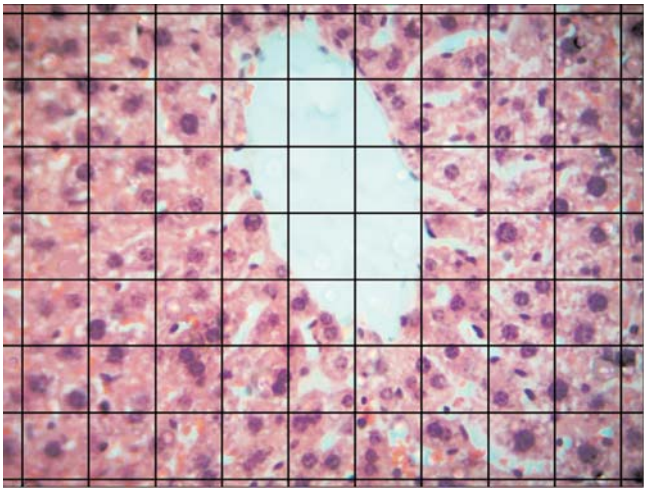

Figure 2. The grids used in the determination of hepatocyte densities. The unit area for each grid square was 0.0018 mm^2. Every second square on the grid was selected for cell counting and a total of 12 grid squares per field were considered. The average cellular count/mm^2 of the 12 unit areas was then used as the cell density. [Color figure can be viewed in the online issue, which is available at www.anatomy.org.tr]

Discussion

ALA reduced the hepatic iron deposition in a manner similar to previous studies using related compounds. For instance, Gao et al.[19] reported a reduction in iron deposition on the mouse liver using danshen, an antioxidant compound. The reduction in iron deposition with ALA treatment could be attributed to its iron chelating properties.[20] This is a similar mechanism to that of deferoxamine and deferipone, known iron chelators that have been shown to reduce hepatic iron deposition in mice liver following iron overload.[21] The dithiolane ring in the chemical structure of ALA confers its ability to bind redox active elements such as iron.[20,22] Since generation of ROS directly correlates with the concentration of free intracellular iron,[23] administration of ALA to iron overload patients could help chelate this free intracellular iron and thus reduce ROS generation and hepatic damage.

ALA treatment, as with other interventions reported elsewhere, resulted in a reduction in the parenchymal damage seen with iron overload. Hazra et al.[24] noted that a flavonoid compound, Katha, was protective against iron overload induced liver damage, while Sarkar et al.[25] studied the effects of *Emblica officinalis*, an antioxidant, on the mouse liver following iron overload, and also noted an improvement in the histoarchitecture compared with iron treatment alone. The reduction in parenchymal damage may be attributed to the antioxidant capacity of ALA which makes it able to scavenge ROS produced during iron overload.[26] Systemic ALA has been shown to be protective against light induced oxidative retinal damage, supporting its protective effects against oxidative damage.[27] This is further supported by

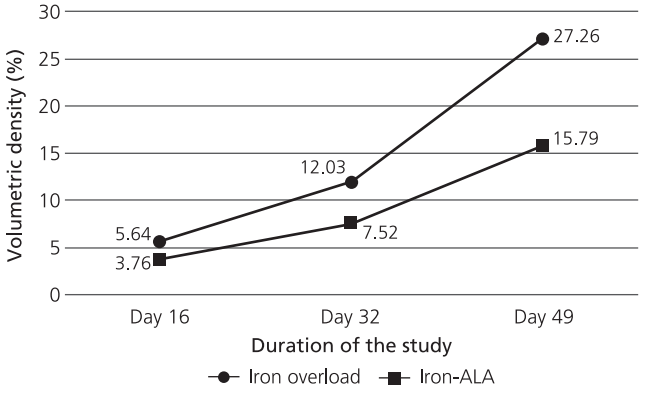

Figure 3. Line graph showing the volumetric densities of the iron deposits in the mouse liver tissue.

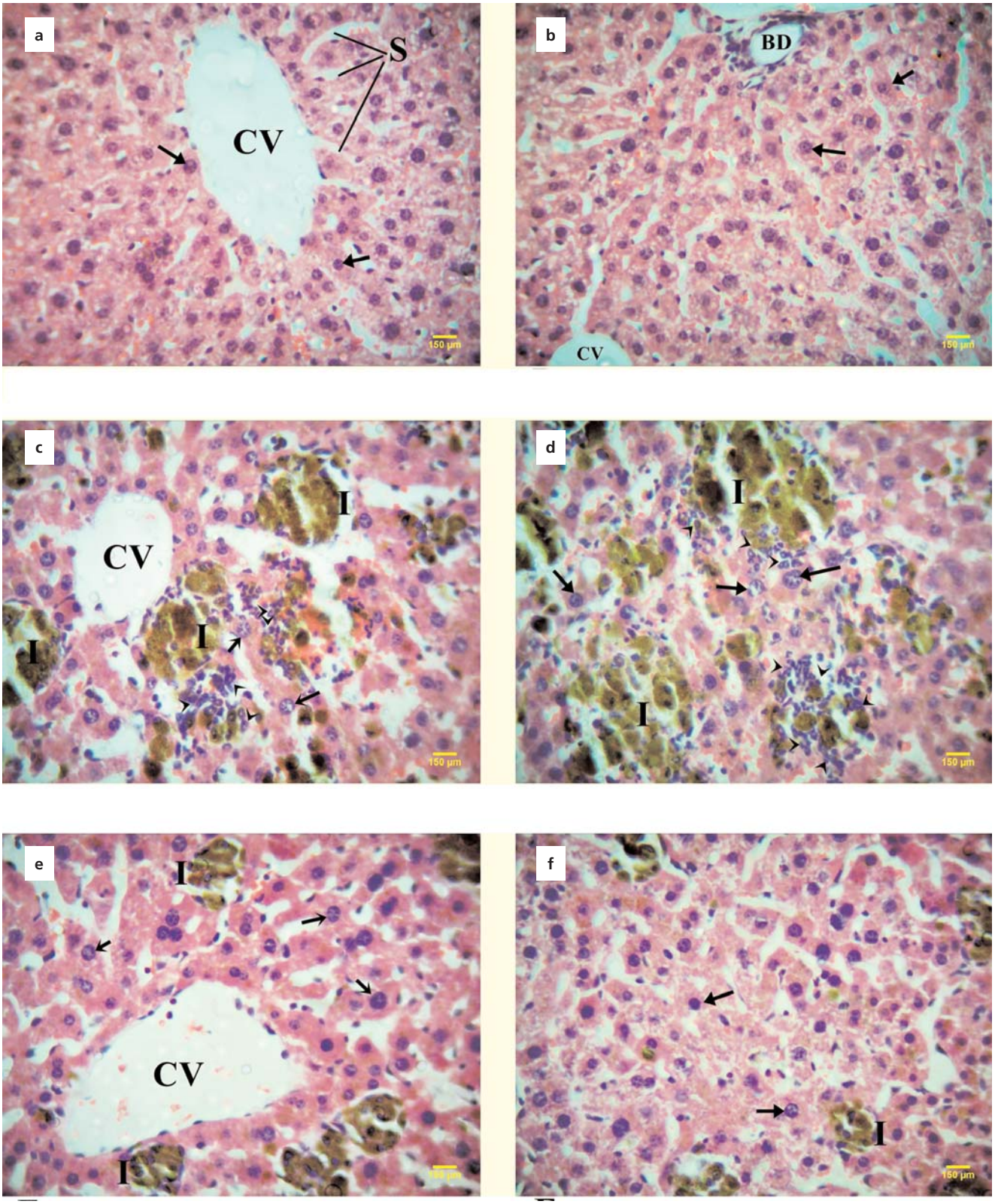

Figure 4. (**a**–**f**) Figure showing the histo-morphological changes in the livers of the control and experimental mice; (**a**, **b**) Liver of a normal control mouse; (**c**, **d**) Liver of a mouse treated with iron dextran for 49 days; (**e**, **f**) liver of a mouse treated with iron and ALA for 49 days. **BD:** bile duct; **CV:** central vein; **I:** iron deposits; **S:** sinusoids; **arrows:** hepatocyte nuclei; **arrowheads:** leukocyte infiltrates. Scale bar=150 µm. [Color figure can be viewed in the online issue, which is available at www.anatomy.org.tr]

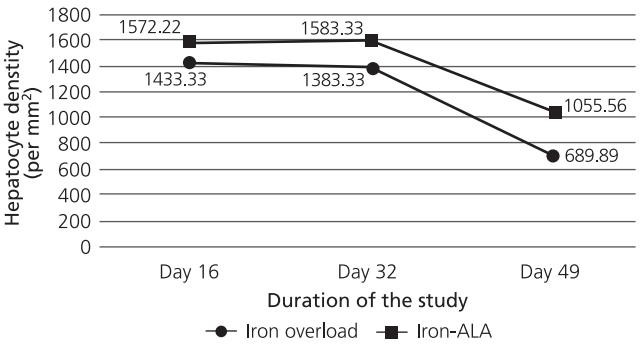

Figure 5. Line graph depicting the changes in hepatocyte densities in the mouse liver tissue.

the works of Rezk and Abdel-Rahman,[28] who found ALA to be protective against lead and gamma-irradiation induced oxidative damage to the lungs and kidneys of albino rats. Additionally, it is postulated that ALA has the ability to regenerate other endogenous antioxidants such as Vitamin C, E and glutathione.[29–31] For instance, biosynthesis of glutathione requires cysteine, an amino acid which is enhanced by ALA through the acceleration of the conversion of cystine to cysteine.[30]

Previous studies have shown that iron overload induced hepatocellular damage causes hepatic dysfunction which is alleviated by application of deferoxamine, an iron chelator.[19,32] Due to its potential iron chelating and antioxidant property, ALA could therefore be used to prevent hepatic cellular damage and subsequent dysfunction in iron overload conditions.

Conclusion

ALA considerably attenuates the structural damage in the liver induced by iron overload. We recommend further clinical studies to investigate the possible utility of ALA in the management of iron overload patients.

References

1. Hentze MW, Muckenthaler MU, Galy B, Camaschella C. Two to tango: regulation of mammalian iron metabolism. Cell 2010;142:24–38.
2. Siddique A, Kowdley KV. Review article: the iron overload syndromes. Aliment Pharmacol Ther 2012;35:876–93.
3. Kohgo Y, Ikuta K, Ohtake T, Torimoto Y, Kato J. Body iron metabolism and pathophysiology of iron overload. Int J Hematol 2008;88:7–15.
4. Hershko C. Iron chelation therapy. New York (NY): Springer; 2012. 28–36.
5. Sheth S. Iron chelation: an update. Curr Opin Hematol 2014;21: 179–85.
6. Brissot P. Optimizing the diagnosis and the treatment of iron overload diseases. Expert Rev Gastroenterol Hepatol 2016;10:359–70.
7. Mobarra N, Shanaki M, Ehteram H, Nasiri H, Sahmani M, Saeidi M, Goudarzi M, Pourkarim H, Azad M. A review on iron chelators in treatment of iron overload syndromes Int J Hematol Oncol Stem Cell Res 2016;10:239–47.
8. Assi TB, Baz E. Current applications of therapeutic phlebotomy. Blood Transfus 2014;12:75–83.
9. Ziegler D, Nowak H, Kempler P, Vargha P, Low PA. Treatment of symptomatic diabetic polyneuropathy with the antioxidant alpha-lipoic acid: a meta analysis. Diabet Med 2004;21:114–21.
10. Goralska M, Dackor R, Holley B, McGahan MC. Alpha lipoic acid changes iron uptake and storage in lens epithelial cells. Exp Eye Res 2003;76:241–8.
11. Suh JH, Moreau R, Heath SH, Hagen TM. Dietary supplementation with (R)-α-lipoic acid reverses the age-related accumulation of iron and depletion of antioxidants in the rat cerebral cortex. Redox Rep 2005;10:52–60.
12. Zhang Y, Zhang Y, Xie Y, Gao Y, Ma J, Yuan J, Li J, Wang J, Li L, Zhang J, Chu L. Multitargeted inhibition of hepatic fibrosis in chronic iron-overloaded mice by *Salvia miltiorrhiza*. J Ethnopharmacol 2013;148:671–81.
13. Budin SB, Othman F, Louis SR, Bakar MA, Radzi M, Osman K, Das S, Mohamed J. Effect of alpha lipoic acid on oxidative stress and vascular wall of diabetic rats. Rom J Morphol Embryol 2009;50:23–30.
14. Ahmadvand H, Jamor P. Effects of alpha lipoic acid on level of NO and MPO activity in diabetic rats. Annals of Research in Antioxidants 2017;2:4–7.
15. Marcos R, Monteiro RA, Rocha E. The use of design-based stereology to evaluate volumes and numbers in the liver: a review with practical guidelines. J Anat 2012;220:303–17.
16. Mandarim-de-Lacerda CA. Stereological tools in biomedical research. An Acad Bras Cienc 2003;75:469–86.
17. Gundersen HJ, Bagger P, Bendtsen TF, Evans SM, Korbo LX, Marcussen N, Møller A, Nielsen K, Nyengaard JR, Pakkenberg B, Sørensen FB. The new stereological tools: disector, fractionator, nucleator and point sampled intercepts and their use in pathological research and diagnosis. APMIS 1988;96:857–81.
18. Bancroft JD, Cook HC. Manual of histological techniques and their diagnostic application. London (UK): Churchill Livingstone; 1994. p. 35–67.
19. Gao Y, Wang N, Zhang Y, Ma Z, Guan P, Ma J, Zhang Y, Zhang X, Wang J, Zhang J, Chu L. Mechanism of protective effects of danshen against iron overload-induced injury in mice. J Ethnopharmacol 2013;145:254–60.
20. Shay KP, Moreau RF, Smith EJ, Smith AR, Hagen TM. Alpha-lipoic acid as a dietary supplement: molecular mechanisms and therapeutic potential. Biochim Biophys Acta 2009;1790:1149–60.
21. Yatmark P, Morales NP, Chaisri U, Wichaiyo S, Hemstapat W, Srichairatanakool S, Svasti S, Fucharoen S. Iron distribution and histopathological characterization of the liver and heart of β-thalassemic mice with parenteral iron overload: effects of deferoxamine and deferiprone. Exp Toxicol Pathol 2014;66:333–43.
22. Altintoprak N, Aydin S, Sanli A, Bilmez ZE, Kösemihal E. The protective effect of intratympanic alpha lipoic acid on cisplatin-induced ototoxicity on rats. J Int Adv Otol 2014;10:217–21.
23. Fernandes MS, Rissi TT, Zuravski L, Mezzomo J, Vargas CR, Folmer V, Soares FA, Manfredini V, Ahmed M, Puntel RL. Oxidative stress and labile plasmatic iron in anemic patients following blood therapy. World J Exp Med 2014;4:38-45.

24. Hazra B, Sarkar R, Ghate NB, Chaudhuri D, Mandal N. Study of the protective effects of Katha (heartwood extract of Acacia catechu) in liver damage induced by iron overload. J Environ Pathol Toxicol Oncol 2013;32:229–40.
25. Sarkar R, Hazra B, Mandal N. Amelioration of iron overload-induced liver toxicity by a potent antioxidant and iron chelator, Emblica officinalis Gaertn. Toxicol Ind Health 2015;31:656–69.
26. Al-Attar AM. Physiological and Histopathological Investigations on the Effects of α-Lipoic Acid in Rats Exposed to Malathion. BioMed Res Int 2010;2010:203503
27. Zhao L, Wang C, Song D, Li Y, Song Y, Su G, Dunaief JL. Systemic administration of the antioxidant/iron chelator α-lipoic acid protects against light-induced photoreceptor degeneration in the mouse retina. Invest Ophthalmol Vis Sci 2014;55:5979–88.
28. Rezk RG, Abdel-Rahman NA. Protective effects of lipoic acid against oxidative stress induced by lead acetate and gamma-irradiation in the kidney and lung in albino rats. Arab Journal of Nuclear Sciences and Applications 2013;46:324–37.
29. Biewenga GP, Haenen GR, Bast A. The pharmacology of the antioxidant lipoic acid. Gen Pharmacol 1997;29:315–31.
30. Suh JH, Wang H, Liu RM, Liu J, Hagen TM. (R)-α-Lipoic acid reverses the age-related loss in GSH redox status in post-mitotic tissues: evidence for increased cysteine requirement for GSH synthesis. Arch Biochem Biophys 2004;423:126–35.
31. Zhang J, Zhou X, Wu W, Wang J, Xie H, Wu Z. Regeneration of glutathione by ·-lipoic acid via Nrf2/ARE signaling pathway alleviates cadmium-induced HepG2 cell toxicity. Environ Toxicol Pharmacol 2017;51:30–7.
32. Liu D, He H, Yin D, Que A, Tang L, Liao Z, Huang Q, He M. Mechanism of chronic dietary iron overload-induced liver damage in mice. Mol Med Rep 2013;7:1173–9.

Online available at:
www.anatomy.org.tr
doi:10.2399/ana.18.074
QR code:

Correspondence to: William O. Sibuor
Department of Human Anatomy, School of Medicine,
University of Nairobi, Nairobi, Kenya
Phone: +254 02 318262
e-mail: williamsibuor@gmail.com

Conflict of interest statement: No conflicts declared.

anatomy
www.anatomy.org.tr
An International Journal of Experimental and Clinical Anatomy

Original Article

www.anatomy.org.tr
Received: October 28, 2018; Accepted: December 5, 2018
doi:10.2399/ana.18.075

Scapular glenopolar angle in anterior shoulder dislocation cases

Özhan Pazarcı, Nazım Aytekin, Seyran Kılınç, Hayati Öztürk

Department of Orthopaedics and Traumatology, School of Medicine, Cumhuriyet University, Sivas, Turkey

Abstract

Objectives: The aim of this study was to assess the glenoid with glenopolar angle measurements in cases with anterior shoulder dislocation and controls.

Methods: The glenopolar angle was measured retrospectively on direct radiographs of patients with shoulder dislocation (n=60), and a control group (n=42).

Results: The glenopolar angle of patients with anterior shoulder dislocation showed an anatomical difference, being significantly lower in anterior shoulder dislocation cases compared to the control group; 32.31±2.01 and 34.5±2.32, respectively ($p<0.001$).

Conclusion: The glenopolar angle, and thus the glenoid alignment is a possible risk factor and should be considered during assessment and management of these cases.

Keywords: glenoid; glenopolar angle; shoulder dislocation

Anatomy 2018;12(3):124–127

Introduction

The shoulder joint is the most mobile joint in the body. This movement is mainly due to the anatomy of the humerus head and the glenoid. The glenohumeral joint is the most frequently dislocated joint.[1] Anterior dislocation is most commonly observed, and there is a high risk of recurrence.[2] The shoulder has a tendency to dislocate after trauma, experienced generally in abduction and external rotation positions. The recurring dislocation rates reduce after arthroscopic treatment, but this situation is still a problem.[2] Maintenance of the glenohumeral joint association is linked to the dynamic and static stabilizers of the shoulder. The roles of capsuloligamentous structures and dynamic muscle balance in shoulder stability is well-defined in the literature.[3] However, there are very few studies on the importance of glenopolar angle (GPA).

GPA is the angle formed by the intersection of the line joining the most caudal and most cranial points of the glenoid cavity and the line joining the most cranial point of the glenoid cavity to the most caudal point of the scapula body.[4,5] GPA is normally used to measure rotational sequence disorders of the glenoid in scapula fractures on anteroposterior radiographs.[6] In this study, GPA was investigated on direct radiographs of anterior shoulder dislocation cases for the first time with an aim to assess the glenoid with GPA measurements in cases with anterior shoulder dislocation.

Materials and Methods

The study included a total of 140 adult patients admitted to Department of Orthopaedics and Traumatology, School of Medicine, Cumhuriyet University from 2013 to 2015. 70 patients were with anterior shoulder dislocation, and the remaining 70 had shoulder pain, but no dislocation or any other shoulder pathology during examinations. Patient information was retrospectively investigated. The age, side, gender and demographic information of patients were noted.

The same senior orthopedic surgeon and the same resident examined all AP shoulder radiographs. Radiographs of Group 1 patients were taken after reduction of shoulder

dislocation. Patients with true shoulder AP view were included in the evaluation, and radiographs of bad positioning and rotation were excluded from the study. Additionally, patients with insufficient file information were excluded. Group 1 comprised 60 and Group 2 comprised 42 cases for GPA measurements (**Table 1**). GPA measurements were made using the hospital PACS system (Medipacs® v3.8.5.1). In the system, the angle between the line from the most caudal to the most cranial points of the glenoid cavity and the line from the most cranial point of the glenoid cavity to the most caudal point of the scapula body were calculated on true AP shoulder radiographs (**Figure 1**).

The study was approved by the ethics committee of the School of Medicine of Cumhuriyet University. Analysis of data was made using the Statistical Package for Social Sciences (SPSS for Windows, version 22.0, Armonk, NY, USA). Data were given as percentage, frequency and the mean. The normality test of the GPA data was examined using the Kolmogorov-Smirnov test. The distribution of the variable was calculated to be normal (p=0.2). Mean differences of GPA values were examined by Student's t-test. The mean difference between groups was investigated using Mann-Whitney U test. The normality test for age was not appropriate (p=0.007).

Table 1
The distribution of groups, gender, sides and accompanying shoulder injuries.

	Category	n	%
Groups	Group 1	60	58.8
	Group 2	42	41.2
Side	Right	55	53.9
	Left	47	46.1
Gender	Male	56	54.9
	Female	46	45.1
Accompanying shoulder injury	No	54	90
	Yes	6	10

Results

The results from a total of 102 patients were assessed. The mean age of 60 patients in Group 1 was 45.68 years (min: 18, max: 85). The mean age of 42 patients in Group 2 was 47.57 years (min: 18, max: 83). There was no significant difference between age groups (p=0.754). The mean follow-up duration for Group 1 patients was 23.46 months. Six patients had accompanying shoulder injuries, including three patients with rotator cuff injury, two patients with

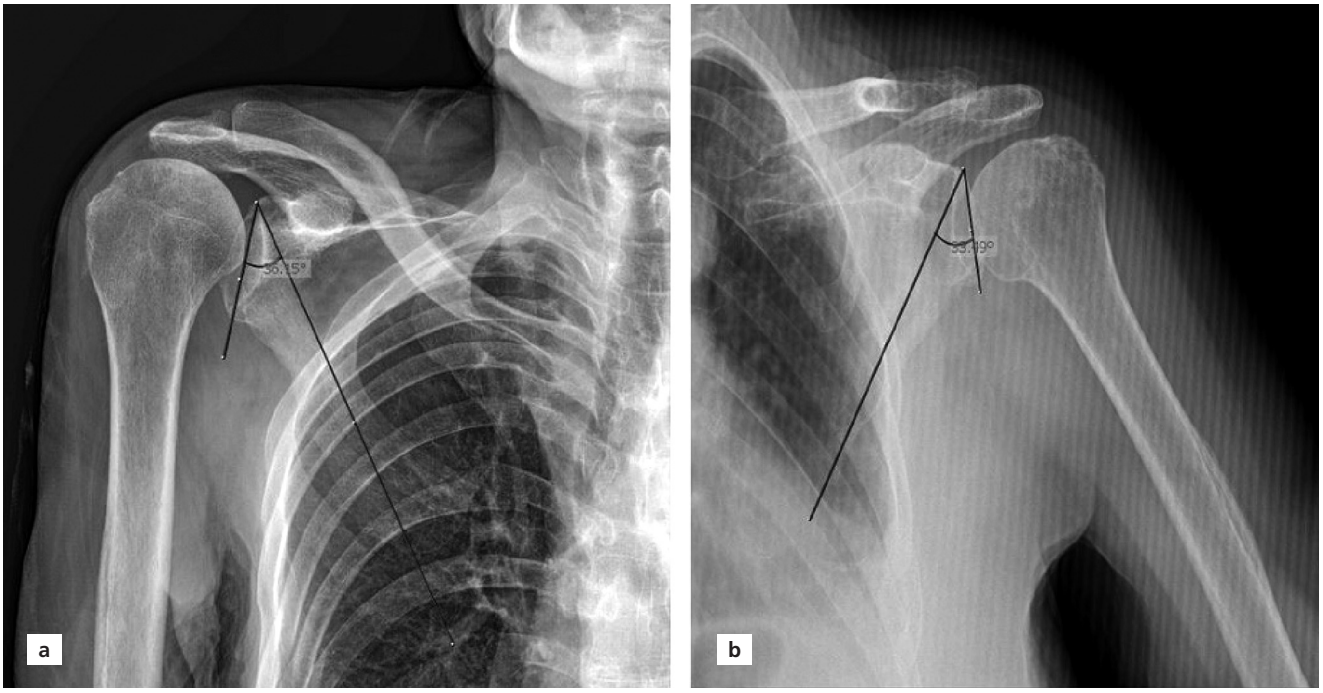

Figure 1. (**a**) Glenopolar angle (GPA) measurement of the angle between the line joining the most caudal and most cranial points of the glenoid cavity and the line from the most cranial point of the glenoid cavity to the most caudal point of the scapula body in a Group 2 patient; (**b**) GPA measurement in a Group 1 patient.

fracture of the greater tubercle of the humerus, and one patient with proximal humerus fracture. These injuries did not involve the glenoid and, therefore, these six patients were not excluded from the study.

The distribution of gender for patients was 34 males and 26 females in Group 1, and 22 males and 20 females in Group 2. **Table 1** shows the distribution of groups, age and sides.

The comparison of GPA by groups, gender and sides is shown in **Table 2**. The GPA in Group 1 was measured 32.31±2.01, while it was 34.5±2.32 in Group 2 (p<0.001) (**Figure 2**). There was no significant difference between males and females (p>0.05).

Table 2
The comparison of GPA (mean±SD) by groups, gender and sides using Student's t-test.

	Category	n	Mean±SD	p-value
Groups	Group 1	60	32.31±2.01	<0.001
	Group 2	42	34.5±2.32	
Side	Right	55	33.21±2.37	0.996
	Left	47	33.21±2.44	
Gender	Male	56	33.15±2.17	0.769
	Female	46	33.29±2.65	

Discussion

The most important finding in this study was that the GPA of patients with anterior shoulder dislocation was significantly low. To our knowledge, this is the first study to investigate the change in GPA with direct radiography in dislocation cases. Glenoid alignment should be considered in anterior shoulder dislocation cases. Previous studies reported glenoid corrective osteotomy was superior to conservative treatment for patients with posterior instability.[7] There is no data on the benefit of corrective osteotomy for anterior stability in the literature. However, there are studies showing a correlation between success rate of prosthesis and stability with the position of the glenoid component in total shoulder prosthesis.[8] A study comprising 128 patients with anterior shoulder instability and a control group of 130 cases investigated the glenoid version and inclination. They concluded that glenoid alignment was a risk factor for anterior shoulder instability and emphasized that care must be taken related to this for recurrent instability treatment.[9] These studies emphasized the effect of glenoid anatomy on shoulder stability. According to our results, GPA measurements on direct radiographs of anterior shoulder dislocation cases will provide rapid information for assessment of glenoid anatomy to orthopedists.

GPA was first described by Bestard et al.,[4] The use of this angle to assess scapula neck fractures.[10] and later gained popularity as a surgical treatment criterion for scapula neck and body fractures.[11,12]

There is no consensus for the optimal radiological technique to measure GPA or the standard values of GPA in the literature.[13] GPA can be measured directly on cadaver specimens, 3D scapula reconstructions, Neer view X-ray images, AP shoulder or AP chest radiographs.[13] In this study, GPA measurement was performed on true (Grashey) AP shoulder radiographs. In the literature, there are studies with measurements made on different imaging views.[14,15] The GPA angle value changes depending on the measurement method. Of these, 3D CT reconstruction, Neer 1 images and cadaver bone specimens provide similar results. AP shoulder and chest radiographs provide lower values compared to these measurements.[14]

There are other studies in the literature that assessed glenoid anatomy. For example, Peter et al.[16] investigated the correlation between glenoid inclination and rotator cuff tears.[16] Gregory et al.[17] investigated the correlation between greater tuberosity angle and rotator cuff tears. Maximilian et al.[18] emphasized the importance of glenoid morphology in instability arthropathy. The above studies emphasize the importance of glenoid anatomy similar to our study. Additionally, an advantage of our study is that information on the glenoid was obtained with GPA measurements on direct radiographs, without advanced tests like MR or 3D CT. A difference of 2.5° was observed between the groups (**Figure 2**). This was statistically significant (p>0.05). GPA can easily be evaluated with X-ray

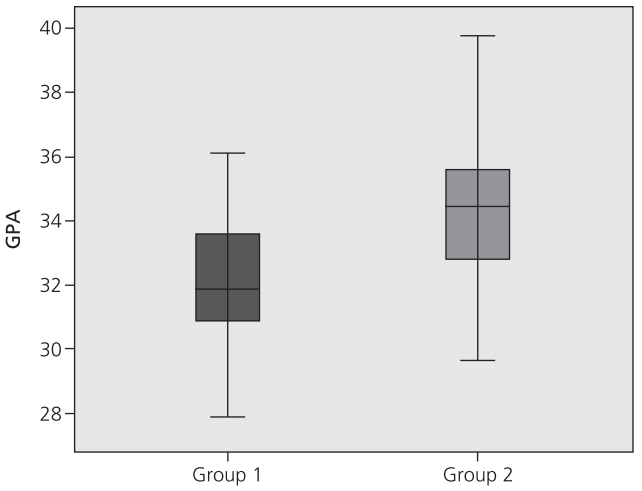

Figure 2. Box plot chart showing the means of GPAs.

in cases of shoulder dislocation. The clinical significance of low GPA is that, this can give the orthopedic surgeon a quick idea about the glenoid.

This study has some limitations. Control group radiographs were chosen from patients admitted to the general orthopedic clinic with shoulder pain. This sample may not be representative of the normal healthy population and may potentially be biased. However, only those with no pathology identified on radiography or examination were included in the control group. Although the GPA was significantly different between the groups, it is difficult to definitively determine whether our findings are clinically significant or not, because other factors may affect the risk of dislocation. Risk factors for patients with glenohumeral instability were described previously.[19] GPA measurements provide information about the nonmodifiable risk factor of glenoid morphology.

Conclusion

The GPA of patients with anterior shoulder dislocation was significantly low compared to the control group, showing an anatomical difference for cases with anterior shoulder dislocation. Should be considered in the assessment and management of these cases.

References

1. Owens BD, Campbell SE, Cameron KL. Risk factors for anterior glenohumeral instability. Am J Sports Med 2014;42:2591–6.
2. Peltz CD, Baumer TG, Mende V, Ramo N, Mehran N, Moutzouros V, Bey MJ. Effect of arthroscopic stabilization on in vivo glenohumeral joint motion and clinical outcomes in patients with anterior instability. Am J Sports Med 2015;43:2800–8.
3. Lugo R, Kung P, Ma CB. Shoulder biomechanics. Eur J Radiol 2008;68:16–24.
4. Bestard EA, Schvene HR, Bestard EH. Glenoplasty in management of recurrent shoulder dislocation. Contemp Orthop 1986;12:47–55.
5. Tuček M, Naňka O, Malík J, Bartoníček J. The scapular glenopolar angle: standard values and side differences. Skeletal Radiol 2014;43: 1583–7.
6. Wijdicks CA, Anavian J, Hill BW, Armitage BM, Vang S, Cole PA. The assessment of scapular radiographs: analysis of anteroposterior radiographs of the shoulder and the effect of rotational offset on the glenopolar angle. Bone Joint J 2013;95–B:1114–20.
7. Lacheta L, Singh TSP, Hovsepian JM, Braun S, Imhoff AB, Pogorzelski J. Posterior open wedge glenoid osteotomy provides reliable results in young patients with increased glenoid retroversion and posterior shoulder instability. Knee Surg Sports Traumatol Arthrosc 2019;27:299–304.
8. Nyffeler RW, Sheikh R, Atkinson TS, Jacob HAC, Favre P, Gerber C. Effects of glenoid component version on humeral head displacement and joint reaction forces: an experimental study. J Shoulder Elbow Surg 2006;15:625–9.
9. Hohmann E, Tetsworth K. Glenoid version and inclination are risk factors for anterior shoulder dislocation. J Shoulder Elbow Surg 2015;24:1268–73.
10. Romero J, Schai O IA. Scapular neck fracture: the influence of permanent malalignment of the glenoid neck on clinical outcome. Arch Orthop Trauma Surg 2001;121:313–6.
11. Cole PA, Hill BW. Scapula fracture. In: Obremskey WT, Sethi MK, Jahangir AA, editors. Orthopaedic traumatology: an evidence based approach. New York (NY): Springer; 2013. p. 71–86.
12. Bozkurt M, Can F, Kirdemir V, Erden Z, Demirkale I, Başbozkurt M. Conservative treatment of scapular neck fracture: the effect of stability and glenopolar angle on clinical outcome. Injury 2005;36: 1176–81.
13. Tucek M, Nanka O, Malik J, Bartonicek J. The scapular glenopolar angle: standard values and side differences. Skeletal Radiol 2014;43:1583–7.
14. Ohl X, Billuart F, Lagacé PY, Gagey O, Hagemeister N, Skalli W. 3D morphometric analysis of 43 scapulae. Surg Radiol Anat 2012;34:447–53.
15. Anavian J, Conflitti JM, Khanna G, Guthrie ST, Cole PA. A reliable radiographic measurement technique for extra-articular scapular fractures. Clin Orthop Relat Res 2011;469:3371–8.
16. Chalmers PN, Beck L, Granger E, Henninger H, Tashjian RZ. Superior glenoid inclination and rotator cuff tears. J Shoulder Elbow Surg 2018;27:1444–50.
17. Cunningham G, Nicodème-Paulin E, Smith MM, Holzer N, Cass B, Young AA. The greater tuberosity angle: a new predictor for rotator cuff tear. J Shoulder Elbow Surg 2018;27:1415–21.
18. Haas M, Plachel F, Wierer G, Heuberer P, Hoffelner T, Schulz E, Anderl W, Moroder P. Glenoid morphology is associated with the development of instability arthropathy. J Shoulder Elbow Surg 2018; pii: S1058– 2746(18)30700–6. doi: 10.1016/j.jse.2018.09.010
19. Cameron KL, Mauntel TC, Owens BD. The epidemiology of glenohumeral joint ınstability: incidence, burden, and long-term consequences. Sports Med Arthrosc Rev 2017;25:144–9.

Online available at:
www.anatomy.org.tr
doi:10.2399/ana.18.075
QR code:

deomed

Correspondence to: Özhan Pazarcı, MD
Department of Orthopaedics and Traumatology, School of Medicine, Cumhuriyet University, 58140, Sivas, Turkey
Phone: +90 534 681 90 45
e-mail: dr.pazarci@gmail.com

Conflict of interest statement: No conflicts declared.

anatomy
www.anatomy.org.tr
An International Journal of Experimental and Clinical Anatomy

Original Article

www.anatomy.org.tr
Received: November 3, 2018; Accepted: November 24, 2018
doi:10.2399/ana.18.077

Lead contamination induces neurodegeneration in prefrontal cortex of Wistar rats

Daniel Temidayo Adeniyi[1], Peter Uwadiegwu Achukwu[2]

[1]*Department of Medical Laboratory Science, School of Basic Medical Sciences, College of Pure and Applied Sciences, Kwara State University, Malete, Kwara State, Nigeria*

[2]*Department of Medical Laboratory Science, Faculty of Health Science and Technology, College of Medicine, University of Nigeria, Enugu Campus, Enugu State, Nigeria*

Abstract

Objectives: Neurodegenerative disorders have been associated with several environmental pollutants such as heavy metals. This study aimed at investigating the neurodegenerative impact of lead concentration obtained from the waterways in Kwara State, Nigeria on Wistar rats.

Methods: Twenty-first filial generation inbred adult male Wistar rats *(Rattus norvegicus)* with an average weight of 150–180 g were divided into two groups of ten animals. The highest mean concentration of lead obtained from the waterways of the three geographical zones of Kwara Nigeria was administered with water (0.009 mg of $Pb(CH_3CO_2).3H_2O$ per milliliter solution) to rats in the treatment group *ad libitum* for 65 days. The harvested prefrontal cortex was processed for paraffin embedding and the sections were stained for haematoxylin and eosin stain and Bielschowsky's silver impregnation stain, and glial fibrillary acidic protein (GFAP) and inducible nitric oxide synthase (iNOS) immunohistochemistry.

Results: The histochemical stainings revealed shreds of evidence of neuronal degeneration in the treatment group compared to the control group. Immunohistochemical analysis revealed marked astrocytosis, the hallmark of neuroinflammation, with induced oxidative stress in the treatment group compared to the control group.

Conclusion: These results indicate lead obtained from the three geographical zones of Kwara Nigeria may have a possible pathogenic role in development of neurodegenerative disorders and emphasize the effects of exposure to this environmental pollutant.

Keywords: environmental pollutants; lead; neurodegenerative disorders; neuroinflammation; oxidative stress

Anatomy 2018;12(3):128–134

Introduction

Neurological impairments are fast becoming common global causes of disabilities.[1] Maulik et al.[2] observed that prevalence of mental disabilities is higher in developing countries compared to those in developed countries. Environmental factors, such as environmental pollution, can influence the prevalence of these mental disabilities.[2] Poor health quality and high contamination level of heavy metals in developing countries may also contribute to these prevalence rates.[3] In recent times, the continual heavy metal contamination in waterways has been a global issue due to its persistence and resultant toxicity.[4,5] Poor waste management and disposal, especially electronic waste (e-waste) disposal and recycling in developing countries were reported to enhance the elevated levels of heavy metal contamination in these regions.[3,6–8]

E-waste is defined as used electronics intended for reuse, resale, salvage, recycling, or disposal.[9] Osibanjo and Nnorom[10] reported that electronic waste devices are usually stored for a while for a perceived value - physical or emotional - before disposal with municipal waste in Nigeria. Because of the absence of a special framework for the separate collection and management of e-waste in Nigeria, these devices are disposed with Municipal Solid Waste (MSW) at open dumpsites and/or into waterways.[9–12] Informal disassembling and recycling of e-waste in backyards was also reported in Nigeria where primitive

methods were used in recovering materials from e-waste.[13–15] The recovered materials are processed to reusable components and the unused portions are also stockpiled or dumped and landfilled.[13,16] E-wastes contain more than a thousand different substances, of which many are toxic, heavy metals inclusive.[17,18] These complex toxic substances, if not properly handled during recycling or disposal, adversely impact the environment.[13,19] Corrosion of e-waste components after disposal result in mobility of incorporated heavy metals which travel with leachate to contaminate the environment.[20] Leaching of these toxic heavy metals eventually contaminates the ground and surface water.[6] The resultant effect is the high levels of heavy metals above the permissible limit recorded in Nigeria waterways.[5,21,22]

Lead is a soft, ductile, flexible and malleable metal with high thermal expansion and electrical conductivity.[23] Being the 5th most widely used metal,[24] it is toxic and found in substantial amount in e-waste.[25] Lead is commonly found in e-waste such as cathode ray tubes (CRTs) in computers monitors and televisions, fluorescent tubes, solder in printed circuit boards, as well as in liquid crystal displays (LCDs) and batteries.[11,26–29] In Nigeria, the population is at risk of lead exposure because of the intense use of leaded gasoline, the poor recovery and recycling of automotive lead-acid batteries, and the uncontrolled e-waste disposal and recycling.[30,31] Lead is not biodegradable. It stores faster in the human body than metabolized or excreted, and hence tends to bio-accumulate in concentrations above that found in the environment.[32] It is a potent neurotoxin that disrupts the functional integrity of the neurons with resultant negative implication on memory and intelligence and cognitive deterioration.[23,33–35]

This study aimed at investigating the neurodegenerative impact of lead concentration obtained from the waterways in Kwara State, Nigeria on Wistar rats as the experimental model.

Materials and Methods

This study was carried out in Kwara State, Nigeria in 2017. Experimental procedures used in this study were approved by the College of Medicine Research Ethics Committee, University of Nigeria, Enugu State (approval number: 025/02/2017) in line with the National Institute of Health (NIH) "Guide to the Care and Use of Animals in Research and Teaching".

The lead (II) acetate trihydrate ($Pb(CH_3CO_2).3H_2O$) salt used was obtained from the Department of Biochemistry, College of Pure and Applied Science, Kwara State University, Malete, Kwara State, Nigeria. 0.009 g of $Pb(CH_3CO_2).3H_2O$ was weighed and dissolved in 1 liter of double distilled demineralized water to form 0.009 mg of $Pb(CH_3CO_2).3H_2O$ per liter to form the final concentration of 0.009 mg of $Pb(CH_3CO_2).3H_2O$ per milliliter solution. This was based on the empirical measurement of heavy metals obtained in the waterways of the Kwara Nigeria in 2016 and reported by Adeniyi et al.[5]

Twenty (20) first filial (F1) generation inbred adult male Wistar rats *(Rattus norvegicus)* with an average weight of about 150–180 g were procured from the animal facility of Institute for Advance Medical Research and Training (IAMRAT), College of Medicine, University of Ibadan and employed in this study. Rats were allowed to acclimatize for 14 days and fed pelletized rat feed and water *ad libitum* throughout acclimatization before use. Plastic cages containing wood shaving bedding were used to house the rats. The bedding was changed once a day. They were kept in standard laboratory conditions under natural light-dark cycle at room temperature and maintained on standard laboratory rat pellets and given water *ad libitum*. These rats were divided at random into two groups of ten animals using the method of Daniel et al.[36] The animals in the first group had access to diet and double distilled demineralized water *ad libitum* while those in the second group had access to diet and lead-contaminated water *ad libitum*. The duration of treatment lasted over a period of 65 days, a long-term standard for rats.[37] The animals were sacrificed by cervical dislocation. The skulls of the sacrificed animals were opened using bone forceps to expose the brain. The skull was opened from the posterior part to leave the tissue intact.[38] The prefrontal cortex was obtained from the anterior cerebral cortex. The harvested tissues were fixed in 10% buffered formol saline, grossed and processed for paraffin tissue embedding following Drury and Wellington[39] technique. The processed sections were stained for histological, histochemical and immunohistochemical evaluation. Neuromorphological and histochemical analysis were carried out using haematoxylin and eosin (H&E) staining technique[40] and Bielschowsky's silver impregnation technique,[41] respectively. Immunohistochemical evaluation was carried out using glial fibrillary acidic protein (GFAP)[42,43] and inducible nitric oxide synthase (iNOS)[44] immunostaining techniques.

The stained sections were viewed and photographed with an Olympus U-D03 microscope (Olympus, Lake Success, NY, USA) captured with Olympus DP21. Photomicrographs of stained sections were obtained and reported.

Results

There was no account of death recorded in the two groups throughout the 65 days of lead administration. The general neuronal morphology of the prefrontal cortex in adult male Wistar rats following administration with lead-contaminated water demonstrated by haematoxylin and eosin staining is shown in **Figure 1**. Sections from the prefrontal cortex of the control Wistar rats (**Figure 1a**) revealed intact and normal sized neurons with clear perikarya, centrally placed nucleus and small-sized neuroglia interspersed within normal neuropil stained slightly eosinophilic; whereas sections from the prefrontal cortex from the treatment group (**Figure 1b**) depicted numerous neurons with distorted morphology with different features of neurodegeneration, which includes red neuron, shrunken neurons with karyolitic nuclei, gliosis with focal neuropil vacuolation degeneration.

The neuronal membrane was demonstrated using Bielschowsky's silver impregnation stain (**Figure 2**). The section from the control group revealed normal neurons with well-outlined neuronal membrane and axons surrounding a clear cytoplasm (**Figure 2a**). The treatment group showed numerous neurons with various degenerative features characterized by pyknotic neurons with condensed chromatin, nuclear shrinkage; with some neuron having no nuclei and neuropil vacuolation (**Figure 2b**).

Glial fibrillary acidic protein (GFAP) immunostaining was used to demonstrate reactive glial immunoreactivity (**Figure 3**). The treatment groups showed strong astrocytic immunoreactivity (**Figure 3b**) compared with the control group (**Figure 3a**). Inducible nitric oxide synthase (iNOS) immunostaining (**Figure 4**) was used for the demonstration of oxidative stress. iNOS reactivity was intensely expressed in the treatment groups (**Figure 4b**) in comparison to the control group (**Figure 4a**).

Discussion

Several parameters were employed in this study to observe the morphology of the neurons in the prefrontal cortex of rats following lead contaminated water consumption. Based on the higher functions of cognitive abilities associated with prefrontal cortex of the brain,[45] the morphology of the neurons located in this region was investigated to compare potential differences following lead exposure.

The results obtained with haematoxylin and eosin staining method (**Figure 1**) showed features of neurodegeneration in the treatment group (**Figure 1b**). The degeneration pattern of the neuron was apoptotic. These apoptotic neuronal cells are characterized by pyknotic nuclei involving irreversible condensation of chromatin in the nucleus and shrinkage of the cells.[46,47] Changes observed in neurons from the treatment group suggested that neuronal cell death occurred in the apoptotic mode. The excessive neuronal cell shrinkage is the result of the tightly packed cells that are smaller in size compared with the control in accordance with the findings of Olajide et al.[48] Stefanis et al.[49] described neuronal apoptotic cells with tightly packed with or without fragment which further supports our observation.

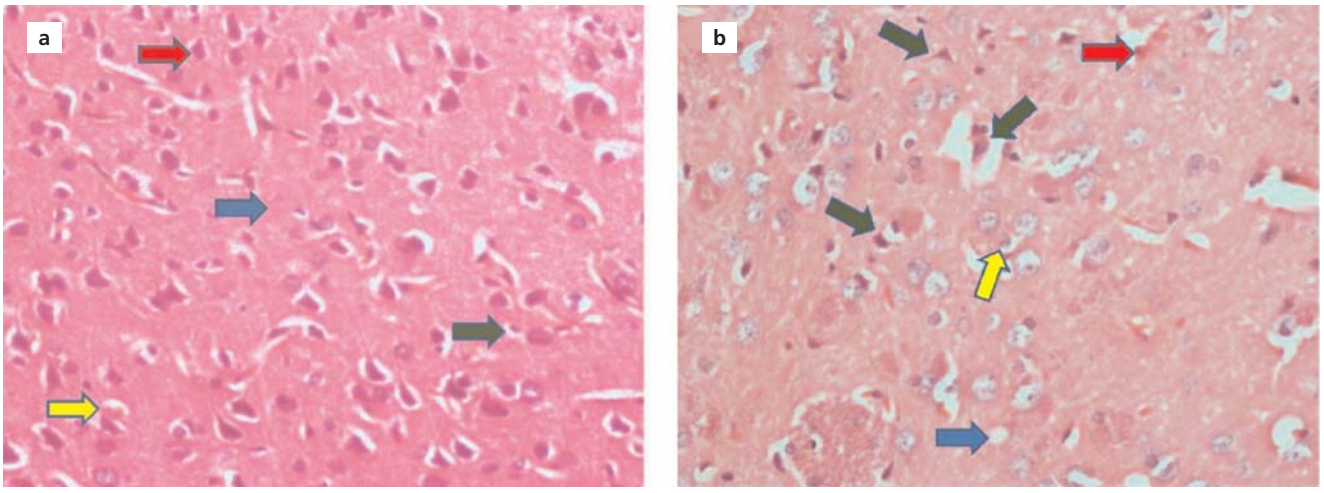

Figure 1. (**a**) Control group had intact neurons (**red arrow**), normal blood vessel (**yellow arrow**) in the neuropil area that stained slightly eosinophilic (**blue arrow**) and glial cells interspersed within this region (**green arrow**). (**b**) The cortical sections of rats from lead-contaminated group showed features of neurodegeneration including red-colored neurons (**red arrow**), shrunken neurons with karyolysis nuclei (**green arrows**), gliosis (**yellow arrow**) and focal neuropil vacuolation (**blue arrow**) (×400 magnification, haematoxylin and eosin stain). [Color figure can be viewed in the online issue, which is available at www.anatomy.org.tr]

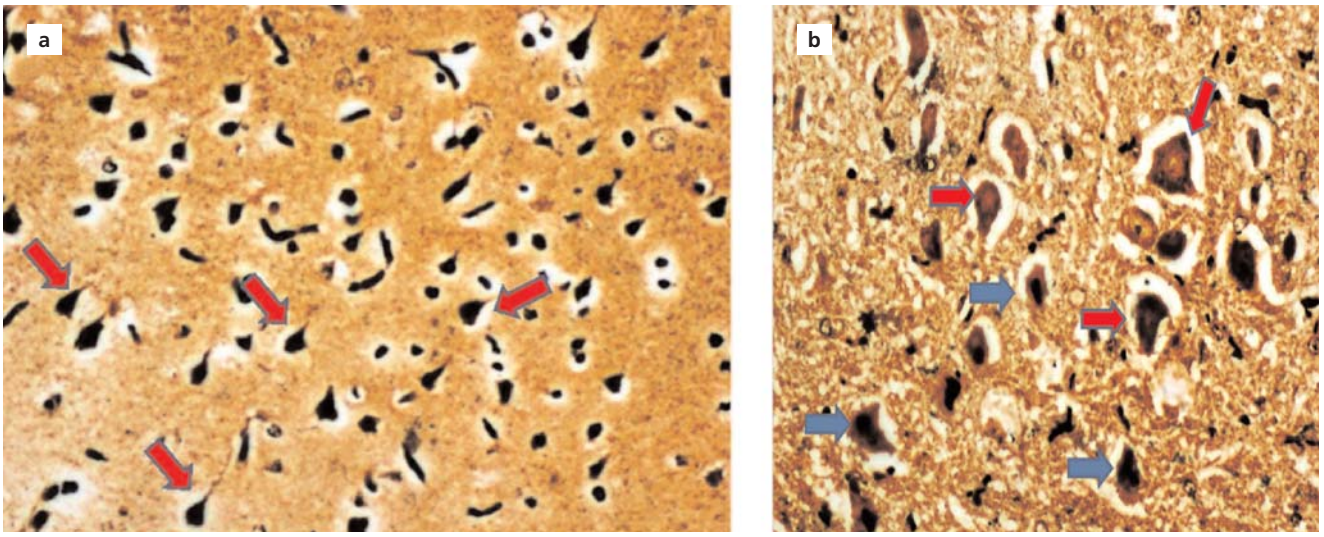

Figure 2. (**a**) The control group appeared normal with intact neurons (**red arrows**). (**b**) Group with administration of water contaminated with lead showed features of neurodegeneration in the cortex characterized by the presence of degenerate neurons with no nuclei (**red arrows**) and some with pyknotic nuclei (**blue arrows**) (×400 magnification, Bielschowsky's silver impregnation staining). [Color figure can be viewed in the online issue, which is available at www.anatomy.org.tr]

The neuronal membrane and presence of neurodegenerative features in the prefrontal cortex of the experimental animals throughout the 65 days of exposure are demonstrated using Bielschowsky's silver staining method as seen in **Figure 2**. Sections from the control group revealed normal neurons with a well-outlined neuronal membrane (**Figure 2a**). The treatment group showed neurons with different degenerative features (**Figure 2b**). The distinct morphological features observed in the treatment group also define apoptotic neuronal cell death in pathological condition.[50]

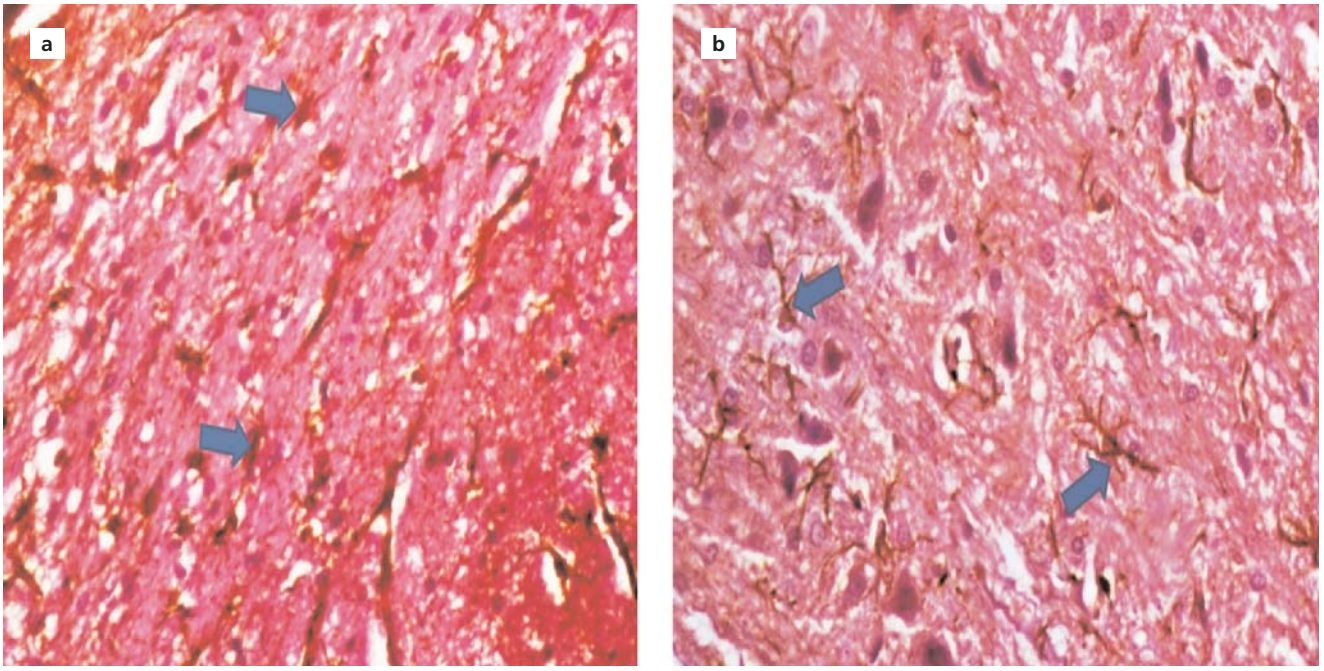

Figure 3. (**a**) Control group showed mild astrocytic immunoreactivity with specific and uniform staining for glial fibrillary acidic protein (GFAP) (**blue arrows**). (**b**) Group with water contaminated with lead administration depicted strong GFAP immunoreactivity with numerous intensely stained astrocytes (**blue arrows**) (×400 magnification, GFAP immunostaining). [Color figure can be viewed in the online issue, which is available at www.anatomy.org.tr]

Immunohistochemical expression of glial fibrillary acidic protein (GFAP) (**Figure 3**) immunostaining revealed GFAP-immunoreactive astroglia-like cells were increased in proportion, forming gliosis in the treatment group when compared with the control. GFAP uniquely marks for astrocytes which provide structural support and strength to the surrounding neurons in the central nervous system.[51,52] The immunoreactivity of GFAP increased during reactive gliosis characterized by astrocyte hyperplasia and hypertrophy as observed in **Figure 3b**.[52] Microglial and astrocytes are effectors of neuroinflammation.[32] Neuroinflammation involving astrogliosis and microglial activation is common to several neurodegenerative disorders.[53] The long-term impact of neuroinflammation-induced cell death is engendered by increased production of reactive oxygen and nitrogen species (RONS).[54–56] Excessive generation of RONS during oxidative stress is the major mechanism for the pathological effect of heavy metals, lead inclusive.[32,57–59] RONS are principally involved in arousing apoptotic cell death by nitrosative or irreversible oxidative damage to neuronal elements.[55,56]

The demonstration of oxidative stress was also shown by immunohistochemical expression of induced nitric oxide synthase (iNOS) (**Figure 4**). iNOS immunoreactivity revealed increased immunointensity in treatment groups (**Figure 4b**) when compared with control groups (**Figure 4a**). Nitric oxide (NO) is mainly synthesized by nitric oxide synthase (NOS) through the conversion of L-arginine to NO and L-citrulline in mammals.[60] NO plays a vital role in both physiological and pathological processes in humans. Excessive production of NO as invoked by neuroinflammation is implicated as one major causative agent for several neurodegenerative disorders pathogenesis.[56] Neuronal NO synthase is documented to be the main NOS isoform in the brain.[61,62] On the contrary, iNOS is not normally expressed or comes with minimal expression in the brain.[63,64] Nevertheless, increased iNOS expression in neuroglia and invading macrophages in response to brain injuries is revealed in pathological conditions.[65,66] Acute injury and iNOS upregulation may result in cell death.[67,68] All the same, chronic neurodegenerative disorders will ensue when a large amount of NO is produced over a prolonged period of time.[69]

Conclusion

The findings of this study show that lead, obtained from the three geographical zones of Kwara Nigeria, may have a possible pathogenic role in development of neurodegenerative disorders and emphasize the effects of exposure to this environmental pollutant.

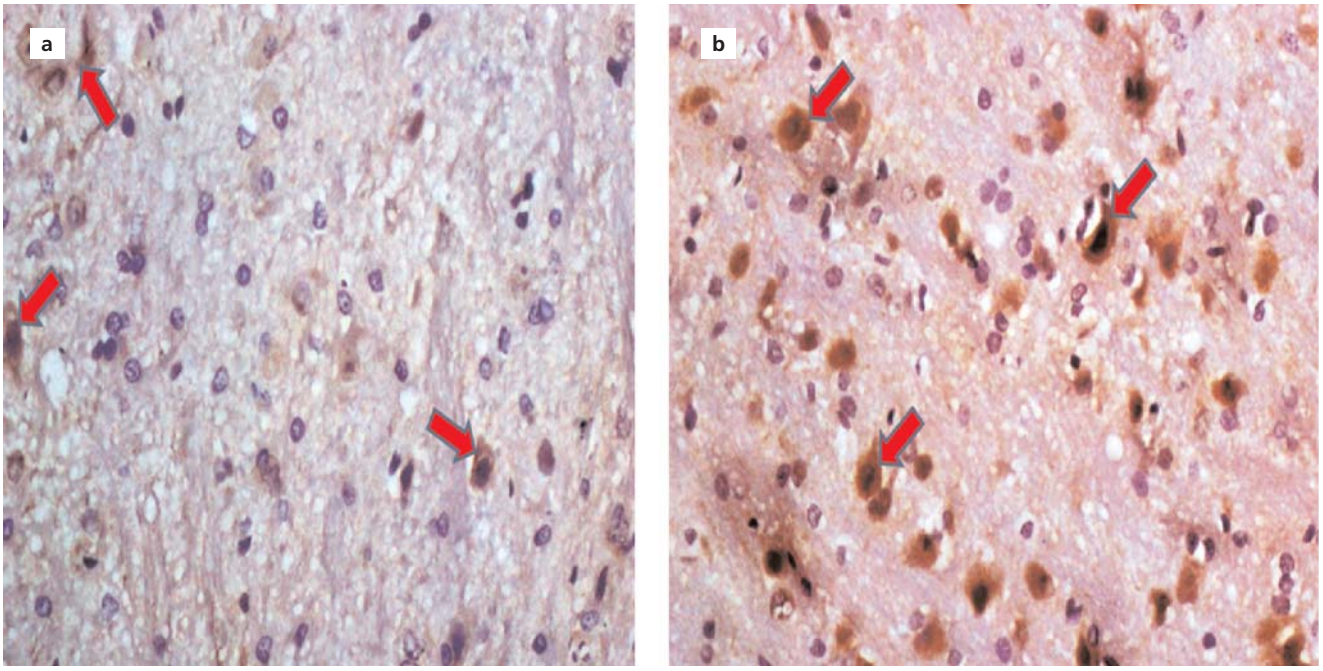

Figure 4. (**a**) Control group showed mild NOS immunostaining (**red arrows**). (**b**) Group administered with lead contaminated water revealed strong iNOS immunoreactivity (×400 magnification, iNOS immunostaining). [Color figure can be viewed in the online issue, which is available at www.anatomy.org.tr]

Acknowledgements

The authors acknowledge Mr. Adekunle Fowotade the technical head of Pathology Department, University of Ilorin Teaching Hospital (UITH) for granting access to use their laboratory for this work and other staff especially Pastor Oluwumi Olutunde and Mrs. Akanbiola for their technical input.

References

1. World Health Organization. World report on disability 2011 [Internet]. [Retrieved: August 11, 2016] Available from: http://www.who.int/disabilities/world_report/2011/en/index.html.
2. Maulik PK, Mascarrnhas MN, Mathers CD, Dua T, Saxena S. Prevalence of intellectual disability: a meta-analysis of population-based studies. Res Dev Disabil 2011;32:419–36.
3. Neal AP, Guilarte TR. Mechanisms of heavy metal neurotoxicity. Toxicol Res 2013;2:99–114.
4. Islam MS, Ahmed MK, Habibullah-Al-Mamun M, Hoque MF. Preliminary assessment of heavy metal contamination in surface sediments from a river in Bangladesh. Environmental Earth Sciences 2015;73:1837–48.
5. Adeniyi TD, Achukwu PU, Abubakar AA. Frequency of electronics waste generated heavy metals in urban waterways. International Journal of Human Capital in Urban Management 2017;2:89–100.
6. Onwughara NI, Umeobika UC, Obianuko PN, Iloamaeke MI. Emphasis on effects of storm runoff in mobilizing the heavy metals from leachate on waste deposit to contaminate Nigerian waters: improved water quality standards. International Journal of Environmental Science and Development 2011;2:55–63.
7. Grant K, Goldizen FC, Sly PD, Brune M, Neira M, van den Berg M, Norman RE. Health consequences of exposure to e-waste: a systematic review. Lancet Glob Health 2013;1:e350–61.
8. Huang J, Nkrumah PN, Anim DO, Mensah E. E-Waste disposal effects on the aquatic environment: Accra, Ghana. Rev Environ Contam Toxicol 2014;229:19–34.
9. Adesina OS. The negative impact of globalization on Nigeria. International Journal of Humanities and Social Science 2012;2:193–201.
10. Osibanjo O, Nnorom IC. The challenge of electronic waste (e-waste) management in developing countries. Waste Manag Res 2007;25:489–501.
11. Afiukwa JN, Agunwamba JC, Eneh OC. Reducing environmental pollution: acid-precipitation of lead from electrical and electronic equipment. Journal of Chemical Society of Nigeria 2015;40:143–6.
12. Onwughara IN, Nnorom IC, Kanno OC. Issues of roadside disposal habit of municipal solid waste, environmental impacts and implementation of sound management practices in developing country: Nigeria. International Journal of Environmental Science and Development 2010a;1:409–17.
13. Onwughara NI, Nnorom IC, Kanno OC, Chukwuma RC. Disposal methods and heavy metals released from certain electrical and electronic equipment wastes in Nigeria: adoption of environmental sound recycling system. International Journal of Environmental Science and Development 2010b;1:290–6.
14. Azuka AI. The influx of used electronics into Africa: a perilous trend. Law Environment and Development Journal 2009;5:90.
15. Robinson BH. E-waste: an assessment of global production and environmental impacts. Sci Total Environ 2009;408:183–91.
16. Schmidt CW. Unfair trade: e-waste in Africa. Environ Health Perspect 2006;114:232–5.
17. Ogungbuyi O, Nnorom IC, Osibanjo O, Schluep M. E-waste country assessment Nigeria. Report of UNEP E-waste Africa project for Nigeria. Ibadan, Nigeria: Basel Convention Coordinating Centre in Nigeria (BCCC-Nigeria); 2012. 230 p.
18. Ousman WZ. Environmental impact assessment of waste electronic and electrical equipment (WEEE) management practices in developing countries through leaching test. African Journal of Environmental Science and Technology 2015;9:671–81.
19. Sepúlveda A, Schluep M, Renaud FG, Streicher M, Kuehr R, Hagelüken C, Gerecke AC. A review of the environmental fate and effects of hazardous substances released from electrical and electronic equipments during recycling: Examples from China and India. Environmental Impact Assessment Review 2010;30:28–41.
20. Li Y, Richardson JB, Bricka RM, Niu X, Yang H, Li L, Jimenez A. Leaching of heavy metals from e-waste in stimulated landfill columns. Waste Manag 2009;29:2147–50.
21. Galadima A, Garba ZN, Leke L, Almustapha MN, Adam IK. Domestic water pollution among local communities in Nigeria – causes and consequences. European Journal of Scientific Research 2011;52:592–603.
22. Izah SC, Chakrabarty N, Srivastav AL. A review on heavy metal concentration in potable water sources in Nigeria: human health effects and mitigating measures. Exposure and Health 2016;8:285–304.
23. Mason LH, Harp JP, Yan DY. Pb neurotoxicity: neuropsychological effects of lead toxicity. Biomed Res Int 2014;840547.
24. Davis JR, Allen P, Lampman S, Zorc TB, Henry SD, Daquila JL, Ronke AW. Metals handbook: properties and selection: nonferrous alloys and special-purpose materials. Novelty (OH): ASM International; 1990. 3470 p.
25. Eneh OC, Agunwamba JC. E-waste management in Africa: recycling of crude lead-extract from e-waste items. Journal of Applied Sciences 2011;11:3215–20.
26. Chen A, Dietrich KN, Huo X, Ho S. Developmental neurotoxicant in E-Waste: an emerging health concern. Environ Health Perspect 2011;119:43–438.
27. Fishbein B. Waste in the wireless world: the challenge of cell phones. New York (NY): Inform; 2002. 106 p.
28. Ibrahim U. E-waste environmental pollution and health risk implications for early child care, growth and development in Nigeria. Sustainable Human Development Review 2017;9:41–54.
29. Song Q, Li J. A systematic review of the human body burden of e-waste exposure in China. Environ Int 2014;68:82–93.
30. Fakayode SO, Olu-Owolabi BI. Heavy metal contamination of roadside topsoil in Osogbo, Nigeria: its relationship to traffic density and proximity to highways. Environmental Geology 2003;44:150–7.
31. Lincoln JD, Ogunseitan OA, Saphores JD, Shapiro AA. Leaching assessments of hazardous materials in cellular telephones. Environ Sci Technol 2007;41:2572–8.
32. Monnet-Tschudi F, Zurich MG, Boschat C, Corbaz A, Honegger P. Involvement of environmental mercury and lead in the etiology of neurodegenerative diseases. Rev Environ Health 2006;21:105–17.
33. Bellinger DC. Very low lead exposures and children's neurodevelopment. Curr Opin Pediatr 2008;20:172–7.
34. Dorsey CD, Lee BK, Bolla KI, Weaver VM, Lee SS, Lee GS, Todd AC, Shi W, Schwartz BS. Comparison of patella lead with blood lead and tibia lead and their associations with neurobehavioral test scores. J Occup Environ Med 2006;48:489–96.
35. Lidsky TI, Schneider JS. Lead neurotoxicity in children: basic mechanisms and clinical correlates. Brain 2003;126:5–19.
36. Daniel AT, Adekilekun TA, Adewale MA, Adekemi AT. Cyanide-induced hyperthyroidism in male Wistar rats. Niger Med J 2014;55:246–9.

37. Adeyemi O, Oloyede OB, Oladiji AT. Physicochemical and microbial characteristics of leachate-contaminated groundwater. Asian Journal of Biochemistry 2007;2:343–8.
38. Van Zutphen LFM, Baumans V, Beynen AC. Principles of laboratory animal science. Amsterdam: Elsevier. 1993. p. 265–276.
39. Drury RA, Wellington EA. Carleton Histological Technique. 5th ed. New York (NY): Oxford University Press; 1980. 190 p.
40. Bancroft JD, Gamble H. Theory and practice of histological technique, 6th ed. Philadelphia: Churchill Livingstone Elsevier, New York; 2008. 240 p.
41. Marsland TA, Glees P, Erikson LB. Modification of Glee's silver impregnation for paraffin sections. J Neuropathol Exp Neurol 1954; 13:587–91.
42. Lyck L, Dalmau I, Chemnitz J, Finsen B, Schroder HD. Immunohistochemical markers for quantitative studies of neurons and glia in human neocortex. J Histochem Cytochem 2008;56:201–21.
43. Delcambre GH, Liu J, Herrington JM, Vallario K, Long MT. Immunohistochemistry for the detection of neural and inflammatory cells in equine brain tissue. PeerJ 2016;4:e1601.
44. Hoehn T, Felderhoff-Mueser U, Maschewski K, Stadelmann C, Sifringer M, Bittigau P, Koehne P, Hoppenz M, Obladen M, Bührer C. Hyperoxia causes inducible nitric oxide synthase-mediated cellular damage to the immature rat brain. Pediatr Res 2003;54:179–84.
45. Semendeferi K, Armstrong E, Schleicher A, Zilles K, Van Hoesen GW. Prefrontal cortex in humans and apes: a comparative study of area 10. Am J Phys Anthropol 2001;114:224–41.
46. Sharifi AM, Baniasadi S, Jorjani M, Rahimi F, Bakhshayesh M. Investigation of acute lead poisoning on apoptosis in rat hippocampus in vivo. Neurosci Lett 2002;329:45–8.
47. Osten P, Margrie TW. Mapping brain circuitry with a light microscope. Nat Methods 2013;10:515–23.
48. Olajide OJ, Akinola OB, Ajao MS, Enaibe BU. Sodium azide-induced degenerative changes in the dorsolateral prefrontal cortex of rats: attenuating mechanisms of kolaviron. Eur J Anat 2016;20:47–64.
49. Stefanis L, Burke RE, Greene LA. Apoptosis in neurodegenerative disorders. Curr Opin Neurol 1997;10:299–305.
50. Wyllie AH, Kerr JF, Currie AR. Cell death: the significance of apoptosis. Int Rev Cytol 1980;68:251–306.
51. Mccall MA, Gregg RG, Behringer RR, Brenner M, Delaney CL, Galbreath EJ, Zhang CL, Pearce RA, Chiu SY, Messing A. Targeted deletion in astrocyte intermediate filament (Gfap) alters neuronal physiology. Proc Natl Acad Sci U S A 1996;93:6361–6.
52. Eng L, Ghirnikar R, Lee Y. Glial fibrillary acidic protein: GFAP-thirty-one years (1969-2000). Neurochem Res 2000;25:1439–51.
53. Blasko I, Stampfer-Koutchev M, Robastscher P, Veerhuis R, Eikelenboom P, Grubeck-Loebenstein B. How chronic inflammation can affect the brain and support the development of Alzheimer's disease in old age: the role of microglia and astrocyte. Aging Cell 2004;3:169–76.
54. Hsiang J, Díaz E. Lead and developmental neurotoxicity of the central nervous system. Current Neurobiology 2011;2:35–42.
55. Nakagawa T, Yokozawa T. Direct scavenging of nitric oxide and superoxide by green tea. Food Chem Toxicol 2002;40:1745–50.
56. Yuste JE, Tarragon E, Campuzano CM, Ros-Bernal F. Implications of glial nitric oxide in neurodegenerative diseases. Front Cell Neurosci 2015;9:322.
57. Antonio-García MT, Massó-Gonzalez EL. Toxic effects of perinatal lead exposure on the brain of rats: involvement of oxidative stress and the beneficial role of antioxidants. Food Chem Toxicol 2008;46:2089–95.
58. Khan D, Qayyum S, Saleem S, Khan F. Lead-induced oxidative stress adversely affects health of the occupational workers. Toxicol Ind Health 2008;24:611–8.
59. Tsang F, Soong TW. Interactions between environmental and genetic factors in the pathophysiology of Parkinson's disease. IUBMB Life 2003;55:323–7.
60. Knowles RG, Moncada S. Nitric oxide synthases in mammals. Biochem J 1994;298:249–58.
61. Huang PL, Dawson TM, Bredt DS, Snyder SH, Fishman MC. Targeted disruption of the neuronal nitric oxide synthase gene. Cell 1993;75:1273–85.
62. Dawson TM, Dawson VL. Nitric oxide synthase: role as a transmitter/mediator in the brain and endocrine system. Annu Rev Med 1996;47:219–27.
63. Lowenstein CJ, Glatt CS, Bredt DS, Snyder SH. Cloned and expressed macrophage nitric oxide synthase contrasts with the brain enzyme. Proc Natl Acad Sci U S A 1992;89:6711–5.
64. Keilhoff G, Seidel B, Noack H, Tischmeyer W, Stanek D, Wolf G. Patterns of nitric oxide synthase at the messenger RNA and protein levels during early rat brain development. Neurosci 1996;75:1193–201.
65. Simmons ML, Murphy S. Induction of nitric oxide synthase in glial cells. J Neurochem 1992;59:897–905.
66. Wallace MN, Fredens K. Activated astrocytes of the mouse hippocampus contain high levels of NADPH-diaphorase. Neuroreport 1992;3:953–6.
67. Adamson DC, Wildemann B, Sasaki M, Glass JD, McArthur JC, Christov VI, Ted M, Dawson TM, Dawson VL. Immunologic NO synthase: elevation in severe AIDS dementia and induction by HIV-1 gp41. Science 1996;274:1917–21.
68. Iadecola C, Xu X, Zhang F, el-Fakahany EE, Ross ME. Marked induction of calcium-independent nitric oxide synthase activity after focal cerebral ischemia. J Cereb Blood Flow Metab 1995;15:52–9.
69. Nathan C, Xie QW. Regulation of biosynthesis of nitric oxide. J Biol Chem 1994;269:13725–8.

Online available at:
www.anatomy.org.tr
doi:10.2399/ana.18.077
QR code:
deomed

Correspondence to: Temidayo Daniel Adeniyi, PhD
Department of Medical Laboratory Science, School of Basic Medical Sciences, College of Pure and Applied Sciences, Kwara State University, Malete, Kwara State, Nigeria
Phone: +234 803 061 2404
e-mail: temidayo.adeniyi@kwasu.edu.ng

Conflict of interest statement: No conflicts declared.

Original Article

www.anatomy.org.tr
Received: November 16, 2018; Accepted: November 27, 2018
doi:10.2399/ana.18.084

anatomy
An International Journal of Experimental and Clinical Anatomy

Localization of the bregma and its clinical relevance

Bilgehan Solmaz

Department of Neurosurgery, Istanbul Education and Research Hospital, Istanbul, Turkey

Abstract

Objectives: External landmarks on the skull are important guides in various neurosurgical procedures. The localization of the bregma is vitally important in bedside ventriculostomy and craniotomies. The aim of the current study was to verify the localization of the bregma.

Methods: This was performed on dry skulls (n=72) and sagittal computerized tomography (CT) images of patients (n=100). The age and the sex of dry skulls were unknown. Of the 100 patients, 48 were males and 52 were females and the mean age for males was 51.14 and for females was 55.34. The distance between nasion to inion and nasion to bregma were measured from both dry skulls and on multiplanar reformation (MPR) sagittal images. The ratio of the two measurements was calculated.

Results: The nasion to bregma distances on 72 dry skulls ranged between 120–140 mm: the average distance was 124.3±6.9 mm. The nasion to inion distance ranged between 295–345 mm; the average was 320.8±14.4 mm. The ratio of nasion to bregma distance to nasion to inion distance was calculated as 0.384. The nasion to bregma distance obtained from 100 CT images scans ranged from 107 to 139 mm (average 126.6±7.3) mm. The nasion to inion distances ranged between 301 and 356 (average 330.2±15.2) mm. The ratio of nasion to bregma distance to nasion to inion distance was calculated as 0.383. Measurements for females were lower than males, but there was no statistical significance between genders. The multiplication of the nasion to inion distance by 0.38 gave the location of bregma for both genders.

Conclusion: An accurate and reliable ratio (0.38 times the distance from nasion to inion) was obtained to define the bregma. The coronal suture lay on each side of bregma, so knowing the exact localization of bregma and of the coronal suture can be vitally important in various surgical procedures to the cranium.

Keywords: coronal suture; craniotomy; external landmark; ventriculostomy

Anatomy 2018;12(3):135–139

Introduction

The bregma, an external promontory on the skull, is an important bony landmark for various neurosurgical interventions such as bedside ventriculostomy and various craniotomies. The coronal suture lateral to the bregma on each side is used as guide to reach the precentral and postcentral gyri and the central sulcus. Therefore, for preoperative and intraoperative localization of the relevant cortical areas, the bony superficial landmarks are of utmost importance. Additionally, a frontal burr hole (Kocher's point) is made anterior to the coronal suture to approach the lateral ventricle and avoid the motor strip. Empirical methods such as finger pad palpation have been used in localizing the bregma and the coronal suture.

This anatomical study aimed to verify the exact localization of the bregma and the coronal suture using dry skulls and computerized tomography (CT). Newer imaging techniques and improved technology such as navigation systems can demonstrate fine details of the region. Although more than 2,000 medical facilities world-wide utilize these systems, many institutions do not have this technological capacity,[1] and in such situations it is valuable to have fine anatomical knowledge of the localization of the bregma as well as the coronal suture.

Materials and Methods

The measurements were obtained from dry skulls and from sagittal CT images. A total of seventy-two adult skulls of

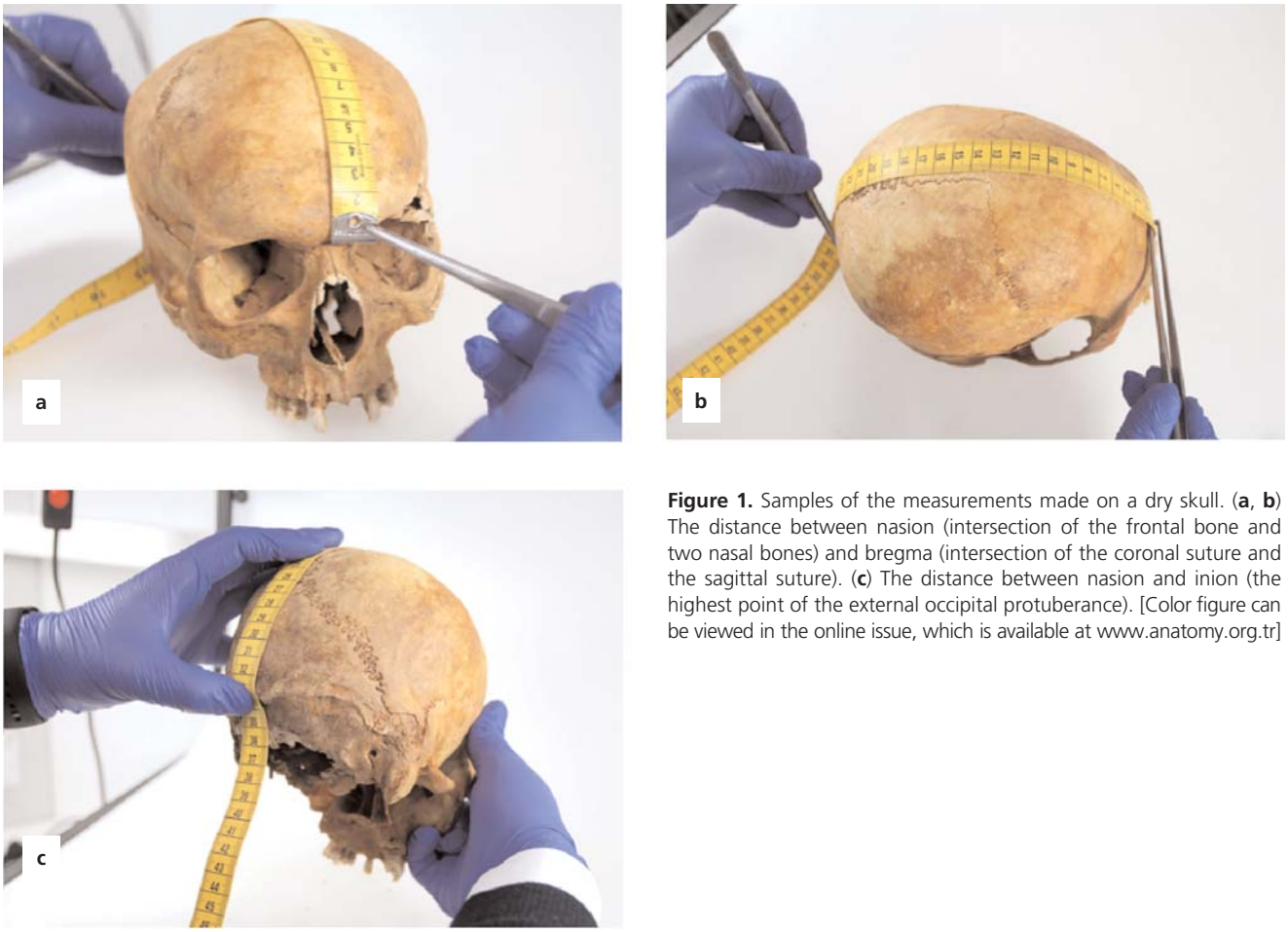

Figure 1. Samples of the measurements made on a dry skull. (**a**, **b**) The distance between nasion (intersection of the frontal bone and two nasal bones) and bregma (intersection of the coronal suture and the sagittal suture). (**c**) The distance between nasion and inion (the highest point of the external occipital protuberance). [Color figure can be viewed in the online issue, which is available at www.anatomy.org.tr]

unknown age and gender were obtained from the Laboratory of Human Anatomy, Istanbul University School of Dentistry, Istanbul, Turkey. The CT images were obtained from patients who underwent CT angiography for a suspicion of a ruptured aneurysm at the Department of Neurosurgery of Marmara University, Istanbul, Turkey, from January 2012 to December 2014. Of the 100 patients, 48 were males and 52 were females, and the mean age was 53.39 (range 18–85) years.

Three anatomical landmarks on the outer surface of the dry skull were defined: nasion (intersection of the frontal bone and two nasal bones), bregma (intersection of the coronal suture and the sagittal suture), and inion (the highest point of the external occipital protuberance). The distance between nasion-inion and nasion-bregma were measured using a tape measure (**Figure 1**). The same measurements were repeated in two-dimensional (2D) multiplanar reformation (MPR) sagittal images with simultaneous correlation of coronal and axial plane CT images by using the Philips IntelliSpace Portal (v5.0.2.40009; Philips Healthcare, Cleveland, OH, USA) software (**Figure 2**). Independent t-test was used to compare means of two groups. Data analysis was done with using SPSS Version 21.0 statistical software (SPSS Inc., Chicago, IL, USA).

Results

The nasion to bregma distance obtained from 72 dry skulls ranged between 120 and 140 mm and the average measurement was 124.3±6.9 mm. The nasion to inion distance ranged between 295–345 (average 320.8±14.5) mm (**Table 1**). The ratio of nasion to bregma distance to nasion to inion distance was calculated as 0.384.

The nasion to bregma distance obtained from 100 CT images ranged between 107–139 (average 126.6±7.3) mm. The nasion to inion distance ranged between 301–356 (average 330.2±15.2) mm (**Table 1**). The ratio of nasion to bregma distance to nasion to inion distance was calculated as 0.383. No statistically significant difference was present between two groups regarding either the nasion to bregma and nasion to inion measurements or the ratio between two groups ($p<0.05$).

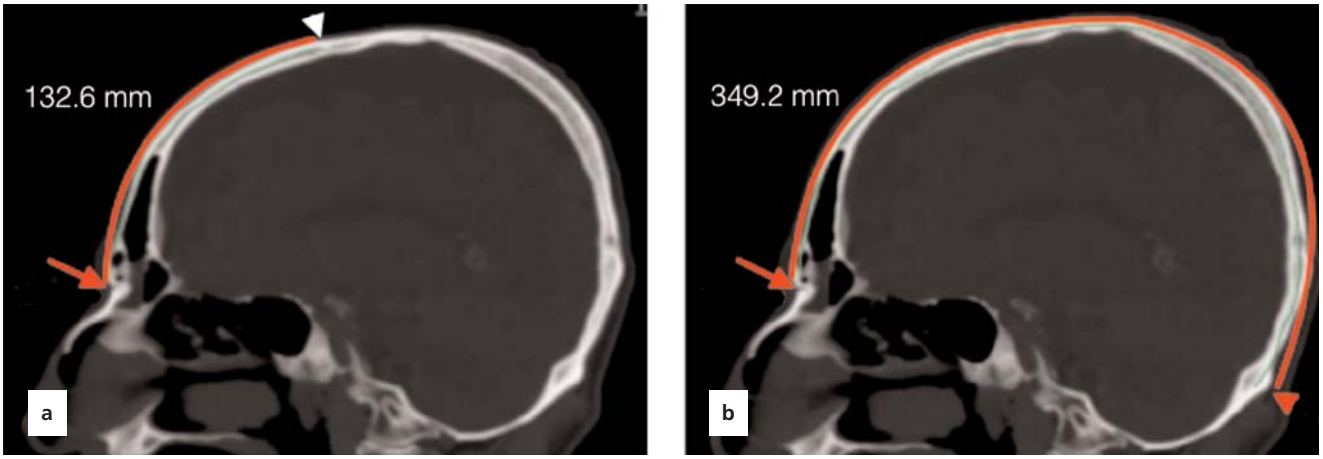

Figure 2. Samples of measurements made on sagittal computerized tomography (CT) images of the patients. (**a**) The distance between nasion (**red arrow**) and bregma (**white arrowhead**). (**b**) The distance between nasion and inion (**red arrowhead**). [Color figure can be viewed in the online issue, which is available at www.anatomy.org.tr]

Discussion

The bregma and the coronal suture are important bony landmarks on the skull. Empiric methods are used to localize these structures. In the present study, we developed an accurate and reliable ratio (0.38 times of the distance between the nasion to inion) which determined the location of bregma and also of coronal suture situated lateral to bregma. The cranial sutures connecting the flat bones of the neurocranium are derived from neural crest cells and paraxial mesoderm. The single coronal suture is one of the synarthroses comprising the cranial vault, separating the frontal from the parietal bones. The coronal suture was first described by Avicenna in his Canon *(al-Qanun fi'l-Tibb)* as "an arc in whose center a perpendicular line has been set up". In the early half of 11th century, William of Saliceto, a prominent surgeon of 13th century, used the term "coronal suture" for the first time.[2]

Numerous craniometric methods have been described to define the location of the central sulcus and the motor cortex.[3–10] Additionally, there are studies which have shown the relation between the coronal suture and central sulcus. However, there are few morphometric studies related to the bregma junction itself.[11] In the literature, the average distance between the nasion to bregma was reported as 126.6 mm on CT. In the present study, we measured this distance as 124.3±6.9 mm on dry skulls and 126.6±7.3 mm on CT. Our CT measurements were exactly the same with the former study; however, dry skull measurements were slightly lower than the CT measurements.[12] The only other study that defined the location of the bregma in terms of a ratio was by Anderson and Makins in 1889.[13] They defined the bregma as two-fifths of the length of nasion to inion (0.4 ratio) and in accordance with our ratio (0.38 ≈ 2/5 nasion to inion).

The bregma and the coronal suture are frequently used as landmarks since they can be easily recognized radiologically and palpated subcutaneously. However, sometimes it can be a challenge to palpate these structures, particularly if not performed by experienced hands. In cases when coronal suture is partly or completely synostotic, it is almost impossible to palpate. With the 0.38 ratio we

Table 1
Descriptive statistics of continuous data.

	Dry skulls (n=72)	CT (male+female) (n=102)	p-value
Nasion-bregma distance mean±SD (mm)	124.3±6.9	126.6±7.3	<0.001
Nasion-inion distance mean±SD (mm)	320.8±14.4	330.2±15.2	<0.001
Ratio Nasion-bregma/Nasion-inion	0.384	0.383	<0.001

n: sample count; **SD:** standard deviation.

suggest, bregma can be midsagittally localized easily with a negligible error.

The coronal suture lies on each side of the bregma but the coronal suture does not extend perpendicular to the midline. Chen et al.[14] stated that the distance to this perpendicular line; that is, the coronal plane from the coronal suture gradually increases with distance from the bregma. In the same way, the central sulcus and the precentral gyrus bow forward as they pass from the midline. Ebeling et al.[15] described the localization of the coronal suture relative to the precentral gyrus being highly variable. Kendir et al.[16] reported that the precentral gyrus was located approximately 4.5 cm and the postcentral gyrus was located approximately 6.5 cm behind the bregma on the midline. Rivet et al.[17] stated that the distance from the coronal suture to the motor cortex was <3 cm in children under 6 years. Sarmento et al.[18] stated that the distance between the coronal suture and the central sulcus ranged from 5 to 6.6 cm, in accordance to measurements of Gusmão et al.[11] and Ribas et al.[12] in the adult. Further, Frigeri et al.[19] reported that the precentral gyrus and central sulcus are closest at a point near where the superior temporal line crossed the coronal suture. Further, at this point all the branches of the middle meningeal artery ran posterior to the coronal suture. Therefore, the location of bregma and coronal suture is used as an important guide during preoperative surgical planning.

The bregma point and croronal suture are important bony landmarks for various neurosurgical procedures such as external ventricular drainage (EVD) placement, endoscopic third ventriculostomy (ETV) and craniotomy.[20] Amongst them, EVD placement is one of the most common emergent and life-saving procedures in neurosurgery practice. For this purpose, freehand pass technique is frequently performed at the bedside by young neurosurgeon trainees. Ventricular catheter is inserted from a frontal burrhole toward the ipsilateral frontal horn of the lateral ventricle. Kocher's point is a common burrhole point that is located 2.5 cm from midline and 1 cm anterior to the coronal suture. ETV is increasingly used as a treatment of choice in various forms of hydrocephalus, particularly those of obstructive types. The entry point and thereby optimal trajectory are crucial to achieve into the third ventricle floor. Similarly, the coronal suture and bregma point are used to estimate the entry point for ETV.

Sutures are primary sites of osteogenesis mediating much of the growth of the skull instead of simple articulations between bones. The coronal suture provides sagittal growth of the skull. A significant increase, from childhood to adolescence, is expected in the length of the cranial vault. An interruption during cranial growth may result in premature ossification. The author of the present study is aware that suture morphogenesis is a highly complex process produced by multiple factors and their interactions cannot be established on a single algorithm. Even so, since the relationship between the cranial dimensions and sutural complexity plays a prominent role in the development of the adult cranium, there may be a developmental anomaly if the suggested ratio (0.38) does not fit.

In the present study, we specified a ratio which is the quantification of a multiplicative relationship, and thus provided a more accurate number representing the detailed topography. Further, giving a ratio can take individual variations into consideration.

Conclusion

Despite the advancements in intraoperative image guided systems, information on constant landmarks such as bregma, inion and nasion points continue to be indispensable for the neurosurgeon. Therefore, localization of the eloquent cortical areas based on superficial landmarks is of utmost importance in cranitomy procedures.

References

1. Basarslan SK, Göcmez C. Neuronavigation: a revolutionary step of neurosurgery and its education. The Medical Journal of Mustafa Kemal University 2014;17:24–31.
2. Di Leva A, Brunner E, Davidson J, Pisano P, Haider T, Stone SS, Cusimano MD, Tschabitscher M, Grizzi F. Cranial sutures: a multidisciplinary review. Childs Nerv Syst 29:2013;893–905.
3. Broca P. Sur le principe des localisations cérébrales. Bull Soc d'Anth II 1861;190–204.
4. DaCosta JC, Spitzka EA. Anatomy, descriptive and surgical: Henry Gray. 17th. ed. Philadelphia (PA): Lea & Febiger; 1908. p. 970.
5. Kido DK, LeMay M, Levinson AW, Benson WE. Computed tomographic localization of the precentral gyrus. Radiology 1980;135: 373–7.
6. Martin N, Grafton S, Viñuela F, Dion J, Duckwiler G, Mazziotta J, Lufkin R, Becker D. Imaging techniques for cortical functional localization. Clin Neurosurg 1992;38:132–65.
7. Rhoton AL Jr. The cerebrum. Neurosurgery 2002:51:S1–51.
8. Schultze OMS, Steward GD: Atlas and textbook of topographic and applied anatomy. Philadelphia (PA): WB Saunders; 1905. p. 37.
9. Taylor AJ, Haughton VM, Syvertsen A, Ho KC. Taylor-Haughton line revisited. AJNR Am J Neuroradiol 1980;1:55–6.
10. Wilkins RH, Rengachary SS (editors). Neurosurgery. New York (NY): McGraw-Hill; 1985. p. 3633–43.
11. Gusmão S, Reis C, Silveira RL, Cabral G. Relationships between the coronal suture and the sulci of the lateral convexity of the frontal lobe: neurosurgical applications. Arq Neuropsiquiatr 2001;59:570–6.
12. Ribas GC, Yasuda A, Ribas EC, Nishikuni K, Rodrigues AJ Jr. Surgical anatomy of microneurosurgical sulcal key points. Neurosurgery 2006;59:177–210.

13. Anderson W, Makins GH. Experiments in cranio-cerebral topography. J Anat Physiol 1889;23:455–65.
14. Chen F, Chen T, Nakaji P. Adjustment of the endoscopic third ventriculostomy entry point based on the anatomical relationship between coronal and sagittal sutures. J Neurosurg 2013;118:510–3.
15. Ebeling U, Rikli D, Huber P, Reulen HJ. The coronal suture, a useful bony landmark in neurosurgery? Craniocerebral topography between bony landmarks on the skull and the brain. Acta Neurochir (Wien) 1987;89:130–4.
16. Kendir S, Acar HI, Comert A, Ozdemir M, Kahilogullari G, Elhan A, Ugur HC. Window anatomy for neurosurgical approaches. Laboratory investigation. J Neurosurg 2009;111:365–70.
17. Rivet DJ, O'Brien DF, Park TS, Ojemann JG. Distance of the motor cortex from the coronal suture as a function of age. Pediatr Neurosurg 40:2004;215–9.
18. Sarmento SA, Jácome DC, de Andrade EM, Melo AV, de Oliveira OR, Tedeschi H. Relationship between the coronal suture and the central lobe: how important is it and how can we use it in surgical planning? Arq Neuropsiquiatr 2008;66:868–71.
19. Frigeri T, Paglioli E, de Oliveira E, Rhoton AL Jr. Microsurgical anatomy of the central lobe. J Neurosurg 122:2015;483–98.
20. Tubbs RS, Loukas M, Shoja MM, Bellew MP, Cohen-Gadol AA. Surface landmarks for the junction between the transverse and sigmoid sinuses: application of the "strategic" burr hole for suboccipital craniotomy. Neurosurgery 2009;65:37–41.

Online available at:
www.anatomy.org.tr
doi:10.2399/ana.18.084
QR code:

Correspondence to: Bilgehan Solmaz, MD
Department of Neurosurgery, Istanbul Education and Research Hospital, Istanbul, Turkey
Phone: +90 532 381 72 57
e-mail: bilgehansolmaz@yahoo.com.tr

Conflict of interest statement: No conflicts declared.

anatomy
www.anatomy.org.tr
An International Journal of Experimental and Clinical Anatomy

Original Article

www.anatomy.org.tr
Received: November 14, 2018; Accepted: November 28, 2018
doi:10.2399/ana.18.088

Evaluation of the prostatic artery origin using computed tomography angiography

Emre Can Çelebioğlu[1], Sinem Akkaşoğlu[2], Selma Çalışkan[2], Ceren Günenç Beşer[3], Tanzer Sancak[1]

[1]*Department of Radiology, School of Medicine, TOBB University, Ankara, Turkey*
[2]*Department of Anatomy, School of Medicine, Ankara Yıldırım Beyazıt University, Ankara, Turkey*
[3]*Department of Anatomy, School of Medicine, Hacettepe University, Ankara, Turkey*

Abstract

Objectives: Radiological anatomy of the prostatic artery is important for any kind of surgical or interventional procedure related to the prostatic region. The aim of this study was to define prostatic arterial anatomy that is critical for both urologists dealing with prostatic interventions and interventional radiologists dealing with prostatic arterial embolization.

Methods: Computed tomography angiography (CTA) is the gold standard for visualizing pelvic arterial anatomy. In this study, morphometric analyses were performed with CTA in 121 patients (41–89 years) retrospectively. The diameters and origins of 242 prostatic arteries were evaluated.

Results: Average diameter of the right prostatic artery was 0.9–2.4 mm; in 39% of the patients the artery originated from the inferior vesical artery. The other origin patterns on the right side were the internal pudendal artery (36%), gluteopudendal trunk (7.4%), obturator (5,8%), inferior gluteal (3.3%), middle rectal (0.8%), umbilical (0.8%) and inferior rectal (0.8%) arteries, and the vesical trunk (0.8%). Average diameter of the left prostatic artery was 0.9–2.7 mm; in 36% of the patients the artery originated from the inferior vesical artery. Other origin patterns revealed for the left side were the internal pudendal artery (31%), obturator artery (13%), gluteopudendal trunk (9.1%), vesical trunk (2.5%) and inferior gluteal artery (2.5%).

Conclusion: CTA is crucial for better understanding of the prostatic arterial anatomy and preventing the complications in surgical or interventional procedures such as prostatic arterial embolization, especially for atherosclerotic patients. The data obtained in this study is significant for determination of pelvic vascular disorders.

Keywords: anatomy; computed tomography angiography; embolization; prostatic artery; variation

Anatomy 2018;12(3):140–144

Introduction

Benign prostatic hyperplasia (BPH) is one of the most frequent health problems in males that impairs the quality of life in sixth and seventh decades.[1,2] Medications such as 5-α-reductase inhibitors and selective α blockers may help decreasing the voiding symptoms in patients with BPH, but the curative treatment option is surgery. Because of the comorbidities in the elderly, open surgical prostatectomy is considered high risk. Alternative treatments are the minimally invasive transurethral therapies and the prostatic artery embolization (PAE).[1,3]

In previous times, PAE was used to stop the bleeding after radical prostatectomy or prostate biopsy. Reduced prostate volume after PAE was reported in experimental animal studies and case series in the literature.[1] PAE has been shown as a minimal invasive technique that can serve as a strong alternative for surgery at BPH with low morbidity rates.[1] Maintenance of sexual functions and eliminations of daily BPH medications are additional benefits of this procedure.[4]

Knowledge of the radiological anatomy of the prostatic arteries (PAs) is very important before any kind of sur-

This study was presented as an oral presentation at the 19th National Anatomy and 1st International Mediterranean Anatomy Congress, September 6–9, 2018, Konya, Turkey, and this presentation was elected as the best oral presentation in the congress.

gical or interventional procedure. Computed tomography angiography (CTA) is the gold standard for showing pelvic arterial anatomy.[5] Prostate surgery may also cause erectile dysfunction due to the condition of the cavernous nerve and vascular variations such as accessory pudendal artery.[6] CTA presents a detailed anatomical knowledge of vascular variations, helps to prevent complications and ensures optimal postoperative sexual function.[6] Variations of the PA have critical importance and should be well known by the interventional radiologists who are dealing with PAE to prevent ischemic damage of bladder, penis or rectum after embolization.[5,7] Preprocedural CTA could be a good option to demonstrate pelvic arterial anatomy before PAE.[7]

Pelvic arterial anatomy and most common variations in males were previously studied. There are cadaveric and radiological studies in the literature enlightening the vascular supply of pelvic organs.[7–9]

In this study, we aimed to define and classify the PA variations in Turkey by CTA and compare the differences of PA anatomy with earlier studies performed in other populations.

Materials and Methods

Ethics committee approval was received by TOBB ETU Faculty of Medicine Clinical Research Ethics Committee (number: KAEK 118/031). A total of 121 patients were included in the study and were evaluated retrospectively by CTA. Each pelvic side was considered seperately, and the diameters and origins of 242 PAs were reported. The ages of the patients were between 41–89 (mean: 65.29±10.66) years. The diameters of the right and left PAs were measured and the mean diameter for each side was determined.

The CTA images of the cases were obtained from the archive system of TOBB ETU University. CTA examinations were obtained with Philips Ingenuity 128 slice computerized tomography device (Philips Medical Systems, Cleveland, OH, USA). Patient dose parameters were adjusted automatically by the device. 0.8 mm slice thickness and a pitch value of 1 were used with a 300/100 ml or 350/100 ml non-ionic iodinated contrast material. We did not administer any IV or sublingual vasodilators before the angiography procedure. Patients in this study population did not use any kind of medications for prostate disease symptoms. CT scans were made at an area between abdominal aorta to common femoral or superficial femoral arteries near femoral heads. Pelvic arterial anatomy was evaluated with the device software (Philips Intellispace Portal 9.0; Philips Medical Systems, Cleveland, OH, USA) and post-process procedures like slice thickness arrangement, maximum intensity projection (MIP), multiplanar reconstructions (MPR) and 3D reconstructions were made by the radiologist with the software, to reach at the utmost level for evaluating the pelvic anatomy of each patient.

Descriptive statistics were used to get the frequency of each vessel category. Statistical Package for Social Sciences (SPSS for Windows, version 21.0; SPSS Inc., Armonk, NY, USA) was used for analyses. Differences between two means were tested by using t-test and $p<0.05$ was considered as statistical significant.

Results

121 patients who underwent CTA imaging for various indications were included in this study. Each pelvic side was considered seperately, and the diameters and origins of 242 PAs were reported.

The mean diameter of the right and left PAs were measured as 1.56±0.35 (0.9–2.4) mm and 1.54±0.3 (0.9–2.7) mm respectively. The minimum, maximum and mean values of the diameters of the right and left PAs are shown in **Figure 1**.

In this study, a total of 242 PAs originating from nine different sources were reported. Of the 121 right PAs, 47 (39%) were found to originate from the inferior vesical artery. Forty-three of the cases (36%) originated from the internal pudendal artery, 9 (7.4%) from the gluteo-pudendal trunk, 7 (5.8%) of from the obturator artery, 4 (3.3%) from the inferior gluteal artery, 1 (0.8%) from the middle

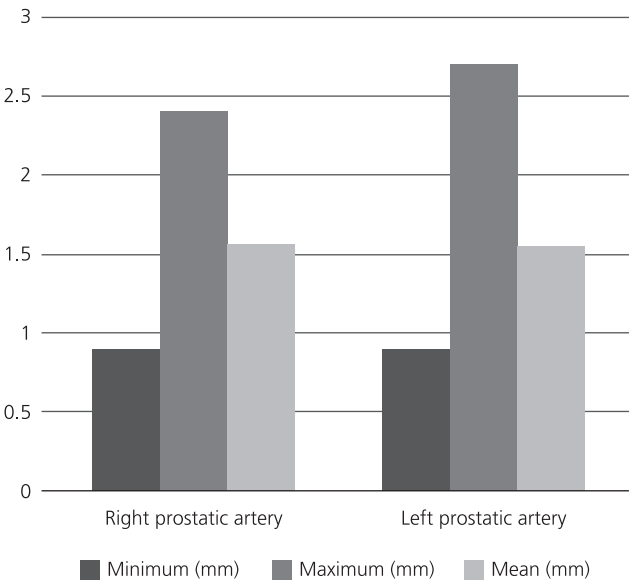

Figure 1. Diameter of the right and left prostatic artery.

rectal artery, 1 (0.8%) from the umbilical artery, 1 (0.8%) from the vesical trunk and 1 (0.8%) from the inferior rectal artery (**Figures 2** and **3**; **Table 1**).

Of the 121 left PAs, 43 (36%) originated from the inferior vesical artery. Thirty-eight (31%) cases originated from the internal pudendal artery, 16 (13%) cases from the obturator artery, 11 (9.1%) from the gluteo-pudendal trunk, 3 (2.5%) from the vesical trunk and 3 (%2.5) from the inferior gluteal artery (**Figures 2** and **3**; **Table 2**).

The origins of right and left PAs are summarized in **Tables 1** and **2**.

In this study, accessory prostatic arteries were also evaluated. Accessory prostatic arteries were found in 10 cases; 8 of them were on the left and 2 of them were on right side.

Table 1
Origin of the right prostatic artery.

Origin	n	Ratio (%)
Internal pudendal artery	43	36
Inferior vesical artery	47	39
Middle rectal artery	1	0.8
Obturator artery	7	5.8
Gluteo-pudendal artery	9	7.4
Inferior gluteal artery	4	3.3
Umblical artery	1	0.8
Vesical trunk	1	0.8
Inferior rectal artery	1	0.8

Discussion

Because of the indistinguishable fat and small nerves and vessels, it is difficult to evaluate the pelvic vascular anatomy in cadavers.[10–12] Besides, cadaveric dissection procedure is likely to damage the relevant structures.[10] Radiologic images present us detailed information about anastomoses, variations and dominance of arteries supplying the prostate. These are important parameters when planning PAE to prevent penis, rectum and bladder from ischemia related to non-target embolization.[10] CTA images are used in this study because of the ability to receive more detailed information about branching patterns of vessels in large patient series in a short time period.

PAs may be depicted by cadaver dissection and imaging modalities such as CTA, digital subtraction angiography (DSA), MR angiography (MRA) and cone beam CT.[5,7–12] Because CTA and MRA are non-invasive procedures, they allow better planning of PAE than digital angiography.[5] Besides, Bilhim et al.[5] claimed that CTA provides more detailed anatomy than MRA. DSA is sometimes incapable of identifying the PA origin because of superimpositions.[10] Cone beam CT has been considered as a good option for better understanding of the pelvic arterial anatomy, with less contrast media and less X-ray doses with similar results, in contrast to CTA. However, it is still an invasive technique that should be done with an arterial puncture intra-procedurally at an angiography suite. It has recently been shown that there are no subjective advantages of cone beam CT over CTA. Besides having a CTA before PA, embolization may affect the puncture site, catheter selection or even abortion of the embolization procedure due to the arterial anatomy or atherosclerotic disease.[10,13] CTA is still

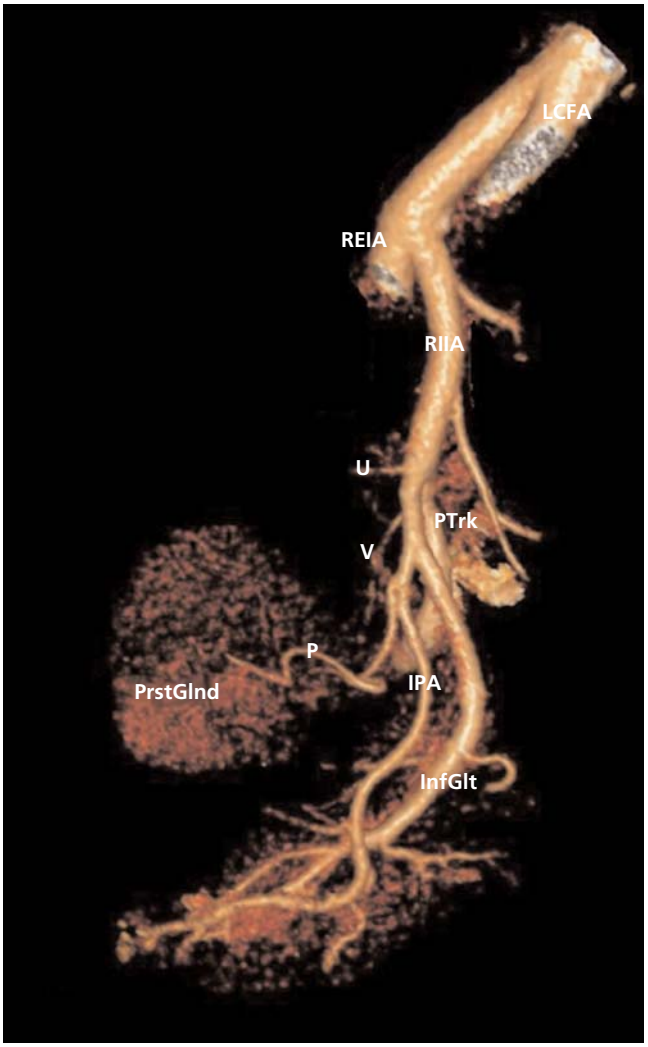

Figure 2. 3D rendered images of right internal iliac artery anterior division. **InfGlt:** inferior gluteal artery; **IPA:** internal pudendal artery; **LCIA:** left common iliac artery; **P:** prostatic artery; **REIA:** right external iliac artery; **RIIA:** right internal iliac artery; **U:** umblical artery; **PrstGlnd:** prostatic gland; **PTrk:** posterior trunk; **V:** vesical artery. [Color figure can be viewed in the online issue, which is available at www.anatomy.org.tr]

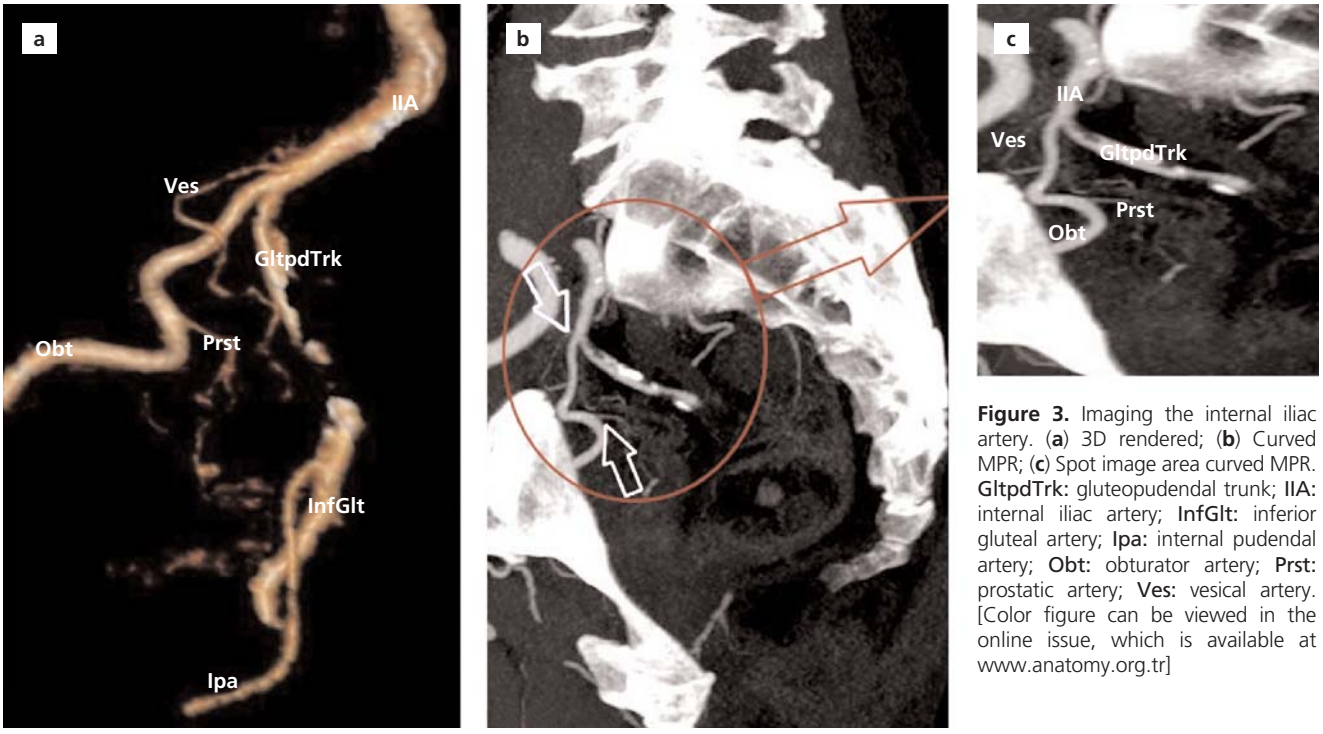

Figure 3. Imaging the internal iliac artery. (**a**) 3D rendered; (**b**) Curved MPR; (**c**) Spot image area curved MPR. **GltpdTrk:** gluteopudendal trunk; **IIA:** internal iliac artery; **InfGlt:** inferior gluteal artery; **Ipa:** internal pudendal artery; **Obt:** obturator artery; **Prst:** prostatic artery; **Ves:** vesical artery. [Color figure can be viewed in the online issue, which is available at www.anatomy.org.tr]

the gold standard method for depicting the pelvic vascular anatomy while planning the PAE.[5,13]

Bouissou and Talazac[14] were the first to describe two cadaveric independent PAs on each pelvic side. They dissected 100 pelvic halves and defined a cranial PA supplying inner and cranial prostate gland and a caudal PA supplying the peripheral and caudal gland. Zhang et al.[10] reported a 3.6% rate of two independent PAs of the pelvic side in their study. Two independent PAs may cause insufficient clinical outcomes after PAE and must be kept in mind. In our study, we found accessory prostatic arteries in 10 cases. This finding is coherent with the literature.

Clegg et al.[15] studied PA in 21 postmortem materials in 1955. They used radio-opaque medium to assist the arterial supply of the prostate. The radiographs of the dissected specimens were obtained. They found that the prostatic gland was supplied by prostatic branch of an artery that was named as prostato-vesical artery. They defined prostato-vesical artery as a well-defined trunk with a variable origin but this is not a current nomenclature. They also reported superior rectal artery giving rise to PA in 32.1% of the cases. In this study, we did not find any PA arising from the superior rectal artery.

Ambrosio et al.[16] studied with 40 pelvic halves in 1980 and found that PA origin was variable (arising from the inferior vesical, internal pudendal, umbilical, obturator, inferior gluteal or internal iliac artery). Similarly, in this study, we did not find any internal iliac artery giving rise to PA.

Moya et al.[8] studied on 10 adult pelvic sides from embalmed cadavers and 34 DSA pelvic angiographies. Fifty-eight PAs were evaluated in their study. They generated six types of PA origins using a total of 735 PAs including their data and previously published data. This study included different patients from different countries and did not present the variations of PA in a certain population. These data were obtained from cadaver dissections, DSA and cone beam CT.[8]

In this study, we evaluated 242 PAs of a single population by the same radiologist using CTA as a single procedure. According to the classification of PAs in the work of

Table 2
Origin of the left prostatic artery.

Origin	n	Ratio (%)
Inferior vesical artery	43	36
Vesical trunk	3	2.5
Gluteo-pudendal trunk	11	9.1
Obturator artery	16	13
Internal pudendal artery	38	31
Inferior gluteal artery	3	2.5

Moya et al.[8] Type I, indicated anterior division of internal pudendal artery to give rise to PA, and Type IV, which presents internal pudendal artery as the origin site of PA, were the most common types.

In the present study, the most common origin of the PA was the inferior vesical artery arising from the anterior division of the internal iliac arteries (Type I in Moya classification). The internal pudendal artery was the second most common site of origin for the PA in our population (Type IV in Moya classification).

In this study, there are differences from the previously published studies in the literature. We suggest that this discrepancy may depend on different patient populations from different countries. However, we need larger patient series to claim this hypothesis in terms of statistics, and this is one of limitations of our study.

Conclusion

It is very important to understand the PA anatomy prior to any surgical or interventional procedure related to the prostate gland. Conventional CTA is the gold standard for depicting PA anatomy, and should be considered as a first line option before surgical or interventional procedures.

References

1. Carnevale FC, Antunes AA, da Motta Leal Filho JM, de Oliveira Cerri LM, Baroni RH, Marcelino AS, Freire GC, Moreira AM, Srougi M, Cerri GG. Prostatic artery embolization as a primary treatment for benign prostatic hyperplasia: preliminary results in two patients. Cardiovasc Intervent Radiol 2010;33:355–61.
2. Garvey B, Türkbey B, Truong H, Bernardo M, Periaswamy S, Choyke PL. Clinical value of prostate segmentation and volume determination on MRI in benign prostatic hyperplasia. Diagn Interv Radiol 2014;20:229–33.
3. Mirakhur A, McWilliams JP. Prostate artery embolization for benign prostatic hyperplasia: current status. Can Assoc Radiol J 2017;68:84–9.
4. Pisco J, Bilhim T, Pinheiro LC, Fernandes L, Pereira J, Costa NV, Duarte M, Oliveira AGJ. Prostate embolization as an alternative to open surgery in patients with large prostate and moderate to severe lower urinary tract symptoms. Vasc Interv Radiol 2016;27:700–8.
5. Bilhim T, Casal D, Furtado A, Pais D, O'Neill JE, Pisco JM. Branching patterns of the male internal iliac artery: imaging findings. Surg Radiol Anat 2011;33:151–9.
6. Park BJ, Sung DJ, Kim MJ, Cho SB, Kim YH, Chung KB, Kang SH, Cheon J. The incidence and anatomy of accessory pudendal arteries as depicted on multidetector-row CT angiography: clinical implications of preoperative evaluation for laparoscopic and robot-assisted radical prostatectomy. Korean J Radiol 2009;10:587–95.
7. Bilhim T, Tinto HR, Fernandes L, Martins Pisco J. Radiological anatomy of prostatic arteries. Tech Vasc Interv Radiol 2012;15:276–85.
8. Moya C, Cuesta J, Friera A, Gil-Vernet Sedo JM, Valderrama-Canales FJ. Cadaveric and radiologic study of the anatomical variations of the prostatic arteries: a review of the literature and a new classification proposal with application to prostatectomy. Clin Anat 2017;30:71–80.
9. Yamaki K, Saga T, Doi Y, Aida K, Yoshizuka M. A statistical study of the branching of the human internal iliac artery. Kurume Med J 1998;45:333–40.
10. Zhang G, Wang M, Duan F, Yuan K, Li K, Yan J, Chang Z, Wang Y. Radiological findings of prostatic arterial anatomy for prostatic arterial embolization: preliminary study in 55 Chinese patients with benign prostatic hyperplasia. PLoS One 2015;10:e0132678.
11. Venuti JM, Imielinska C, Molholt P. New views of male pelvic anatomy: role of computer-generated 3D images. Clin Anat 2004;17:261–71.
12. Ding HM1, Yin ZX, Zhou XB, Li YB, Tang ML, Chen SH, Xu DC, Zhong SZ. Three-dimensional visualization of pelvic vascularity. Surg Radiol Anat 2008;30:437–42.
13. Desai H, Yu H, Ohana E, Gunnell ET, Kim J, Isaacson A. Comparative analysis of cone-beam CT angiogram and conventional CT angiogram for prostatic artery identification prior to embolization. J Vasc Interv Radiol 2018;29:229–32.
14. Bouıssou H, Talazac A. Arterial vascularization of the normal and the pathological prostate. Ann Anat Pathol (Paris). 1959;4:63–79.
15. Clegg EJ. The arterial supply of the human prostate and seminal vesicles. J Anat 1955;89:209–16.
16. Ambrósio JD, De Almeida JS, De Souza A. Origin of prostatic arteries in man. Rev Paul Med 1980;96:52–5.

Online available at: www.anatomy.org.tr
doi:10.2399/ana.18.088
QR code:

Correspondence to: Ceren Günenç Beşer, MD, PhD
Department of Anatomy, School of Medicine, Hacettepe University, Sıhhıye, Ankara, Turkey
Phone: +90 532 521 22 78
e-mail: cerengnc@hacettepe.edu.tr

Conflict of interest statement: No conflicts declared.

Teaching Anatomy

www.anatomy.org.tr
Received: October 15, 2018; Accepted: December 3, 2018
doi:10.2399/ana.18.069

anatomy
www.anatomy.org.tr
An International Journal of Experimental and Clinical Anatomy

Physical and emotional impact of cadaver dissection on innovative medical education students: a survey in Ethiopia

Melese Shenkut Abebe

Department of Anatomy, School of Medicine, College of Medicine and Health Science, Wollo University, Dessie, Ethiopia

Abstract

Objectives: Although many studies have been conducted worldwide to investigate the positive and negative experiences of the cadaver room, there is no documented research in medical schools delivering the new innovative medical education (NIME) curriculum which involves teaching students who already receive a bachelor degree in any natural science including health sciences and having at least two years of work experience. Therefore, this study aimed to assess the effect of cadaver dissection both physically and emotionally on NIME students.

Methods: A survey was done on 82 first and second-year NIME students using standard structured questionnaire. The students were evaluated according to gender, religion and ethnicity.

Results: Students experienced multiple symptoms in the dissection room. The most prevalent physical symptoms were nausea (32%), palpitation (20.7%) and sweating (17.1%). In addition to these, sadness (41.5%), fear (34.1%) and worry (29.3%) were mostly reported emotional experiences. Females were more significantly nervous than males ($p=0.03$). Students of Oromo ethnicity reported a significantly higher degree of fainting ($p=0.03$), dizziness ($p=0.02$), and palpitation ($p=0.02$) than other ethnic students. Sweating and breathlessness were significantly decreased in year two compared to year one students ($p<0.05$). The smell of the cadaver was the most stressing aspect of the cadaver room. Females had nightmares more significantly than males in the post-dissection period ($p=0.04$).

Conclusion: Students experience a variety of physical and emotional symptoms during dissection. These can affect the performance of the students. this study provides data for these symptoms in NIME students, and their relation to gender, religion and ethnicity.

Keywords: cadaver dissection; emotional impact; medical students; physical impact

Anatomy 2018;12(3):145–151

Introduction

Anatomy, the study of the structures of the human body is one of the first, most basic and important subjects studied by medical students when they begin their medical education.[1] Dissection of the dead human body has been central to medical education since Renaissance.[1,2] Indeed, the Greek roots of the word anatomy indicate cutting apart; so, many anatomists are adamant that dissection is the best way to learn anatomy.[3,4] Some scholars described dissection as the most universal and universally recognizable step in becoming a doctor.[2] An old fashioned way of anatomy teaching in medical schools is based on the use of human cadaveric specimens, either taking the whole body specimens for complete dissection or as prosected specimens.[2]

In the 18th century, the study of gross anatomy was dependent on cadaveric dissection, because that was the only available method for three-dimensional studies of the gross anatomical structures. However, with the passage of time and, as a result of advances in science and technology, there have been revolutionary changes in teaching methodologies.[5] In spite of that, cadaveric dissection cannot be dismissed as obsolete and is still of paramount importance in medical education.[4]

In addition, the use of the human body dissection for teaching medical students helps them to identify the real, natural and unbiased organs of the human being. It is also a means to learn anatomical variation before they are exposed to the real patient. This will let them prepare to face the challenges during their clinical practice.[6–8]

However, it is good to realize that cadaver dissection has multiple physical and psychological effects on students. These experiences especially worsen during the first period of dissecting the cadaver.[9]

In Ethiopia, there are two types of medical education curriculum; the conventional curriculum used to teach students directly coming from the high school, and the other called new innovative medical education (NIME) curriculum to teach students who already receive a bachelor degree in any natural science including health sciences and have at least two years of work experience.

Wollo University is one of the 13 institutions that launched the new NIME curriculum. In the NIME curriculum, the anatomy course is given as integrated with other basic science courses.

Therefore, dissection of the cadaver is done in the first two pre-clinical years of the NIME curriculum.

Multiple types of research have been conducted worldwide and indicated both positive and negative experiences of the cadaver room.[10–14] However, there is no documented research conducted in medical schools delivering the NIME curriculum. This study aimed to assess the effect of cadaver dissection both physically and emotionally on NIME students.

Materials and Methods

This research was conducted on 85 first and second year NIME students of Wollo University in 2016. The students were informed about the objective of the study and the volunteer students were briefed on the questionnaire used as a data collection tool. A standardized questionnaire was used for data collection. The questionnaire includes sociodemographic characteristics and physical and emotional impacts of cadaver dissection on the students. The survey was done at one time after the first system dissection schedule for year one students, and after completion of all system dissection for the second-year students. For the first-year students, those who didn't attend the first system dissection and repeaters were excluded from the study. In addition to this, for both year students, those who didn't avail at the time of data collection were also excluded. The ethical review committee of the School of Medicine, Wollo University approved this work earlier to data collection. The data were entered into Epi Info 7 (Centers for Disease Control and Prevention, 2005) and analyzed using the Statistical Package for Social Sciences (SPSS for Windows, version 22.0, Armonk, NY, USA). $p<0.05$ was considered as statistically significant.

Results

This study was conducted on 85 first and second-year new innovative medical students of Wollo University. From both years, 82 students filled the questionnaire. The average age range for most of the students (70.7%) is 24–27 years. 84.1% and 81.7% of the students were males and Ethiopian Orthodox Christian followers, respectively. The majority (87.8%) of the students were from health science (paramedical science) educational background. In addition to this, 57.3% of the students were urban residents and 80.5% of them were Amhara in ethnicity as showed in **Table 1**.

In the present survey, most of the respondents 75 (91.5%) agreed with the ethical acceptability of cadaver dissection for teaching medical students. All Muslim students agreed on the ethical acceptance of human body utilization for teaching purpose, while 89.6% of Christian students agreed. From a total of 82 students, 95.1% of them preferred cadaver dissections as the best method of learning anatomy and 75.65% of the students didn't think dissecting cadaver is replaced by other methods of teaching. Among the different teaching approaches on the cadaver, self or instructor assisted dissection was preferred by 92.7% of the students. Only 62.2% of the respondents were excited in the first visit of dissection room (**Table 2**).

Since most of the students (87.7%) were from health science background 31.7% of them had previous exposure to the dead body. The previous exposure to dead body resulted in slight and high degree of trauma in 17.1% and 18.3% of the students, respectively.

The top three most stressing components of the dissection room were the smell of the cadaver 45.1%, religious incompatibility 32.9%, and touching a certain part of the cadaver 28% (**Table 3**). Females were more stressed by looking or touching certain parts of the cadaver and by the practical exam compared to males, while males were stressed by the smell, dissection workload, infectiousness of the cadaver and religious incompatibility. Looking at certain parts of the cadaver, smell of the cadaver, fear of infection and the practical exam were stressors for Christian students.

Nausea 32%, palpitation 20.7% and sweating 17.1% were the most prevalent physical symptoms experienced in the dissection room. From the emotional symptoms reported by the students, sadness 41.5% was the first followed by fear (34.1%) and worry (29.3%) (**Table 4**).

Table 1
Sociodemographic characteristics of the NIME students of Wollo University.

Variables		n	%
Age	24–27	58	70.7
	28–31	22	26.8
	32–35	1	1.2
	>35	1	1.2
Gender	Male	69	84.1
	Female	13	15.9
Religion	Orthodox Christian	67	81.7
	Muslim	15	18.3
Educational background	Health sciences	72	87.8
	Teaching	1	1.2
	Applied sciences	3	3.7
	Agriculture	3	3.7
	Veterinary medicine	1	1.2
	Other	2	2.4
Ethnicity	Amhara	66	80.5
	Oromo	2	2.4
	Tigre	8	9.8
	Gurage	3	3.7
	Other	3	3.7
Residence	Urban	47	57.3
	Rural	35	42.7
Year of study	Year one	45	54.9
	Year two	37	45.1

Females were more nervous, depressed, sad and felt eye irritation than the males. On the other hand, males sweated, felt nausea, and fainted.

In religion comparison, Christian students commonly felt dry mouth, fear, depression, and satisfaction; in contrast, Muslim students showed nervousness, sadness, irritation of the eye and vomiting.

Oromo students significantly reported fainting, dizziness and palpitation as compared to the other three ethnic students ($p<0.05$). Although not statistically significant,

Table 2
Responses of the students on general information about cadaver dissection.

Questions	Responses	n	%
Cadaver dissection is ethically acceptable	No	7	8.5
	Yes	75	91.5
Dissection is best method of learning Anatomy	No	4	4.9
	Yes	78	95.1
Cadaver dissection is replaced by other methods	No	62	75.6
	Yes	20	24.4
Preferred method of learning in the cadaver room	Deal with prosected specimen	5	6.1
	Self or instructor assisted dissection	76	92.7
	Deal with dissected cadaver	1	1.2
First visit to the dissection room was exciting	No	31	37.8
	Yes	51	62.2
Have self-mental preparedness prior to the dissection room	No	10	12.2
	Yes	72	87.8

Table 3
Student's response of their most stressful component of the dissection room. For all comparisons p>0.05.

The most stressful component of the dissection room	All % (n=82)	Gender (%)		Religion (%)	
		Male	Female	Christian	Muslim
Looking at certain part of the cadaver	26.8	24.6	38.5	22.4	46.8
Touching certain part of the cadaver	28.0	27.5	30.8	28.4	26.7
The smell of the body	45.1	46.4	38.5	44.8	46.7
Dissection workload	12.2	13	7.7	14.9	0
Religious incompatibility	32.9	33.3	30.8	37.3	13.3
Fear of infection	22.0	24.6	7.7	20.9	26.7
Thinking of practical exam	17.1	15.9	23.1	14.9	26.7

most of the physical and emotional symptoms were less likely to be seen in year one compared to second-year students. However, sweating and breathlessness were significantly less as 26.7% in year one compared to 5.4% in second-year, and 11.1% in year one compared to 0% in second-year students (p<0.05). Instead, nausea, palpitation, and dryness of the mouth were relatively higher for second-year students compared to the first year (**Table 5**).

The most common way of coping strategies used by the students in the cadaver room was focusing on task 46.3% (n=38) followed by seeking advice from instructor or lab assistant 43.9% (n=36) and thirdly stay within the group 25.6% (n=21) as presented in **Table 6**. In addition to this, Christian students sought advice from lab assistant or their instructor, while Muslim students wanted to focus on their task as a coping mechanism in the dissection room. Females prayed and stayed in the group, and males sought an advice.

As shown in **Table 7**, most of the symptoms decreased gradually. However, loss of appetite and headache were still felt after leaving the dissection room. Both males and females, and Christian and Muslim students reported decrement symptoms after they left the cadaver room. However, female students reported insomnia which was statistically significant (p=0.04).

Discussion

Cadaver dissection has been used for a long time as a cornerstone of dealing anatomical science for medical education. Dissection of the human body helps students gets a

Table 4
Physical and emotional symptoms experienced by the students in the cadaver room.

Physical symptoms	All (%) (n=82)	Gender (%)		Religion (%)		Ethnicity (%)			
		Male	Female	Christian	Muslim	Amhara	Oromo	Tigre	Gurage
Fainting	4.9	5.8	0	4.5	6.7	3	50*	12.5	0
Dizziness	12.2	11.6	15.4	11.9	13.3	9.1	100*	12.5	33.3
Nausea	32.9	33.3	30.8	32.8	33.3	34.8	100	25	0
Vomiting	3.7	4.3	0	3	6.7	1.5	50	12.5	0
Palpitation	20.7	18.8	30.8	20.9	20	22.7	100*	0	0
Sweating	17.1	18.8	7.7	16.4	20	18.2	50	12.5	0
Breathlessness	6.1	5.8	7.7	6	6.7	6.1	50	0	0
Irritation of the eye	9.8	7.2	23.1	6.7	10.4	7.6	100	33.3	33.3
Dryness of the mouth	7.3	7.2	7.7	9	0	7.6	50	33.3	33.3
Worry	29.3	30.4	23.1	32.8	13.3	31.8	0	38.5	0
Fear	34.1	31.9	46.2	35.8	26.7	33	100	33	66.7
Satisfaction	18.3	11.6	7.7	11.9	6.7	9.1	0	37.5	33.3
Sadness	41.5	39.1	53.8	37.3	60	39.4	0	50	33.3
Depression	14.6	11.6	30.8	14.9	13.3	15.2	50	12.5	33.3
Nervousness	12.2	8.7	30.8*	10.4	20	10.6	50	33.3	33.3

*p<0.05.

Table 5
Physical and emotional symptoms of the respondents by year.

Variables	Year of study n (%)		p-value
	Year one	Year two	
Fainting	4 (8.9)	0	*
Dizziness	6 (13.3)	4 (10.8)	*
Nausea	12 (26.7)	15 (40.5)	*
Vomiting	3 (6.7)	0	*
Palpitation	9 (20)	8 (21.6)	*
Sweating	12 (26.7)	2 (5.4)	0.011
Breathlessness	5 (11.1)	0	0.036
Irritation of the eye	5 (11.1)	3 (8.1)	*
Skin irritation	2 (4.4)	0	*
Dryness of the mouth	2 (4.4)	4 (10.8)	*
Worry	13 (28.9)	11 (29.7)	*
Fear	16 (35.6)	12 (32.4)	*
Satisfaction	8 (17.8)	7 (17.9)	*
Sadness	20 (44.4)	14 (37.8)	*
Depression	9 (20)	3 (8.1)	*
Nervousness	6 (13.3)	4 (10.8)	*

*p>0.05.

meaningful and unbiased structure of human beings. In spite of this, students are experiencing a variety of physical and emotional symptoms at the time of dissection. These impacts can affect the performance of the students.

The ethical acceptability of cadaver dissection as agreed by most students irrespective of religion indicates that cadaver is a valuable gift to medical education. This is supported by the findings of Agnihotri and Sagoo[15] and Rajeh et al.[16]

Our students agreed that cadaver dissection should not be replaced with plastic models or 3D images (75.6%) and is the best method of learning anatomy (95.1%). Self or instructor assisted dissection was preferred by 92.7% of our respondents to studying prosected specimen or dissected cadaver. This is in close proximity with the findings of Agnihotri and Sagoo,[15] Johnson,[17] Shugaba et al.,[18] but different from the study of McLachlan et al.[2] This difference may be due to the student's perception and level of understanding of new technology. Based on our findings, the idea of replacing the cadaver dissection technique with plastic models, computer-assisted training or other methods is challenged, as the utilization of human body dissection helps students to grasp the three-dimensional anatomy and concept of countless variations.[19]

This survey is intended to show the impacts of cadaver dissection immediately after the first-time dissection and after repeated dissections. Therefore, according to this investigation, nausea, palpitation and sweating were the

Table 6
Strategies used by students to help them cope with dissection. For all comparisons p>0.05.

Variables	All (%)	Gender (%)		Religion (%)	
		Male	Female	Christian	Muslim
Focusing on the task	46.3	46.4	46.2	40.3	60.3
Self-prayer	9.8	7.2	23.1	11.9	0
Stay within the group	25.6	24.6	30.8	26.9	20
Temporary departure from the dissection room	1.2	1.4	0	1.5	0
Seeking advice from lab assistance/instructors	43.9	44.9	38.5	47.8	26.7

Table 7
Responses on the symptoms that continue after leaving the dissecting room.

Symptoms	All (%)	Gender (%)			Religion (%)		
		Male	Female	p-value	Christian	Muslim	p-value
Loss of appetite	40.2	40.6	38.5	*	41.8	33.3	*
Insomnia or nightmare	13.4	10.1	30.8	0.04	14.9	6.7	*
Dizziness	11.0	10.1	15.4	*	10.4	13.3	*
Headache	22.0	18.8	38.5	*	20.9	26.7	*
Loss of concentration on study	13.4	11.6	23.1	*	14.9	6.7	*
Symptoms decrease gradually	90.2	91.3	84.6	*	88.1	100	*

*p>0.05.

most prevalent physical symptoms experience in the dissection room. This finding is almost consistent with a research conducted in Tanzania at Muhimbili University which showed disgust, fear, nausea, loss of appetite and sweating as the commonest symptom.[11] Another research done in India by Vinay et al.[20] indicated the commonest symptoms as eye irritation (63.33%), headache (10%), decrease in appetite (12%), nausea (3.3%) and sweating (35.33%).

The research conducted in Foundation University Medical College, Rawalpindi, Pakistan pointed out eye soreness and fatigue (39.9%) and throat irritation (41.6%) as the most common physical symptom. This finding was different from ours, possibly due to different laboratory setup, age and educational background of our students as our study subjects had a minimum of bachelor degree.[21]

The most prevalent emotional symptoms depicted in this research were sadness, fear and worry. This finding is also similar to the above researchers.

In the comparison done between males and females, females were more nervous than males. This variable showed a significant difference (p=0.03). This may indicate a gender difference in behavioral response to cadaver dissection.[22] Students with Oromo ethnicity reported a significantly higher degree of fainting (p=0.03), dizziness (p=0.02), and palpitation (p=0.02) than other ethnic students. No significant differences were found for the other symptoms.

As presented in **Table 6**, this study also compared the decrement of the symptoms between the two batch students. The prevalence for most of the symptoms decreased for the second-year students. This is because of repeated exposure to the dissection. This finding was also reported in other studies.[20,23,24]

According to a research conducted in Hawasa University and the University of Gondar, Ethiopia, most stressing component of the dissection room was the smell of the dissection room. This is also the same in this study as stated by 45.1% of the respondents, and also in line with the study of Bataineh et al.[25] This is because of the established use of formalin as a preservative of cadavers in our country, Ethiopia.[24,26] There were some ups and downs in the frequency of responses between males and females, and Christians and Muslims; however, none of these were statistically significant.

In this study, 90.2% of the symptoms decreased gradually. However, loss of appetite, headache, and nightmares were still felt after leaving the dissection room. Post-dissection continuity of the above two symptoms may be due to long time (minimum of 3 hours) exposure at one dissection schedule. This may lead to an excessive intake of irritant chemical (mainly formalin) that may bring loss of appetite and headache. Females had nightmares more than males in the post-dissection period (p=0.04). Nevertheless, no significant difference was observed in Christian and Muslim respondents. Karau et al.[27] presented similar findings.

The commonest way of coping strategy used by the students was focusing on task followed by seeking advice from instructor or lab assistant and thirdly stay within the group. Comparison of gender and race presented in **Table 7** did not show a significant difference between males and females and Christians and Muslims. Most students in Oman (65%) and Jordan (89.8%) used rationalization to cope with fear and disturbance associated with cadaver dissection.[28] Other coping mechanisms listed in this research are utilized in different degrees by the above students. The age and work experience of our subjects may be the factors that bring a difference in prioritizing coping mechanisms.

This study has some limitations having incorporated only two batches of medical students, of a number of 85. On the other hand, the concentration of embalming fluid on air in the dissection room could not be measured due to our laboratory facilities.

Conclusion

Even though dissection of the human body is the best methods of learning anatomy, multiple physical and emotional symptoms are experienced by the students. Commonly students felt nausea, palpitation, sweating sadness, fear, and worry in our cadaver room. Even some of the symptoms are worsen for female. These findings are also reported by different investigators. Therefore, all medical schools of Ethiopia should conduct nation-wide research to assess commonest symptoms, their causes and the maximum level of embalming solution in the cadaver room.

Acknowledgments

The deepest gratitude is extended to the students who voluntarily participated to fill in the questionnaire.

References

1. Parker LM. What's wrong with the dead body? Use of the human cadaver in medical education. Med J Aust 2002;176:74–6.
2. McLachlan JC, Bligh J, Bradley P, Searle J. Teaching anatomy without cadavers. Med Educ 2004;38:418–24.
3. O'Carroll RE, Whiten S, Jakson D, Sinclair DW. Assessing the emotional impact of cadaver dissection on medical students. Med Educ 2002;36:550–4.
4. Snelling J, Sahai A, Ellis H. Attitudes of medical and dental students to dissection. Clin Anat 2003; 16:165–72.
5. Hancock D, Williams M, Taylor A, Dawson B. Impact of cadaver dissection on medical students. New Zealand Journal of Psychology 2004;33:20–3.
6. Cahill KC, Ettarh R. Attitudes to anatomy dissection in an Irish medical school. Clin Anat 2009; 22:386–91.
7. Older J. Anatomy: a must for teaching the next generation. Surgeon 2004; 2:79–90.
8. Rajkumari A, Singh Y. Body donation and its relevance in anatomy learning - a review. J Anat Soc India 2007; 56:44–7.
9. Nnodim J. Preclinical student reactions to dissection, death, and dying. Clin Anat 1996;9:175–82.
10. Dempster M, Black A, McCorry N, Wilson D. Appraisal and consequences of cadaver dissection. Med Educ Online 2006; 11:4592.
11. Russa A, Mligiliche L. Inspiring Tanzanian medical students into the profession: appraisal of cadaveric dissection stress and coping strategies. Ital J Anat Embryol 2014; 119:268–76.
12. Tschernig T, Schlaud M, Pabst R. Emotional reactions of medical students to dissecting human bodies: a conceptual approach and its evaluation. Anat Rec 2000;261:11–3.
13. Vijayabhaskar P, Shankar PR, Dubey AK. Emotional impact of cadaver dissection: a survey in a medical college in western Nepal. Kathmandu Univ Med J (KUMJ) 2005;3:143–8.
14. Williams AD, Greenwald EE, Soricelli RL, DePace DM. Medical students' reactions to anatomic dissection and the phenomenon of cadaver naming. Anat Sci Educ 2014;7:169–80.
15. Agnihotri G, Sagoo MG. Reactions of first year Indian medical students to the dissection hall experience. National Journal of Integrated Research in Medicine 2010;1:4–9.
16. Rajeh NA, Badroun LE, Alqarni AK, Alzhrani BA, Alallah BS, Almghrabi SA, Almalki LA. Cadaver dissection: a positive experience among Saudi female medical students. Journal of Taibah University Medical Sciences 2017; 12:268–72.
17. Johnson JH. Importance of dissection in learning anatomy: personal versus peer teaching. Clin Anat 2002; 15:38–44.
18. Shugaba AI, Usman YM, Shimwen FJ, Uzokwe CB, Shinku F, Rabiu AM, Hassan ZI. Attitude of Jos University medical students to their initial encounter with cadavers in the dissecting room. Journal of Experimental and Clinical Anatomy 2015;14:101–4.
19. Winkelmann A. Anatomical dissection as a teaching method in medical school: a review of the evidence. Med Educ 2007; 41:15–22.
20. Vinay KV, Martin LA, Vishal K, Pradeep K. Attitude of first year Indian medical students towards cadaver dissection. International Journal of Anatomy and Research 2015;3:1255–58.
21. Khan H, Mirza T. Physical and psychological effects of cadaveric dissection on undergraduate medical students. J Pak Med Assoc 2013; 63:831–4.
22. Izunya A, Oaikhena G, Nwaopara A. Attitudes to cadaver dissection in a Nigerian medical school. Asian Journal of Medical Sciences 2010;2:89–94.
23. Lee Y, Lee Y, Kwon S, Park S. Reactions of first-year medical students to cadaver dissection and their perception on learning methods in anatomy. Korean J Med Educ 2011;23:275–83.
24. Getacew D. Reaction of medical students to experiences in dissection room. Ethiop J Health Sci 2014;20:337–42.
25. Bataineh ZM, Hijazi TA, Hijleh MF. Attitudes and reactions of Jordanian medical students to the dissecting room. Surg Radiol Anat 2006;28:416–21.
26. Mulu A, Tigabu D. Medical atudents' attitudinal changes towards cadaver dissection. Ethiop J Health Sci 2012;22:51–8.
27. Karau PB, Wamachi A, Ndede K, Mwamisi J, Ongeti K. Physical and emotional impact of dissection: findings from a pioneer medical class in a Kenyan Medical School. Anatomy Journal of Africa 2016;5:746–59.
28. Abu-hijleh MF, Hamdi NA, Moqattash ST, Harris PF, Heseltine GF. Attitudes and reactions of Arab medical students to the dissecting room. Clin Anat 1997;10:272–8.

Online available at:
www.anatomy.org.tr
doi:10.2399/ana.18.069
QR code:
deomed

Correspondence to: Melese Shenkut Abebe, MSc
Department of Anatomy, School of Medicine, College of Medicine and Health Science, Wollo University, Dessie, Ethiopia
Phone: +251 912 368 855
e-mail: melese19@yahoo.com

Conflict of interest statement: No conflicts declared.

anatomy
www.anatomy.org.tr
An International Journal of Experimental and Clinical Anatomy

Case Report

www.anatomy.org.tr
Received: October 30, 2018; Accepted: November 20, 2018
doi:10.2399/ana.18.089

A rare muscle variation – accessory piriformis muscle

Albert Gradev, Lina Malinova, Lazar Jelev

Department of Anatomy, Histology and Embryology, Medical University of Sofia, Sofia, Bulgaria

Abstract

During routine anatomical dissection of the right lower limb of a 68-year-old male cadaver, a rare muscle variation was revealed and identified as an accessory piriformis muscle. This variant muscle started from the anterior surface of the sacrum below the usual piriformis muscle and extended in a well-identifiable lateral tendon also inserting to the greater trochanter of the femur. In the case described, the accessory piriformis pierced through the proximal part of the sciatic nerve. The length of the additional small muscle was 85 mm with the broadest part of the muscle belly as 9 mm. The course of the variant muscle, especially its tendinous part, might irritate the sciatic nerve and cause piriformis syndrome and other sciatica-like symptoms. The neurologists who diagnose piriformis syndrome and surgeons performing nerve releasing surgery should be well aware of the described rare muscle variation.

Keywords: nerve compression syndrome; piriformis muscle; sciatic nerve; variation

Anatomy 2018;12(3):152–154

Introduction

The piriformis is a flat, triangular muscle that originates from the anterior surface of the sacrum, and then passes through the greater sciatic foramen to finally insert into the greater trochanter of the femur.[1] Despite its small size and insignificant function as a lateral hip joint rotator, the piriformis has a great importance for the topography of the deep gluteal region. The upper and lower muscle borders form together with the greater sciatic foramen the main foramina for the gluteal neuro-vascular bundles. The piriformis has also special and sometimes variable relations with the largest nerve of the lower limb – the sciatic nerve.[2] Some piriformis-sciatic nerve variations might be related to nerve compression symptoms described as piriformis syndrome.[3] A rare type of piriformis muscle variation is described here that may be a contribution to the understanding of this nerve compression syndrome.

Case Report

During routine anatomical dissection of the right lower limb of a 68-year-old male cadaver, skin over gluteal region was dissected up to mid-thigh. The gluteus maximus was transected in the middle to expose the deeper structures. Upon dissecting the neurovascular bundles passing through the supra-and infrapiriform foramina, an interesting variation, related to the piriformis muscle and the sciatic nerve was revealed (**Figures 1a** and **b**). The piriformis muscle presented a complete structure with the usual origin and insertion. As usual, the sciatic nerve emerged from the infrapiriform foramen. There was an interesting additional small muscle identified, that also started from the anterior surface of the sacrum and passed through the greater sciatic foramen below the usual piriformis. The variant muscle presented a well identifiable lateral tendon that pierced through the proximal part of the sciatsic nerve and inserted to the greater trochanter. The length of the additional small muscle was 85 mm with the broadest part of the muscle belly of 9 mm.

Discussion

In the literature, there are several variations of the piriformis described – divided piriformis, cleavage of muscle

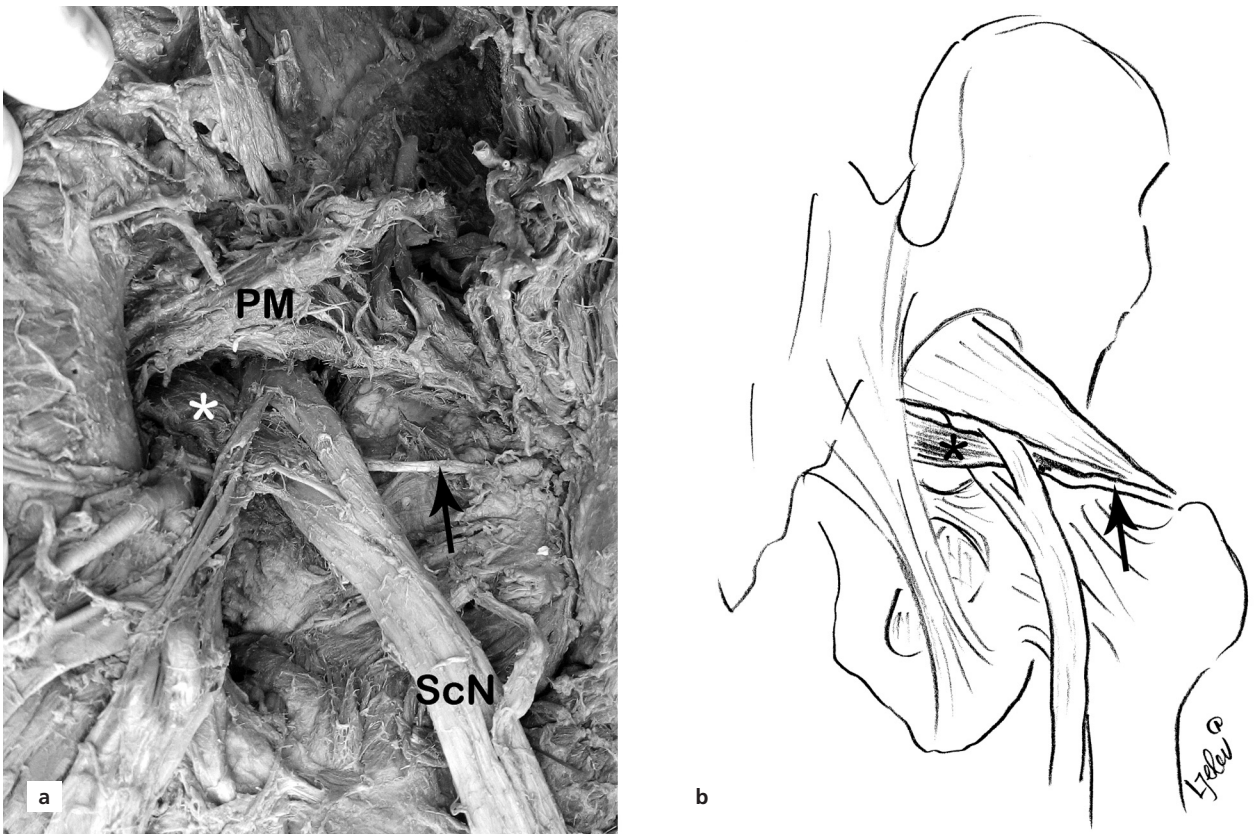

Figure 1. Photograph (**a**) and schematic diagram (**b**) of the deep gluteal region. The usual piriformis muscle was partially damaged by the student dissection. The accessory piriformis (*) and its lateral tendon (**arrow**) passing through the sciatic nerve. **PM:** piriformis muscle; **ScN:** sciatic nerve.

bellies, merging with other muscles, or even absence.[4,5] The most important muscle variations, however, are those related to the structure of the proximal sciatic nerve.[6] Six basic types of piriformis-sciatic nerve variations are described in the literature and their distribution among the human population are presented in details.[7,8]

The muscle described here resembles a variation of the piriformis muscle. It is not simply a case of a divided or cleavaged muscle, because it has a separate origin and insertion and distinct proportion of muscle belly to tendon. It can be accepted that this is an accessory muscle. In our case, the sciatic nerve passed below the usual piriformis and was pierced by the accessory piriformis muscle. From a review of the pertinent literature, it seems that the accessory piriformis is quite a rare muscle variation. A similar small muscle below the usual piriformis is also described by Carro et al.[9] In their case, however, the accessory piriformis did not penetrate through the sciatic nerve fibers. In two other reports,[10,11] the anomalous sacral attachment of the piriformis with accessory fibers extending over the sacral nerve, seen on MRI, were also described as accessory piriformis muscle.

The reported aberrant muscle might provoke symptoms of compression of the sciatic nerve and be the cause of piriformis syndrome, coccygodynia and following muscle atrophy in the zone innervated by the sciatic nerve. Piriformis syndrome includes hip pain, buttock pain, sciatica and intolerance to sitting.[3,12,13] In up to 16.2% of surgical case series, piriformis syndrome is caused by anatomical variations.[14] The accessory piriformis, piercing the sciatic nerve, might be one of the rare causes of nerve compression. Therefore, the surgeons who operate in this region must be well aware of the reported muscle variation, as well as the neurologists who diagnose piriformis syndrome and other related sensory symptomatology.

References

1. Clemente CD. Anatomy of the human body. 30th ed. Philadelphia (PA): Lea and Febiger; 1985. pp. 565–71.
2. Beaton LE, Anson BJ. The relation between the sciatic nerve and of its subdivisions to the piriformis muscle. Anat Rec 1938;70:1–5.

3. Jankovic D, Peng P, van Zundert A. Brief review. Piriformis syndrome: etiology, diagnosis, and management. Can J Anaesth 2013; 60:1003–12.
4. Bergman RA, Afifi AK, Miyauchi R. Illustrated encyclopaedia of human anatomic variation. Opus I: Muscular system [Revised on January 1, 2019] [Retrieved: March 2019]. Available from: https://www.anatomyatlases.org/AnatomicVariants/MuscularSystem/Text/P/24Piriformis.shtml
5. Brenner E, Tripoli M, Scavo E, Cordova A. Case report: absence of the right piriformis muscle in a woman. Surg Radiol Anat 2019 Feb 13. doi: 10.1007/s00276-018-02176–6
6. Natsis K, Totlis T, Konstantinidis GA, Paraskevas G, Piagkou M, Koebke J. Anatomical variations between the sciatic nerve and the piriformis muscle: a contribution to surgical anatomy in piriformis syndrome. Surg Radiol Anat 2014;36:273–80.
7. Adibatti M, Sangeetha V. Study on variant anatomy of sciatic nerve. J Clin Diagn Res 2014;8:AC07–9.
8. Sinha MB, Aggarwal A, Sahni D, Harjeet K, Gupta R, Sinha HP. Morphological variations of sciatic nerve and piriformis muscle in gluteal region during fetal period. Eur J Anat 2014;18:261–6.
9. Carro LP, Hernando MF, Cerezal L, Navarro IS, Fernandez AA, Castillo AO. Deep gluteal space problems: piriformis syndrome, ischiofemoral impingement and sciatic nerve release. Muscles Ligaments Tendons J 2016;6:384–96.
10. Lee EY, Margherita AJ, Gierada DS, Narra VR. MRI of piriformis syndrome. AJR Am J Roentgenol 2004;183:63–4.
11. Sen A, Rajesh S. Accessory piriformis muscle: an easily identifiable cause of piriformis syndrome on magnetic resonance imaging. Neurol India 2011;59:769–71.
12. Beers MH, Porter RS, Jones TV, Kaplan JL, Berkwits M. The Merck manual of diagnosis and therapy. 18th ed. New Jersey (NJ): Merck Research Laboratories; 2006. p. 2635.
13. Han SK, Kim YS, Kim TH, Kang SH. Surgical treatment of piriformis syndrome. Clin Orthop Surg 2017;9:136–44.
14. Smoll NR. Variations of the piriformis and sciatic nerve with clinical consequence: a review. Clin Anat 2010;23:8–17.

Online available at:
www.anatomy.org.tr
doi:10.2399/ana.18.089
QR code:

Correspondence to: Lazar Jelev, MD, PhD
Department of Anatomy, Histology and Embryology, Medical University of Sofia, BG-1431, Sofia, Bulgaria
Phone: +359 897 87 27 51
e-mail: ljelev@abv.bg

Conflict of interest statement: No conflicts declared.

Historical View

www.anatomy.org.tr
Received: May 10, 2018; Accepted: September 14, 2018
doi:10.2399/ana.18.060

anatomy
An International Journal of Experimental and Clinical Anatomy

Da Vinci's foot illustration and its errors

Didem Dönmez, Menekşe Karahan, Oğuz Taşkınalp

Department of Anatomy, School of Medicine, Trakya University, Edirne, Turkey

Abstract

Leonardo da Vinci is an important philosopher, astronomer, architect, engineer, inventor, mathematician, anatomist, musician, sculptor, writer and painter who lived in the Renaissance period. In addition to his skills in numerous diverse areas of study, he has important contributions to anatomy, cornerstone of medicine. Leonardo da Vinci performed many cadaver dissections. His anatomical illustartions are brilliant, despite the limitations of his time. However, a number of errors have been found in these illustrations. Here, we interpreted the illustration of da Vinci named "The anatomy of a foot".

Keywords: foot; illustration; Leonardo da Vinci

Anatomy 2018;12(3):155–157

Leonardo da Vinci's early years

Da Vinci was born on 15 April 1452 in Mount Albano, Florence. He was the son of Sar Pierro da Vinci, a lawyer. Her mother was a peasant woman. Due to the requirements of that period, her parents never got married. Leonardo's father married to a noble woman and Leonardo had to live with his grandparents who raised him well.[1]

Leonardo da Vinci's Interest in Anatomy

Leonardo da Vinci's interest in anatomy began in Milan when he was working for Ludovico Maria Sforza. Da Vinci's favorite tools were sharp knives, chisels and bone saws. He had no assistant at that time. That's why he had to transcribe quickly his observation right after each dissection section. It is still not known how he preserved the cadavers.[2] He performed approximately 30 cadaver dissections.[3] After 1510, he collaborated with a young professor named Marcantonio della Torre. Later on, with the advance of science, dissection studies increased. In this way, the accuracy of the teachings of the previous period began to be questioned, and it was then found that Leonardo da Vinci's work had some mistakes.[4–7] For example, his work "The anatomy of a foot" is confusing like "Mona Lisa".

"The Anatomy of a Foot"

At a quick glance to the illustration, to the alignment of the metatarsal bones and phalanges, we can say this is the lateral side of the foot. Also, the phalanges are gradually becoming smaller. So, the illustrated tendons in this work probably belong to the peroneus brevis and peroneus longus muscles. In addition, the location of the nerve lying from the back of the leg to dorsum of the foot implies this is the superficial peroneal nerve. This nerve becomes superficial by penetrating the deep fascia in the junction between upper 2/3 and lower 1/3 of the posterior leg. It's divided into two branches at the dorsum of the foot: the dorsal medial cutaneous nerve and the dorsal intermedial cutaneous nerve.[8] It's not possible to say this is the peroneus tertius muscle (**Figure 1a**), because the tendon of the peroneus tertius muscle passes under the extensor retinaculum.

However, there is another tendon in the drawing (marked in **Figure 1a**). This also refutes the idea of being the lateral side of the foot. If it's the medial side, it can be assumed that the tibialis posterior, flexor digitorum longus and flexor hallucis longus muscles are observed behind the medial malleolus. On the medial side, we should clearly see the extensor hallucis longus muscle with a thick tendon. Also, the structure with the question mark can be assumed as the great saphenous vein (**Figure 1b**). However, this structure goes to the posterior of the leg, and therefore, does not suit with the path of the great saphenous vein. It's not possible to say this is the tibialis anterior muscle, because the muscle

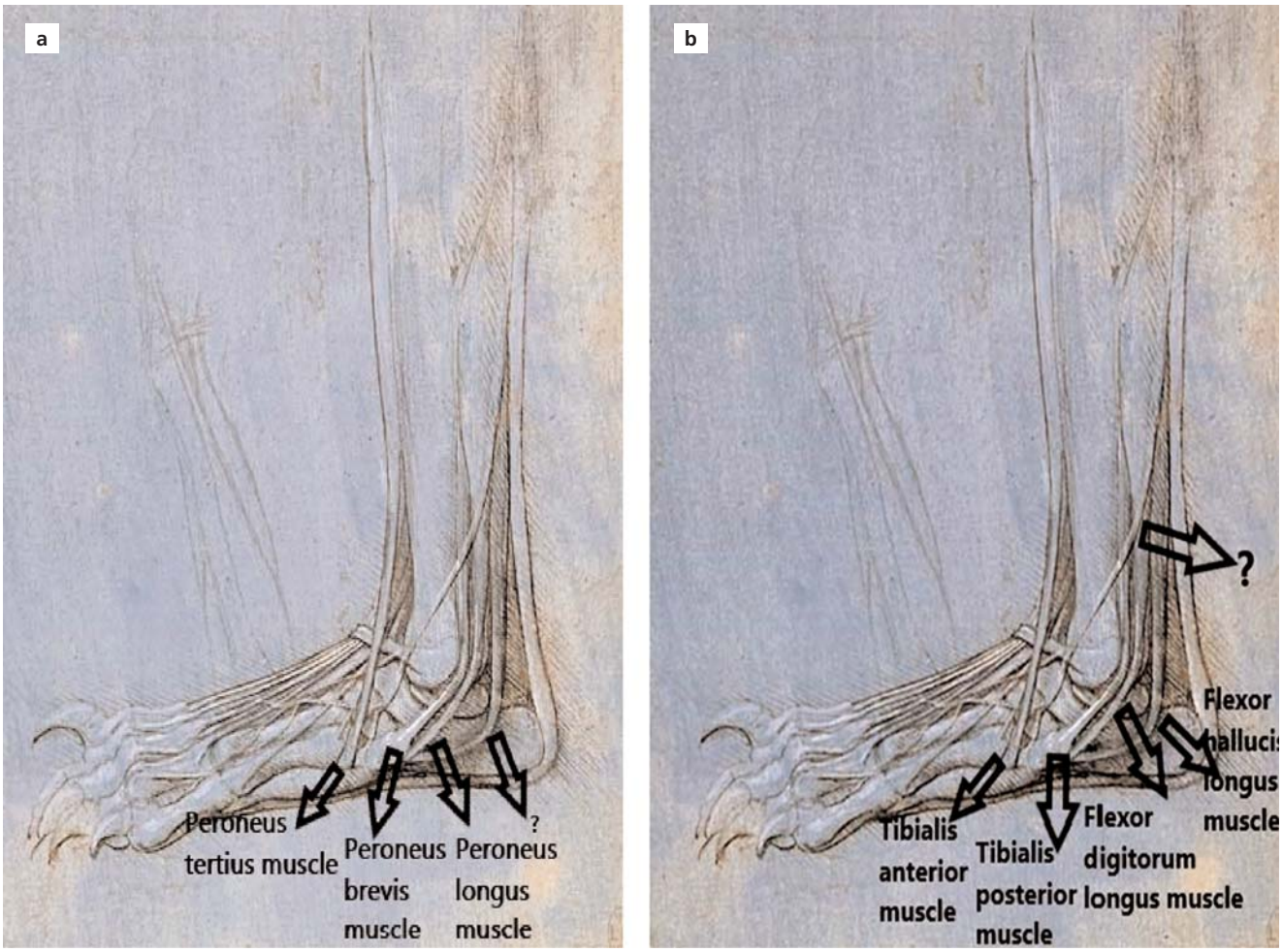

Figure 1. . Lateral (**a**) and medial (**b**) views of the human foot showing tendons which support the foot, respectively.[9] [Color figure can be viewed in the online issue, which is available at www.anatomy.org.tr]

passes under the extensor retinaculum. So, we could not come to a decision on which side this may be.

Jastifer et al. [10] examined another drawing of foot by Leonardo da Vinci. In this work, the anatomical structures supporting the medial arch of the foot are clearly seen. Compared to the work studied in this article, the two drawings look quite different from each other. The work we studied can be one of his early works. In this respect, this piece reminded us Mona Lisa's face.

Conclusion

Leonardo da Vinci has been influencing people for centuries with his magnificent intelligence. His anatomical work presented new details for the surgical treatment of previously unexplored areas. Therefore, surgeons and anatomists owe him as his works facilitated and improved their practice. We can understand his respect for his work from his words before his death: "I have offended God and mankind because my work did not reach the quality it should have".[1]

References

1. Jose AM. Anatomy and Leonardo da Vinci. Yale J Biol Med 2001;74: 185–95.
2. White M. Leonardo: the first scientist. London (UK): Little, Brown; 2001. 384 p.
3. Toledo-Pereyra LH. Leonardo da Vinci: the hidden father of modern anatomy. J Invest Surg 2002;15:247–9.
4. Bowen G, Gonzales J, Iwanaga J, Fisahn C, Loukas M, Oskouian RJ, Tubbs RS. Leonardo da Vinci (1452–1519) and his depictions of the human spine. Childs Nerv Syst 2017;33:2067–70.
5. Clayton M, Philo R. Leonardo da Vinci: anatomist. London (UK): Royal Collection Trust; 2012. 260 p.
6. O'Malley CD, Saunders JB de CM. Leonardo da Vinci on the human body: the anatomical, physiological, and embryological draw-

ings of Leonardo da Vinci: with translations, emendations and a biographical introduction. New York (NY): Henry Schuman; 1952. 506 p.

7. Tubbs RI, Gonzales J, Iwanaga J, Loukas M, Oskouian RJ, Tubbs RS. The influence of ancient Greek thought on fifteenth century anatomy: Galenic influence and Leonardo da Vinci. Childs Nerv Syst 2018;34:1095–101.
8. Garg K. Human anatomy: regional and applied dissection and clinical. New Delhi: CBS Publishers; 2010. 472 p.
9. The anatomy of a foot - by Leonardo da Vinci. [Internet].[Cited 2018 May 8]. Available from: [https://www.leonardodavinci.net/ the-anatomy-of-a-foot].
10. Jastifer JR, Toledo-Pereyra LH. Leonardo da Vinci's foot: historical evidence of concept. J Invest Surg 2012;25:281–5.

Online available at:
www.anatomy.org.tr
doi:10.2399/ana.18.060
QR code:

Correspondence to: Didem Dönmez, MD
Department of Anatomy, School of Medicine,
Trakya University, Balkan Campus, 22040, Edirne, Turkey
Phone: +90 284 235 76 41/1510
e-mail: didemdonmez@trakya.edu.tr

Conflict of interest statement: No conflicts declared.

anatomy
www.anatomy.org.tr
An International Journal of Experimental and Clinical Anatomy

Erratum

www.anatomy.org.tr
Received: November 22, 2018; Accepted: November 25, 2018
doi:10.2399/ana.18.S2S140.err001O74

Correction: (O-74) Virtual reality technology in anatomy education

Anatomy 2018;12(3):158 ©2018 Turkish Society of Anatomy and Clinical Anatomy (TSACA)

Topuz Y[1], Özdener DN[2], Verimli U[3]

[1]*Department of Information Technologies and Security, Beykoz University, Istanbul, Turkey*
[2]*Department of Computer Education and Instructional Technology, Marmara University Atatürk Faculty of Education, Istanbul, Turkey*
[3]*Department of Anatomy, School of Medicine, Marmara University, Istanbul, Turkey*

Author names for abstract of poster presentation published in Volume 12, Supplement 2, September 2018, page S140; O-74 "Virtual reality technology in anatomy education" is erroneously published as: Topuz Y, Özdener DN. Corrected version is as follows: **Topuz Y, Özdener DN, Verimli U**.

Online available at:
www.anatomy.org.tr
doi:10.2399/ana.18.S2S140.err001O74
QR code:

Correspondence to: Yasemin Topuz, MD
Department of Information Technologies and Security,
Beykoz University, Istanbul, Turkey

Announcement

www.anatomy.org.tr
Received: December 21, 2018; Accepted: December 24, 2018
doi:10.2399/ana.18.090

anatomy
www.anatomy.org.tr
An International Journal of Experimental and Clinical Anatomy

International Meeting of Anatomia Clinica & International Symposium of Clinical and Applied Anatomy (ISCAA), 24th to 26th June 2019, Madrid, Spain

Anatomy 2018;12(3):159

Dear colleagues,

We are happy to announce that Abstract Submission and Registration to the **International Meeting of Anatomia Clinica** (European Association of Clinical Anatomist, EACA) and the International Symposium of Clinical and Applied Anatomy (ISCAA), which will take place from 24th to 26th June 2019 in Madrid (Spain) is now open.

Visit www.eaca2019.com to get an account which will allow you to submit abstracts, register to the meeting.

Deadline for receipt of abstracts – 11 April 2019

The accepted abstracts will be published in the Surgical and Radiologic Anatomy journal.

We look forward to meeting you all in Madrid, June 2019 for an enjoyable Meeting!

Sincerely,

Prof. Jose Sanudo
President of the Congress

Department of Human Anatomy & Embryology,
Faculty of Medicine,
Complutense Universtiy of Madrid
Av. Ciudad Universitaria s/n 28040-Madrid. Spain.
Tel: +34 91 394 1381
e-mail: jrsanudo@ucm.es

Online available at:
www.anatomy.org.tr
doi:10.2399/ana.18.090
QR code:

deomed

anatomy
www.anatomy.org.tr
An International Journal of Experimental and Clinical Anatomy

www.anatomy.org.tr
Anatomy 2018;12(3):160 ©2018 Turkish Society of Anatomy and Clinical Anatomy (TSACA)

Author Index to Volume 12, 2018

(The bold typed references are the ones in which the person is the first author.)

Acknowledgment

www.anatomy.org.tr
Anatomy 2018;12(3):160 ©2018 Turkish Society of Anatomy and Clinical Anatomy (TSACA)

Acknowledgment of Reviewers for Volume 12, 2018

The Editorial Staff of Anatomy expresses their appreciation to the following reviewers who have evaluated the manuscripts for Volume 12, 2018.

Esat Adıgüzel
Nihal Apaydın
Yüksel Aydar
Ebru Ballı
Çağatay Barut
Mustafa Büyükmumcu
Servet Çelik
Burcu Erçakmak
Tolga Ertekin
Mete Ertürk
Zeliha Fazlıoğulları
Georg Feigl
Nadir Gülekon
Ceren Günenç Beşer
Z. Aslı İkiz
David Kachlick
S. Tuna Karahan
Piraye Kervancıoğlu
Zeliha Kurtoğlu
Bernard Moxham
Helen Nicholson
Eren Öğüt
Davut Özbağ
Cenk Murat Özer
Tuncay Veysel Peker
Mustafa F. Sargon
Levent Sarıkçıoğlu
Isabel Stabile
Lütfiye Bikem Süzen
Ümit S. Şehirli
Gülgün Şengül
Trifon Totlis
M. İbrahim Tuğlu
Emel Ulupınar
İlknur Uysal
Hülya Üçerler
Nadire Ünver Doğan
Tuncay Varol
Ural Verimli

Table of Contents

Volume **12** / Issue **3** / December **2018**

(Continued from back cover)

Teaching Anatomy

Case Report

Historical View

Erratum

Announcement

Index

Acknowledgment

On the Front Cover:
Course of the anterior interosseous nerve (AIN). **Arrowheads:** AIN; **FDP:** flexor digitorum profundus; **FPL:** flexor pollicis longus; **m:** median nerve; **PQ:** pronator quadratus; **PT:** pronator teres. From Kibar S, Bilecenoğlu B, Filgueira L, Uz A. Morphometry of the anterior interosseous nerve: a cadaveric study. *Anatomy* 2018;12(3):111–114.

Colored images of the published articles can be found in the online version of the journal which is available at www.anatomy.org.tr

www.anatomy.org.tr

anatomy

An International Journal of Experimental and Clinical Anatomy

Table of Contents

Volume **12** / Issue **3** / December **2018**

Original Articles

(Contents continued on inside back cover)

deomed®